Title
Mapping Dysregulated Metabolic Pathways in Cancer Using Chemoproteomic and Metabolomic Platforms

Author
Louie, Sharon M

Publication Date
2017

Peer reviewed|Thesis/dissertation

Mapping Dysregulated Metabolic Pathways in Cancer Using Chemoproteomic and Metabolomic Platforms

by

Sharon M Louie

A dissertation submitted in partial satisfaction of the

requirements for the degree of

Doctor of Philosophy

in

Metabolic Biology

in the

Graduate Division

of the

University of California, Berkeley

Committee in charge:

Professor Daniel K. Nomura, Chair
Professor James A. Olzmann
Professor Kunxin Luo

Spring 2017

ABSTRACT

Mapping Dysregulated Metabolic Pathways in Cancer
Using Chemoproteomic and Metabolomic Platforms

by

Sharon M Louie

Doctor of Philosophy in Metabolic Biology

University of California, Berkeley

Professor Daniel K. Nomura, Chair

Cancer cells reprogram cellular metabolism to support growth and maintain pathogenicity. Since Otto Warburg's discovery nearly a century ago that cancer cells have heightened glucose uptake and aerobic glycolysis, many studies have identified additional metabolic alterations required to maintain proliferation and cancer pathogenicity, such as heightened *de novo* lipogenesis and glutamine-dependent anaplerosis[1–3]. These studies have provided a foundation for understanding the metabolic alterations that support tumorigenesis and cancer pathogenicity, but additional studies are required to uncover novel dysregulated metabolic pathways to fully understand the biochemical consequences of cancer.

In chapter one, we present several potential mechanisms that yield insight into the relationship between lipids and cancer. In chapter two, using an isotopic metabolomic platform, we elucidate the role of exogenous fatty acids in several types of cancer cells, putting forth an additional mechanism to describe the role of lipid metabolism in cancer. Although dysregulated lipid metabolism is a key feature of many cancers, the metabolic alterations in certain subtypes of cancer remain poorly understood. In chapter three, we use a reactivity-based chemoproteomic platform in combination with a metabolomic platform to identify GSTP1 as a novel metabolic enzyme target that is heightened in triple negative breast cancers (TNBCs), a highly malignant subtype of breast cancer that is poorly understood. Taken together, these studies highlight critical metabolic alterations in cancer to not only uncover novel metabolic pathways that drive cancer, but also lead to the development of novel therapeutic options for the treatment of cancer.

DEDICATION

Throughout graduate school, I have been surrounded by an amazing support system. I would like to thank my friends, colleagues, and family for being a part of this. I am extremely grateful to have had a wonderful group of people supporting me, both intellectually and emotionally, through my graduate school tenure.

A special thank you to all of the following people.

Firstly, to my mentor, Dan, who encouraged me to embark on this journey. Thank you for believing in me and seeing something in me from the very beginning.

To all of my labmates, former and present. Without all of you, this would not have been possible. You guys are the only people who truly understand what goes down in the Nomura lab. Thank you for all of your support with research and life outside of research, for bringing fun to the lab, for being some of the best colleagues and friends I have met, and for sharing all the tough times and celebrating the successes with me. A sincere gratitude to all of you for the laughs and for making this journey way more fun and entertaining than I could have ever imagined.

A special appreciation for my fellow Nomura lab BG, Lindsay, for being there and bearing witness to every single step of graduate school. I am so grateful that we started and ended this journey together. Thank you for being an amazing colleague and friend, reminding me about all of our deadlines, rewording all of my emails, incessantly practicing our presentations, introducing me to the wonderful life at the gym, and so much more.

A heartfelt thank you to my baymate, Jessica, for being an incredible friend and being the upbeat, cheerful presence over the last few years. Thank you for being my constant supply of laughter and entertainment. You have made graduate school so much more enjoyable.

My undergraduate mentees, Lucky and Justin. Thank you for teaching me how to teach and for all of your hard work in lab. Both of you contributed immensely to this work.

To all my friends for reminding me that there is so much more to life outside of research. I can always count on you guys to listen to me no matter what was going on.

To my family - my parents, grandparents, and sisters. Thank you for being the steady force in life. No matter what was going on with research, your unwavering support helped me achieve this. Thank you for listening to my stories, for your words of encouragement, and for all of the food that powered me through this journey.

Finally, to my fiancé, Kevin. Thank you for your unconditional love and for listening to all of my stories and complaints, practicing my presentations with me through Facetime,

and for being there every single step of the way. I could not have achieved this without your patience.

TABLE OF CONTENTS

LIST OF FIGURES

LIST OF ABBREVIATIONS

"e" after lipid designation	ether lipid
"L" before lipid designations	lyso-
"p" after lipid designation	plasmalogen
2DG	2-deoxyglucose
AC	acyl carnitine
ACC	acetyl coenzyme A carboxylase
acetyl CoA	acetyl coenzyme A
ADP	adenine diphosphate
AMP	adenine monophosphate
ASC	adipose stromal cells
ATGL	adipose triglyceride lipase
ATP	adenosine triphosphate
BMI	body mass index
C1P	ceramide-1-phosphate
CDNB	1-chloro-2,4-dinitrobenzene
CDP	cytidine monophosphate
COX-2	cyclooxygenase-2
CPT1	carnitine palmitoyltransferase 1
CREB	cAMP response element binding protein
DAG	diacylglycerol
DHAP	dihydoxyacetone phosphate
dUTP	deoxyuridine triphosphate

EMT	epithelial-to-mesenchymal transition
ER	estrogen receptor
FASN	fatty acid synthase
FFA	free fatty acid
G3P	glyceraldehyde-3-phosphate
GAPDH	glyceraldehyde-3-phosphate dehydrogenase
GMP	guanine monophosphate
GSH	reduced glutathione
GSSG	oxidized glutathione
GSTP1	glutathione-S-transferase pi 1
GTP	guanine triphosphate
HER2	human epidermal growth factor receptor 2
HIF1α	hypoxia-inducible factor 1 alpha
HSL	hormone sensitive lipase
IC50	50% inhibitory concentration
IGF	insulin-like growth factor
IL6	interleukin 6
IP3	inositol trisphosphate
KEGG	Kyoto encyclopedia of genes
LC-MS	liquid chromatography-mass spectrometry
LPCAT	lysophosphatidylcholine acyltransferase
MAG	monoacylglycerol
MAGL	monoacylglycerol lipase

MAPK	mitogen activated protein kinase
mTOR	mammalian target of rapamycin
NAD/NADH	nicotinamide adenine dinucleotide
NADP/NAPDH	nicotinamide adenine dinucleotide phosphate
NAE	N-acylethanolamine
PA	phosphatidic acid
PAF	platelet activating factor
PAI-1	pasminogen activator inhibitor-1
PAPS	phosphoadenosine phosphosulfate
PC	phosphatidylcholine
PE	phosphatidylethanolamine
PEP	phosphoenolpyruvate
PG	phosphatidylglycerol
PGE2-1	prostglandin E2 synthase-1
PI	phosphatidyl inositol
PPP	penthose phosphate pathway
PR	progesterone receptor
PS	phosphatidylserine
qPCR	quantitative polymerase chain reaction
S1P	sphingosine-1-phosphate
shRNA	short hairpin RNA
SK-1	sphingosine kinase-1
SM	sphingomyelin

SRM	single reaction monitoring
TAG	triacylglycerol
TBTA	Tris[(1-benzyl-1*H*-1,2,3-triazol-4-yl)methyl]amine
TCA	tricarboxylic acid
TCEP	(tris(2-carboxyethyl)phosphine)
TNBC	triple negative breast cancer
TNFα	tumor necrosis factor alpha
TZD	thiazolidinedione
UDP	uridine diphosphate
UDP-GlcNac	UDP-acetylglycosamine
UMP	uridine monophosphate
UTP	uridine triphosphate
WAT	white adipose tissue

ACKNOWLEDGEMENTS

Adapted with permission from Biochimica et Biophysica Acta – Molecular and Cell Biology of Lipids, Volume 1831, Issue 10, Pages 1499-1508, October 2013, Sharon M Louie, Lindsay S. Roberts, Daniel K. Nomura, “Mechanisms linking obesity and cancer.” Copyright © 2013 with permission from Elsevier.

Adapted with permission from Biochimica et Biophysica Acta – Molecular and Cell Biology of Lipids, Volume 1831, Issue 10, Pages 1566-1572, October 2013, Sharon M Louie, Lindsay S. Roberts, Melinda M. Mulvihill, Kunxin Luo, Daniel K. Nomura, “Cancer cells incorporate and remodel exogenous palmitate into structural and oncogenic signaling lipids.” Copyright © 2013 with permission from Elsevier.

Adapted with permission from Cell Chemical Biology, Volume 23, Issue 5, Pages 567-578, May 2016, Sharon M Louie, Elizabeth A. Grossman, Lisa A. Crawford, Lucky Ding, Roman Camarda, Tucker R. Huffman, David K. Miyamoto, Andrei Goga, Eranthie Weerapana, Daniel K. Nomura, “GSTP1 Is a Driver of Triple-Negative Breast Cancer Cell Metabolism and Pathogenicity.” Copyright © 2016 with permission from Elsevier.

INTRODUCTION

Cancer cells depend on the reprogramming of cellular metabolism to initiate tumorigenesis and maintain their pathogenic features. Proliferating cancer cells have vastly different metabolic needs compared to normal differentiated cells[4]. Hence, metabolism is rewired to balance the biosynthetic needs of the proliferating cells with its metabolic requirements to maintain cell growth and survival. Since Otto Warburg's discovery in the 1920s that cancer cells have heightened glucose uptake and aerobic glycolysis, recent studies have identified many other metabolic alterations in cancer cells, including heightened glutamine-dependent anaplerosis and *de novo* lipogenesis, which serve as metabolic platforms for cancer cells to generate biomass for cell division and metabolites that modulate cancer cell signaling, epigenetics, and pathogenicity[1–3]. While most studies have focused on glucose and glutamine metabolism, cancer cells utilize additional nutrients, such as lipids, that contribute to tumorigenesis[3].

White adipose tissue has traditionally been described as an inert tissue for energy storage. More recently, evidence has emerged to reclassify white adipose tissue as an important metabolic tissue that plays a role in inflammation, immunity, and cancer[5]. Epidemiological evidence has established an association between adipose tissue and cancer, more specifically obesity and cancer[6,7]. In chapter one, we highlight the mechanisms underlying how elevated lipids and lipid signaling, inflammation, insulin signaling, and adipokines support tumorigenesis.

Heightened *de novo* lipogenesis is a hallmark of nearly all cancers[8]. Previously, cancer cells were thought to rely almost entirely on *de novo* lipogenesis for lipids used for membrane biosynthesis and signaling molecules. Yet, evidence has emerged that tumorigenic impairments conferred by inactivation of a lipolytic enzyme monoacylglycerol lipase (MAGL), in cancer cells, could be rescued by exogenous fatty acids *in situ* or by a high fat diet *in vivo*[9]. These studies suggest that exogenous fatty acids may play a role in cancer pathogenesis. In chapter two, we investigate the role of exogenous fatty acids in several types of cancer cells using an isotopic fatty acid tracing metabolomic method, putting forth an alternate mechanism linking obesity to cancer, where cancer cells can uptake exogenous fatty acids and remodel them into structural and oncogenic signaling lipids.

While targeting dysregulated metabolism, such as inhibition of fatty acid synthase (FASN) to disrupt *de novo* lipogenesis or inhibition of the FB3 isoform of phosphofructokinase (PFKFB3) to disrupt glycolytic metabolism, is a promising strategy for cancer treatment, the metabolic pathways that drive pathogenicity in certain types of cancer, more specifically breast cancer subtypes that are correlated with heightened malignancy and poor prognosis, remain poorly understood[10,11]. In chapter three, we employ a reactivity-based chemoproteomic platform to identify metabolic enzymes that are heightened in triple negative breast cancers (TNBCs), a malignant subtype of breast cancer that shows poor prognosis and remains without targeted therapies.

CHAPTER ONE

Mechanisms Linking Obesity and Cancer

Introduction

The incidence of obesity has been steadily increasing over the past few decades. In 2007–2008, the prevalence of obesity among US adults was 33.8% and of overweight 68.0%, after adjusting for age[12]. These epidemic proportions of obesity are not only mirrored in the rest of the developed world, but also now in many developing countries, making obesity one of the most serious health problems worldwide[13]. While there are many comorbidities associated with obesity, such as the well-established relationship with type 2 diabetes and cardiovascular diseases, a clear epidemiological relationship between obesity and the prevalence of a variety of cancers has also been uncovered[6,7].

Cancer is currently the leading cause of death in developed countries and second in developing countries[14]. Several studies have shown significantly elevated risk for leukemia, lymphoma and myeloma with high body-mass index (BMI) in a dose-dependent manner[15], as well as an increased risk for pancreatic[16], prostate[17], breast[18], colon, endometrial, liver, kidney, esophagus, gastric, and gallbladder cancers[19] in obese adults. Furthermore, as childhood obesity rates continue to follow those of adults[20], their risks for cancers later in life are significantly higher[21]. Although the epidemiological associations between cancer progression and prognosis are firmly established, the link between obesity and cancer initiation and the molecular mechanisms underlying these associations are still being elucidated.

White adipose tissue has traditionally been considered an inert tissue almost exclusively for energy storage. Recently, white adipose has emerged as an important endocrine and metabolic organ as well as a key player in immunity and inflammation[5]. With this new understanding of adipose tissue function, researchers have delved into the relationship of these secondary effects of obesity, which may in fact be responsible for the increased propensities for various cancers. Considering the prevalence of obesity, the lethality of cancer, and the rise in childhood obesity, there is an imminent need for research to delineate the underlying mechanism(s) through which obesity drives cancer and to exploit those findings to develop interventions and potential therapeutics to combat this deadly combination. This chapter focuses on the mechanisms that have been proposed to underlie how obesity drives cancer pathogenesis, with emphasis on elevated lipids and lipid signaling, inflammation, insulin signaling, and adipokines **(Figure 1)**.

Elevated Lipids in Cancer

Obesity is primarily characterized by excess fat storage, adipocyte mass, and coordinate increases in certain types of lipids. I will first discuss the evidence for how fat from sources including cancer cell *de novo* lipogenesis, from the breakdown of adipose tissue in cachexia, or from neighboring adipocyte lipid-transfer, can be utilized as oncogenic signaling lipids by the cancer cells and thereby influence cancer pathogenicity. This then sets the stage for potential mechanisms through which lipid stores in obesity may also influence cancer pathogenicity.

Fatty acid synthase

One piece of supporting evidence for the utilization of lipids by cancer cells is the upregulation of fatty acid synthase (FASN), an enzyme that makes endogenous fatty acids, which can be modified and packaged into structural lipids required for cell division. Elevated FASN enzyme, mRNA, and enzymatic activity have been seen in human breast cancer cell lines[22], ovarian tumors[23], prostate tumors[24] and cancer precursor lesions in the colon, stomach, esophagus and oral cavity[10]. The increase in FASN seems to be necessary for eliciting the malignant effects, such as proliferation and survival, though this itself is not the cause of malignancy[25]. One study found FASN inhibition as an off-target effect of the weight-loss drug Orlistat.

This FASN inhibition induced an antiproliferative effect in prostate cancer cells in culture, which was rescued by addition of palmitate, the product of FASN[26]. Furthermore, when FASN was chemically inhibited in both breast and prostate cancer tumor xenografts, there was a significant antitumor effect[10]. These data together show the importance of FASN in cancer cell growth, survival and proliferation *in vitro* and *in vivo*. This FASN overexpression in cancer is also mirrored in a variety of tissues in obesity, and one may postulate that the fatty acids formed through FASN in other tissues may also provide fatty acid sources to the cancer[27]. Additionally, in a study examining FASN polymorphisms and the risk of prostate cancer, one of the polymorphisms associated with prostate cancer was also significantly, positively correlated with BMI[24]. Between increases in FASN in obesity and a heightened propensity for an unfavorable FASN polymorphism, there is also evidence that FASN plays an important role in the way through which obesity may drive some cancers.

MAGL

The increased activity of FASN in cancer cells is also matched by an increase in lipolytic enzymes, such as monoacylglycerol lipase (MAGL), to promote the mobilization of lipid stores for remodeling of cellular lipids and generation of pro-tumorigenic signaling lipids. The MAGL pathway is upregulated in multiple types of aggressive human cancer cells and high-grade primary tumors[28] and releases free fatty acids (FFAs), which in turn fuel the generation of fatty acid-derived lipid signaling molecules such as lysophosphatidic acid and prostaglandins. Impairments of MAGL-dependent tumor growth are rescued by a high-fat diet *in vivo*, suggesting that exogenous sources of fatty acids can also contribute to cancer malignancy. Thus, elevated levels of fatty acids, derived either from the cancer cell or exogenous fat sources, may promote a more aggressive tumorigenic phenotype[28].

Cachexia

In subjects, with late-stage, highly malignant cancer these exogenous sources of fats may be derived from the breakdown of fat mass. Cachexia commonly accompanies late-stage cancers and causes subjects to lose both muscle and fat mass through catabolic processes. In cachectic subjects, there is a marked increase in adipose triglyceride lipase (ATGL)[29] an enzyme that breaks triglycerides into diglycerides as well as hormone-sensitive lipase (HSL), an enzyme that breaks diglycerides into free fatty

acids[30]. This then leads to increased levels of circulating free fatty acids, which can be repackaged into important oncogenic signaling lipids as well as membrane structural lipids necessary for cell proliferation[31]. Moreover, there is evidence that the lipids released in these processes can be directly utilized by the cancer cells for fuel[32]. While cachexia contrasts obesity in that it is a condition marked by muscle and adipose catabolism, it provides additional evidence that cancer cells can utilize free fatty acids for both fuel and oncogenic signaling lipids. In a state of obesity, however, the free fatty acid substrates for fuel or signaling molecules must be derived from adipocyte stores.

Transfer of Lipids from Adipocytes to Tumor

One study showed that cancer cells can access and use lipids from neighboring adipocyte stores *in vitro* by co-culture of ovarian cancer cells and adipocytes. This led to the direct transfer of lipids from the adipocytes to the cancer cells, which induced lipolysis in the adipocytes and β-oxidation in the cancer cells. This indicates that cancer cells can directly use these transferred lipids as an energy source, which in turn promotes tumor growth[33]. These data are of particular importance in considering the implications of obesity, mainly excess adipocyte mass, on cancer prevalence and aggressiveness and the synergistic interplay of adipocytes and cancer cells.

Adipose Stromal Cells

In another study using a mouse model, obesity was shown to facilitate tumor growth irrespective of diet, suggesting a direct role of adipose tissue in cancer progression[34]. White adipose tissue-derived mesenchymal stem cells, termed adipose stromal cells (ASC), may represent a cell population linking obesity to the increased incidence of cancer. When transplanted into mice, adipose stromal cells can promote tumor growth by serving as perivascular adipocyte progenitors. ASCs were shown to traffic from endogenous white adipose tissue (WAT) to tumors, where they can be incorporated as pericytes into blood vessels and differentiate into adipocytes[34]. Intratumoral adipocytes were shown to be associated with an increase in tumor vascularization and an increase in proliferation of adjacent malignant cells[34]. These results suggest that ASCs recruited from adipose tissue have a direct role in inducing tumor development.

Lipid Signaling

Another mechanism through which obesity may drive cancer pathogenesis is through converting high-fat diet supplied fatty acids or *de novo* synthesized fatty acids into protumorigenic signaling lipids. Signaling lipids derived from other cell types or from the cancer cell itself can then signal onto the cancer cell through paracrine or autocrine interactions. Studies have shown that aggressive cancer cells upregulate MAGL to generate fatty acids to be incorporated in oncogenic signaling lipids that drive cancer pathogenicity. However, the function of MAGL can be supplanted also by exogenous fatty acid sources that arise from high-fat diets[28]. The enzymes that synthesize or break down these signaling lipids are also often times dysregulated in cancer to promote their signaling. There is a wide range of lipid signaling molecules that have the capacity to trigger oncogenic responses, including proliferation, motility, invasiveness, tumor

growth, immunological responses, and metastasis. Imbalances in these lipid signaling pathways can fuel various aspects of cancer[35].

LPA

Lysophosphatidic acid (LPA) is a bioactive phospholipid that stimulates cell proliferation, migration, and survival by acting on G-protein coupled receptors[36]. LPA and LPA receptors are highly expressed in multiple cancer lines including ovarian[37], breast[38], and colon[39]. Interestingly, autotaxin (ATX), the primary enzyme producing LPA, is upregulated in highly aggressive metastatic breast cancer[38], indicating that LPA is a key contributor to the aggressive phenotypes of cancer.

LPA functions by activating G-protein coupled receptors, which can feed into multiple effector systems. LPA activates G_q, which stimulates the effector molecule phospholipase C, thereby generating multiple second messengers leading to activation of protein kinase C[40]. The LPA-dependent activation of PKC mediates the activation of the β-catenin pathway, leading to its cell proliferative effects in colon cancer cells[39]. LPA also activates G_i, leading to inhibition of adenylyl cyclase and therefore inhibition of cAMP accumulation. G_i also stimulates the mitogenic Ras-MAPK cascade and also the PI3K pathway, contributing to cell proliferation and migration[41–43]. LPA has also been shown to mediate cell proliferation, invasion, and migration in human breast cancer through activation of G_i protein, which activates the ERK 1/ERK2 pathway[44].

Debio-0719, a specific inhibitor of the LPA receptor 1, suppressed development of metastasis from the breast to the liver in the 4T1 breast cancer model[45]. Pharmacological or genetic blockade of MAGL lowers LPA levels indirectly through lowering the levels of fatty acids required for acylation of glycerol-3-phosphate through the *de novo* LPA synthesis pathway, leading to impaired cancer cell migration, invasion, and tumor growth[28]. Furthermore, knockdown of β-catenin by RNAi abolished LPA induced proliferation in colon cancer cells[39], suggesting a critical role for LPA in the initiation and progression of cancer.

Prostaglandins

Prostaglandins play a role in regulating the migratory and invasive behavior of cells during development and progression of cancer. Many human cancers exhibit high prostaglandin levels due to upregulation of cyclooxygenase-2 (COX-2) and prostaglandin E2 synthase-1 (PGE2-1), key enzymes in eicosanoid biosynthesis. Prostaglandins are derived from the 20-carbon chain fatty acid, arachidonic acid. COX-2 is highly expressed in metastatic breast cancer[46] and knocking out COX-2 in mice reduced mammary tumorigenesis and angiogenesis[47]. High COX-2 and PGE2 levels have been implicated in the loss of e-cadherin, and subsequently, cell migration as cells become more migratory during epithelial-to-mesenchymal transition (EMT)[48]. The expression of COX2, along with the epidermal growth factor receptor ligand epiregulin and the matrix metalloproteinases 1 and 2, can collectively facilitate mammary tumor metastasis into the lungs by the assembly of new tumor blood vessels and the release of tumor cells into circulation[49]. In mice with orthotopically implanted mammary tumors, pharmacological intervention with anti-EGFR antibody, metalloproteinase inhibitor, and

a COX2 inhibitor showed reduced rates of primary tumor growth[49]. In addition, overexpression of COX-2 in transgenic mice induced increases in microvessel density and tumor growth, suggesting the role of prostaglandins in the upregulation of angiogenic factors[50]. Furthermore, prostaglandin E2 promotes colon cancer growth through the G-protein coupled receptor, EP2, by signaling the activation of PI3K and Akt, which subsequently inactivates glycogen synthase kinase and activates the β-catenin signaling pathway[51].

The hydrolytic pathways that release the arachidonic acid from complex phospho- or neutral-lipid stores to generate prostaglandins have also been implicated in cancer progression. Phospholipase A2 (PLA2) is an enzyme that releases fatty acids from phospholipids, generating arachidonic acid and lysophospholipids[52]. Mice deficient for cytosolic phospholipase A2 are protected against the development of lung tumors, suggesting that PLA2 plays a key role in tumorigenesis by altering cytokine production[53]. MAGL blockade also leads to reduced prostaglandins by reducing the arachidonic acid precursor pool required for generating prostaglandins, leading to impaired cancer cell pathogenicity[28]. These mechanisms suggest a profound role for prostaglandins in promoting cancer development and growth.

Sphingosine-1-phosphate

Sphingolipids play an important role in modulating growth and survival. Sphingosine-1-phosphate (S1P) is a biologically active lipid that plays a role in regulating growth, survival, and migration. S1P is generated by the conversion of ceramide to sphingosine by the enzyme ceramidase, which is subsequently catalyzed by sphingosine kinase-1 (SK-1) to S1P[54]. High expressions of SK-1 and S1P have been implicated in various types of cancers, including ovarian[55], gastric[56], and colon[57] cancers. SK-1 plays a critical role in determining the balance between pro-apoptotic ceramide and pro-survival S1P. Increased SK-1 expression and subsequently S1P levels reduce sensitivity to ceramide-mediated apoptosis and overexpression of pro-survival protein Bcl-2 in human melanoma cells[58]. Overexpression of SK-1 also activates the proliferative and anti-apoptotic PI3K/Akt pathways[59]. In addition, SK-1 promotes tumor progression in colon cancer by regulation of the focal adhesion kinase pathway, which stimulates cell motility, and thus cell invasion and migration[60]. Accordingly, S1P stimulates migration and invasion in OVCAR3 ovarian cancer cells[55]. Furthermore, S1P lyase, which degrades S1P, has been shown to be downregulated in colon cancer and S1P expression promotes apoptosis[61]. Taken together, the upregulation of SK-1, which generates S1P, stimulates proliferative pathways, contributing to the growth and survival of cancers.

PAF

Platelet-activating factor (PAF) is a proinflammatory lipid signaling molecule that can be generated by the remodeling of phosphatidylcholine, a membrane lipid, to PAF by the action of lysophosphatidylcholine acyltransferase (LPCAT)[62]. PAF activity has been implicated in several cancers, including thyroid[63] and breast[64] cancers. PAF promotes proliferation, migration, and angiogenesis in human breast cancer cells[64]. One mechanism for the tumorigenic properties of PAF is through the overexpression of

cAMP-response element binding protein (CREB). PAF has been shown to activate CREB, which modulates gene expression in response to cAMP and cell stimulation with growth factors. Addition of PAF to melanoma cells stimulates CRE-dependent transcription and metastasis[65]. Taken together, PAF contributes to the onset and development of tumors through inducing angiogenesis and metastasis.

Phosphoinositides

Phosphatidylinositols can be reversibly phosphorylated at three distinct positions on the inositol headgroup, generating unique phosphoinositides that have diverse roles in signaling[35]. Phosphoinositides signal through cytosolic effector proteins to activate downstream signaling molecules. The plasma membrane localized phosphatidylinositol-4,5-bisphopshate (PtdIns(4,5)P2) serves as the substrate for two phosphoinositide-dependent signaling events. Cleavage of PtdIns(4,5)P2 by phospholipase C generates two second messengers, membrane-bound diacylglycerol (DAG) and the soluble inositol-1,4,5- trisphosphate (IP3)[35]. In addition, PtdIns(4,5)P2 can alternatively be converted to phosphatidylinositol-3,4,5-trisphosphate (PtdIns(3,4,5) P3) by phosphoinositide 3-kinase (PI3K)[35]. PtdIns(3,4,5)P3 is another second messenger involved in cell growth signaling and elevated levels have been implicated in cancer[66]. PI3K, the enzyme that generates PtdIns(3,4,5)P3, plays a key regulatory function in cell survival, proliferation, migration, and apoptosis[67]. PI3K has been shown to play a mitogenic and anti-apoptotic effect in endometrial cancer[68]. Furthermore, inhibition of the enzyme blocks growth and promotes apoptosis in small-cell lung cancers[69]. Altogether, phosphoinositides have been implicated to play a profound role in the promotion of tumorigenesis.

Inflammation

In addition to simply storing excess fat, the state of obesity induces a low-grade, chronic, metabolically-linked, inflammatory state, different from traditional inflammation, called metaflammation[70]. Although it is unclear how this inflammatory state is initiated, one proposed mechanism is through hypoxia. During weight gain and adipose tissue expansion, there are times when some cells are too distant from the organ's vasculature causing them to become poorly oxygenated and resulting in localized hypoxia[71]. This then activates hypoxia-inducible factor (HIF)-1α, which mediates the infiltration of macrophages and monocytes into the adipose tissue and finally the secretion of tumor necrosis factor-α (TNF-α)[72].

In this metaflammatory state, TNF-α has been found to be elevated in and secreted from the white adipose tissue[73]. However, other work has shown that TNF-α is actually released from macrophages and monocytes, which have increased infiltration into the adipose tissue in obese subjects[74]. While TNF-α was originally found to mediate endotoxin-induced tumor necrosis[75], it has also been implicated in cancer angiogenesis [76]and metastasis[77] as well as cell survival[78], growth, and differentiation[79,80]. One proposed mechanism of TNF-α-induced carcinogenesis is through activation of the nuclear transcription factor NF-κB by inhibiting the inhibitor of NF-κB (IκB). This pathway

has been shown to be involved in the development of lymphoma[81], pancreatic[82] and liver[83] cancers. Activated NF-κB prevents apoptosis allowing enhanced cell survival[78] and eventually inflammation-associated cancer[83]. However these effects may differ in different cell-types and experimental conditions[84]. Moreover, activation of NF-κB in cancer cells can activate cell cycling through c-Myc[78] and cyclin D1[79] leading to increased cell growth and proliferation. While both the relationship between obesity-induced inflammation and the activation of NF-κB by TNF-α are well-established, whether there are other roles of NF-κB in obesity-associated cancers remains unknown.

Interleukin-6 is another cytokine shown to be elevated in obesity and IL-6 levels are positively correlated with BMI[85]. IL-6 secretion from the white adipose tissue is induced by TNF-α[73] as well as the hypoxic conditions of the adipose[86]. Circulating IL-6 signals through the Janus kinase-signal transducer and activator of transcription-3 (JAK-STAT3) signal cascade[87]. IL-6 induced JAK-STAT3 signal transduction stimulates cell proliferation, differentiation[88] and metastasis[89]. In animal models lacking endogenous IL-6, the effect of obesity on tumorigenesis was not seen[90]. IL-6 mediated cell proliferation has been proposed to act through the mitogen-activated protein kinase (MAPK) pathway. Upon inhibition of MAPK, there was no proliferation in the presence of IL-6[91] indicating the integral role of IL-6 in cell proliferation in inflammation.

In addition to TNF-α and IL-6, there are other cytokines produced during the obesity-induced inflammatory state such as plasminogen activator inhibitor-1 (PAI-1). PAI-1 inhibits plasminogen activators such as urokinase and tissue plasminogen activator. These plasminogen activators convert plasminogen, a zymogen, to the active enzyme, plasmin. Plasmin is a serine protease, which breaks down the extracellular matrix, a critical step in cancer invasion and metastasis[92]. After the extracellular matrix is broken down and as the cancer becomes more aggressive, PAI-1 is upregulated to inhibit the aberrant activity of plasmin. Therefore, elevated PAI-1 levels are observed in subjects with poor cancer prognoses, (rates of relapse, death, etc.)[93]. PAI-1 has also been shown to inhibit cell-adhesion to vitronectin and promote migration from vitronectin to fibronectin, where it has a stimulatory effect on vascularization, thus promoting angiogenesis[94]. Moreover, the absence of PAI-1 prevents invasion and tumor vascularization, both of which can be rescued upon injection of an adenoviral vector expressing PAI-1[95]. These inflammatory response data indicate the multi-faceted importance of elevated cytokine levels in cancer malignancy, their measured levels as potential cancer malignancy biomarkers, and their inhibition as a novel cancer or obesity induced cancer drug target.

Some of these inflammatory pathways stimulated as a result of obesity intersect with other seemingly unrelated pathways altered in obesity. This interplay may lead to a synergistic effect of multiple mechanisms through which obesity drives cancer. For example, TNF-α overexpression in white adipose tissue has also been shown to play an important role in mediating insulin resistance in obesity[96] and a lack of TNF-α function results in improved insulin sensitivity in mice[97].

Insulin Signaling

Obesity is associated with an increased risk of developing insulin resistance. Insulin resistance is a major metabolic abnormality in most patients with type 2 diabetes characterized by elevated levels of circulating insulin[98]. Insulin resistance develops with the accumulation of fatty acid metabolites within insulin responsive tissues. Besides the overall increase in adiposity, distribution of body fat is a critical determinant of insulin sensitivity. Lean individuals with a more peripheral distribution of fat are more insulin sensitive than lean individuals who have their fat distributed predominantly centrally in the abdominal and chest areas[99–101]. Insulin resistance is a pathological condition characterized by a decrease in the efficiency of insulin signaling for blood sugar regulation. A recent meta-analysis of observational studies has revealed that insulin resistance is a significant risk factor for endometrial cancer[102]. Furthermore, cancer patients with preexisting type 2 diabetes have a worse cancer prognosis than matched patients without diabetes[103,104]. In addition, patients with HER2-positive breast cancer with expression of the IGF-1 receptor are more likely to be resistant to the preoperative chemotherapeutic drugs, trastuzumab and vinorelbine, compared to matched patients without expression of the IGF-1 receptor[105]. These data suggest that insulin resistance may promote a poorer response to cancer treatment or a more aggressive cancer phenotype in patients with preexisting diabetes. The dysregulation of insulin signaling is a major contributor to the increased risk of cancer associated with obesity.

In the obese state, characterized by insulin resistance, tissues are exposed to elevated levels of insulin and insulin signaling. In fed rats, acute elevation of insulin stimulates lipid synthesis and acetyl-CoA carboxylase activity in liver and adipose tissues[106]. Similarly, insulin also stimulates fatty acid synthesis in human breast cancer cells[107]. In addition, many groups have demonstrated the proliferative effects of elevated insulin. Insulin promotes proliferation in the human breast cancer line MCF-7 by facilitating the transit of cells through G1[108]. More recently, insulin has been shown to induce proliferation in hepatocellular carcinoma cells by upregulating AKR1B10, a tumor marker that plays a critical role in tumor development and progression by promoting lipogenesis[109]. Furthermore, Wang *et al*. recently showed that insulin has mitogenic and anti-apoptotic effects on endometrial cancer[68].

In addition to insulin, insulin-like growth factors, IGF-1 and IGF-2, also play a role in insulin signaling. IGF-1 and IGF-2 are hormones that are primarily produced in the liver and share sequence homology with insulin[110]. Hyperinsulinemia has been shown to increase production of IGF-1 in the liver[111]. IGF-1 and IGF-2 bind to IGF receptors, which can heterodimerize with insulin receptors. Activation of the receptors results in phosphorylation of IRS proteins, which activates the oncogenic Ras-MAPK and PI3K-Akt pathways[112,113]. The PI3K/Akt signaling pathway is frequently activated in human cancers where it induces cell proliferation[114]. One downstream effector of Akt is mTOR, which promotes protein translation and cancer growth[115]. Furthermore, tumors with constitutive activation of the PI3K pathway are insensitive to dietary restrictions, which can normally delay the incidence and decrease growth of various types of tumors by reducing the levels of circulating insulin and IGF-1, suggesting a link between obesity

and cancer[116]. IGF-1 has also been shown to mediate PTEN suppression and enhances cell invasion and proliferation via activation of the PI3K/Akt signaling pathway in pancreatic cancer cells[117]. Thus, the effect of obesity on the elevated levels of IGFs plays a crucial role in determining the proliferative effects of the oncogenic signaling pathways on cancer growth.

The aggressive phenotypes of various types of cancers have been linked to the IGF family. Increased expression of IGF-1, IGF-2, and/ or IGF-1R have been shown in gliobaslatomas, neuroblastomas, meningiomas[118], medulloblastomas[119], breast cancer[120], and prostate cancer[121]. Several groups have documented the role of the IGF family in cancer metastasis as well. Barozzi *et al*.[122] found that the overexpression of IGF-2 was predictive of liver metastasis. Hakam *et al*.[123] also showed an increase in the expression of IGF-1R during progression from colonic adenomas toward primary colorectal adenocarcinomas and metastases. The combined effects of insulin and the insulin-like growth factors on cell proliferation and metastasis may increase the risk for cancer in the hyperinsulinemic state that is associated with obesity. Somewhat controversially, one cross-sectional study did find a negative correlation between IGF-1 levels and both insulin resistance and BMI[124]. These results, however, only consider total IGF-1, not the relative amounts of bound and free IGF-1. Another study[125] found that in obesity total IGF-1 is unchanged compared to normal weight control. However, free IGF-1 is significantly increased and IGF binding proteins reduced. The ratio of free to bound IGF-1 may be an important factor in IGF-1-driven carcinogenesis, and this change may be induced by perturbations of the IGF-1 production and signaling pathway as a result of chronic hyperinsulinemia.

In accordance with the correlative studies, transgenic expression of IGF-1, IGF-2, or IGF-1R in mice drives development of various cancers. The transgenic overexpression of IGF-1 in mice enhances development of breast cancer[126], prostate cancer[127], and skin cancer[128]. The transgenic overexpression of IGF-2 drives development of lung cancer[129] and breast cancer[130]. Overexpression of IGF-1 receptor drives development of salivary and mammary adenocarcinomas[131] and pancreatic cancer[132]. These transgenic overexpression studies suggest that increased signaling through the IGF-1R pathway can drive cancer development, even in the presence of physiological levels of insulin.

The role of the IGF system in driving tumor development and progression in the obese state has also been explored in genetic models of obese mice with liver-specific deletion of IGF-1. IGF-1 deficiency in the mice abolished the obesity-associated enhancement of subcutaneous tumor growth where tumors in the IGF-1 deficient mice were smaller than tumors in the control mice. Furthermore, IGF-1 deficiency in the liver showed a reduction of liver metastases of a colorectal cancer cell line that was injected into the venous circulation[133].

Adipokines

Leptin

In addition to its fat-storing capacity, adipose tissue is the largest endocrine organ, secreting adipokines. Adipokines are adipocyte-derived hormones that play a role in maintaining energy homeostasis. Leptin, one such adipokine, is a central mediator that regulates appetite and energy homeostasis. By secreting leptin from adipocytes, the change in leptin level communicates body energy status to the brain, which responds by activating the leptin receptor and adjusting food intake[134]. Several groups have shown an overexpression of leptin receptors in various cancers, including cancers of the breast[135], prostate, and colon[136].

Obesity can lead to alterations in leptin regulation. Chronic overexpression of leptin induces leptin resistance, resulting in increased circulating leptin, similar to the increased insulin levels seen in insulin resistance that is associated with increased adiposity[137,138]. The close association between adiposity and leptin levels may suggest a role for this neuroendocrine hormone in the increased incidence of cancer in obesity. Elevated circulating leptin has been shown to increase the risk of prostate[139], breast[140], colon[141], thyroid[142], and ovarian[143] cancer.

Elevated leptin in cancer has been suggested to have several pro-tumorigenic effects. Leptin has been shown to have mitogenic action in cancers of the breast[144], colon[141], and endometrium[145] and have mitogenic and anti-apoptotic effects in cancers of the ovarian[143] and prostate[139]. Increases in cell migration have also been shown by elevated circulating leptin in thyroid cancer[142] and endometrial cancer[145].

Several mechanisms have been explored by which leptin contributes to tumor development and progression. Leptin signals through a transmembrane receptor (LRb) that contains intracellular tyrosine residues that become phosphorylated to mediate downstream LRb signaling, which controls STAT3 and ERK activation[146]. STAT3 signaling is required for proper leptin regulation of energy balance[147]. Leptin induces STAT3 phosphorylation in the human breast cancer line, MCF7, and blocking phosphorylation with the specific inhibitor AG490 abolished leptin-induced proliferation[144]. Furthermore, leptin increases HER2 protein levels through a STAT3 mediated upregulation of Hsp90 in breast cancer cells. Inhibition of the STAT3 signaling cascade by AG490 abrogated leptin induced HER2 expression[148]. In gastrointestinal epithelial cell specific knockout of SOCS3, leptin production was enhanced and activated STAT3 signaling to increase development of gastric tumors in mice. Administration of an anti-leptin antibody to the knockout mice reduced hyperplasia of gastric mucosa, the initiation step of gastric tumor [149]. These studies suggest that enhancement of leptin receptor signaling by STAT3 contributes to tumor development and progression.

These signaling pathways stimulate leptin to have proliferative and mitogenic effects, contributing to the initiation and progression of cancers. Activation of leptin receptors leads to phosphorylation of MAPK and increased proliferation in MCF7 breast cancer

cells[150] and in HT29 colon cancer cells[151]. Treatment with leptin and inhibitors of MAPK and PI3K inhibited the proliferative effects on prostate cancer cells[139]. Chronic elevation in leptin also caused ERK1/2[152] activation in human breast cancer cells and ERK1/2 and Akt phosphorylation in human prostate cancer cells[139]. Activation of these pathways induces cell proliferation, which plays a critical role in tumor progression.

Additional *in vivo* studies support the pro-tumorigenic effects of elevated leptin levels. Mammary tumors transplanted into obese leptin receptor deficient (db/db) mice grow to eight times the volume compared to tumors in the wild-type mice, suggesting the role of obesity in increased tumor growth[153]. Surprisingly, tumors transplanted into leptin-deficient (ob/ob) mice showed a reduction of tumor outgrowth compared to wildtype or db/db mice. Residual tumors from ob/ob mice showed reduced tumor initiating activity, suggesting fewer cancer stem cells. In contrast to the obese db/db mice, the obese ob/ob mice were leptin-deficient, suggesting that leptin deficiency is sufficient to suppress obesity induced tumor growth. The reduced outgrowth and tumor burden in leptin-deficient mice indicates that leptin can promote increased tumorigenesis in an obese state[153].

Although db/db or ob/ob mice have been used to study the role of leptin in obesity-associated cancers, these leptin receptor or leptin deficient mice suffer from defective development of the ductal epithelium, resulting in models unsuitable to address mammary tumorigenesis. Park *et al*. focused on the role of peripheral leptin signaling in breast cancer progression through transgenic overexpression of the leptin receptor in neurons of db/db mice and crossing the brain-specific long form of leptin receptor transgenic mice into the background of the mouse mammary tumor model MMTV-PyMT, thus generating peripheral LEPR-B mutants[154]. The rate of tumor growth in the peripheral LEPR-B mutants was reduced by twofold compared to PyMT mice. Furthermore, the lack of peripheral leptin receptors reduced tumor progression and metastasis through ERK1/ 2 and Jak2/STAT3 mediated pathways. Under obese conditions, tumor cells exhibit high local levels of leptin, leading to an increase in LEPR-B mediated pathways, which increases tumor progression. Globally, the effects of elevated leptin in obesity can drive tumor growth and development.

Adiponectin

Adiponectin is another adipokine that is associated with cancer risk. Adiponectin is a key mediator in development and progression of several types of cancers[155] and circulating adiponectin levels are decreased in patients with diabetes and obesity-associated cancers[156].

The two classical adiponectin receptors are seven transmembrane proteins[157] that activate the downstream target AMPK. Expression of the adiponectin receptors, AdipoR1 and AdipoR2, is decreased in obesity, diminishing adiponectin sensitivity[158].

Epidemiological studies have suggested a link between circulating adiponectin levels and cancer. Adiponectin levels were inversely correlated with the risk of colorectal

cancer[159], endometrial cancer[160], esophageal cancer[161], prostate cancer[162], and breast cancer[163].

Several studies have explored the mechanisms by which adiponectin inhibits carcinogenesis. Adiponectin negatively influences growth of most obesity-related cancer types, such as prostate[164] and colon[165] cancers. A study on breast cancer also proved a negative effect of adiponectin on migration[166]. MMTV-PyVT transgenic mice with reduced adiponectin expression developed mammary tumors by downregulating PTEN and upregulating PI3K/Akt signaling[167]. Thus, the proliferative effects of reduced adiponectin may be mediated through the PI3K/Akt signaling cascade. Furthermore, binding of adiponectin to its receptors provokes activation of AMPK, a critical regulator of proliferation in response to energy status[168]. AMPK plays a role in regulation of growth arrest and apoptosis by stimulating p21 and p53[169] and is also an inhibitor of mTOR, thus suppressing cell proliferation[170]. Adiponectin has also been shown to activate PPAR-α, thus enhancing fatty acid combustion and energy consumption, leading to a decrease of triacylglycerides in the liver and skeletal muscle, reversing the accumulation of adiposity[157]. Recently, a new mechanism has been shown whereby the balance between ceramide and S1P mediates many of the effects of adiponectin. AdipoR1 and AdipoR2 enhance ceramidase activity[171]. An accumulation of ceramide promotes an array of activities related to metabolic diseases, often in direct opposition to adiponectin[172]. The activity of ceramidase converts ceramide to S1P, a potent inducer of proliferation and inhibitor of apoptosis[173]. Contrary to the proliferative effects of S1P, it has also been shown to activate AMPK[174]. Thus, ceramidase is an essential initiator of adiponectin actions by generating S1P, which activates AMPK. Although S1P has proliferative effects, it is degraded in the liver, the primary target tissue where adiponectin plays a role in insulin sensitization. Many of the effects of adiponectin are mediated by ceramidase activity and the resulting alteration of the ratio of ceramide to S1P plays a role in cell growth[175].

Although adiponectin levels have been shown to inversely correlate with the risk of several types of cancers, it is noteworthy to suggest that the protective effect of adiponectin may be specific to certain types of cancers and stage of tumor progression. A study comparing rates of tumor growth in the mouse mammary tumor model MMTV-PyMT and adiponectin-null mice showed defects in angiogenesis and reduced rates of tumor growth in adiponectin-null mice in early stages of tumorigenesis[176]. Despite the defects in angiogenesis, tumor growth in the adiponectin knockout mice persisted and developed into late stages of carcinoma, at which point the anti-angiogenic stress at early stages led to an adaptive mechanism to bypass the dependence of adiponectin driven angiogenesis. This study suggests a pro-angiogenic contribution of adiponectin toward mammary tumor growth *in vivo* in the early stages of tumorigenesis, but not in late stages[176].

Since adiponectin levels are inversely correlated with obesity[177], studies implicating a protective effect of adiponectin in tumorigenesis and the analysis of the PyMT tumor model by Landskroner-Eiger *et al*. showing a pro-angiogenic role of adiponectin at early

stage tumors indicate the complex role of adiponectin in tumorigenesis, and possibly a biphasic effect of adiponectin at early stages[176].

Overall, the above studies suggest that leptin plays a role in tumor development and progression, whereas adiponectin plays a role in tumor inhibition. In one prostate cancer model, adiponectin reduced cell proliferation and this effect was blocked by treatment with leptin[178]. Thus, leptin and adiponectin have been suggested to have opposing roles in cancer development and progression.

Conclusion

Several mechanisms have been suggested to explain the association between cancer and obesity, involving elevated lipid levels and lipid signaling, inflammatory responses, insulin resistance, and adipokines. However, it remains unclear how the convergence of these pathways drives obesity-linked cancer. Thus, whether therapeutic interventions can prevent the effect of obesity on cancer is still controversial.

One potential therapeutic intervention for patients with obesity and type 2 diabetes is to take insulin, drugs that increase insulin secretion like sulphonylureas, or insulin-sensitizing drugs, such as metformin or thiazolidinediones (TZDs). Data suggest that patients who take insulin or drugs that increase insulin secretion have a higher risk of cancer than patients taking insulin-sensitizing drugs[179,180]. In addition, patients taking insulin or insulin secreting drugs have a worse cancer outcome than those taking insulin-sensitizing drugs[181,182]. Epidemiological data also show that taking metformin or TZDs may be associated with lower cancer incidence, possibly due to a reduction in circulating insulin levels[183]. Although not all data sets have shown this association, the association between high circulating insulin levels and cancer risk is evident.

Another potential therapeutic implication is through lowering inflammation as a strategy for chemoprevention. Epidemiological data showed that in patients with higher BMI, aspirin is more effective in preventing colorectal cancers[184], possibly by reducing circulating cytokines. Although this effect was not seen at lower doses[184], there seems to be a therapeutic potential in modulating inflammation. Although the effectiveness of therapeutic interventions is controversial, the growing incidence of obesity suggests that lifestyle changes and therapeutics may reduce or prevent adiposity that could additionally reduce the incidence and mortality from cancer.

Although it remains unclear how obesity contributes to cancer, we have highlighted several mechanisms that have been put forth as evidence for this link. In chapter two to follow, we propose an additional mechanism describing the role of exogenous fatty acids in cancer to further couple the role of lipids to cancer.

Figure

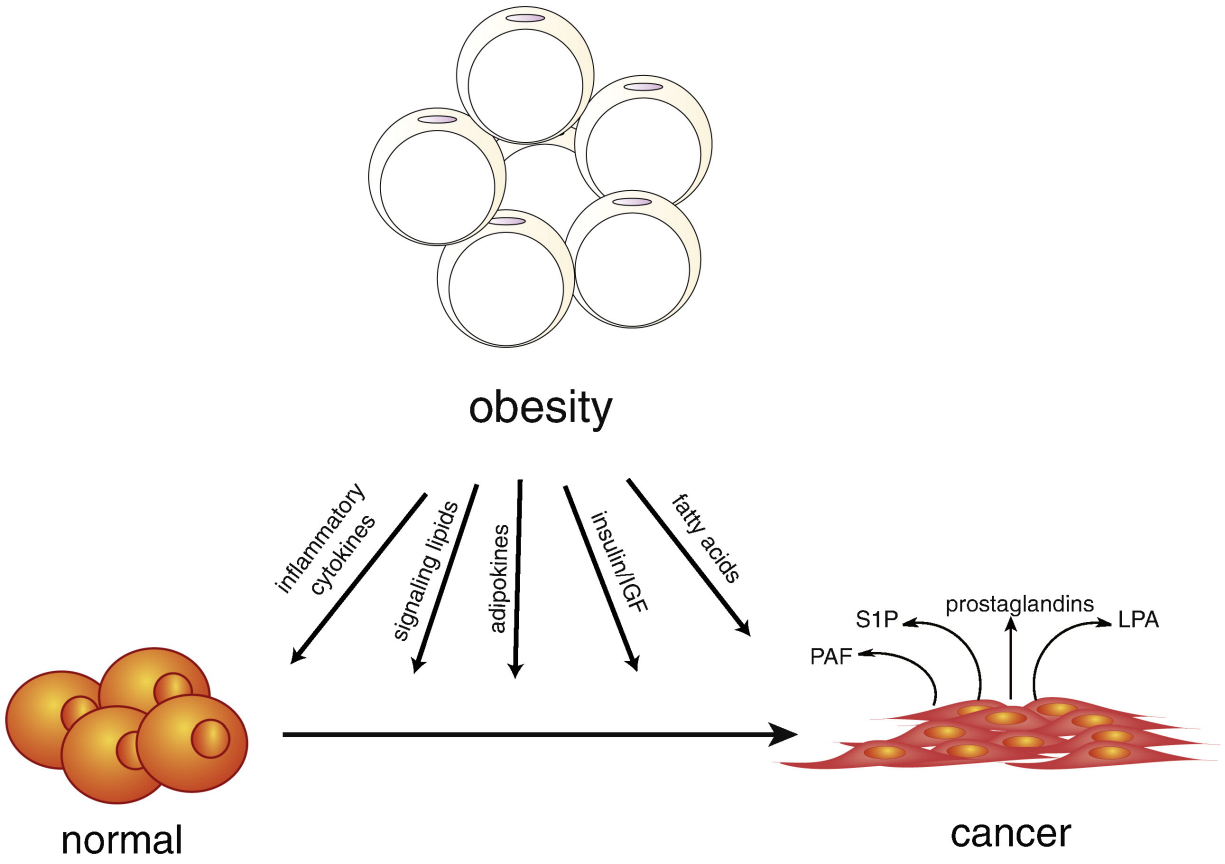

Figure 1. **Obesity-Related Mechanisms Underlying Cancer**
Cancer cells have heightened *de novo* lipogenesis through elevated fatty acid synthase (FASN) and both obesity or cancer cell-derived lipolytic enzymes generate free fatty acids to the tumor to provide structural and oncogenic lipid signaling molecules such as platelet activating factor (PAF), sphingosine-1-phosphate (S1P), lysophosphatidic acid (LPA), and prostaglandins. Obesity also causes a low-grade inflammation and the release of inflammatory cytokines. Obesity can also lead to type II diabetes and hyperinsulinemia and insulin signaling which can fuel cancer. Furthermore, obesity leads to dysregulation in adipokines including elevated leptin and reduced adiponectin levels, which can collectively stimulate tumor growth.

CHAPTER TWO

Cancer Cells Incorporate and Remodel Exogenous Palmitate into Structural and Oncogenic Signaling Lipids

Introduction

Heightened *de novo* lipogenesis is a fundamental hallmark of nearly all cancers and is required for cellular transformation and cancer progression[25]. Fatty acid synthase, the enzyme responsible for *de novo* synthesis of fatty acids, is upregulated across multiple types of human tumors and blocking FASN has been shown to attenuate cell proliferation, tumorigenicity, and cancer malignancy[25]. Early studies, using radioactivity-based methods measuring bulk lipids, have shown that *de novo* synthesis of fatty acids from glucose and other carbon sources account for 93% of the total cellular lipid content in certain cancer types[185]. Cancer cells are thus thought to rely almost solely on *de novo* lipogenesis, rather than exogenous fatty acids for generation of cellular lipids[186]. In addition to lipogenic pathways that subserve cancer proliferation, we have previously shown that aggressive human cancer cells also upregulate lipolytic pathways to mobilize free fatty acids to generate oncogenic signaling lipids that in turn fuel aggressive features of cancer[28]. We found that the tumorigenic impairments conferred by inactivating a lipolytic enzyme monoacylglycerol lipase (MAGL) in cancer cells, could be rescued by exogenous fatty acids *in situ* or by high-fat diet feeding *in vivo*[28]. These results put forth the possibility that exogenous fatty acids, despite the dominant role of *de novo* fatty acid synthesis, may also play an important role in cancer pathogenesis. In this study, we investigated whether cancer cells are capable of incorporating exogenous free fatty acids (FFA) and used advanced metabolomic platforms to comprehensively understand how FFAs are remodeled within cancer cells, and whether this exogenous FFA-derived lipid metabolism is altered during cancer progression.

Isotopic Fatty Acid Tracing-Based Metabolomics Reveals that Cancer Cells Incorporate Exogenous Fatty Acids into Structural and Signaling Lipids

To understand how cancer cells incorporate exogenous lipids and whether this lipid metabolism is altered during cancer progression, we treated a panel of aggressive versus non-aggressive human cancer cells from breast, ovarian, prostate, and melanoma cancers *in situ* with nonisotopic or isotopic palmitic acid (C16:0 free fatty acid (C16:0 FFA)), 10 μM in 0.5% fatty-acid free BSA for 4 h). These aggressive human cancer cells (231MFP, SKOV3, PC3, and C8161) have been previously shown to possess heightened motility, invasiveness, and *in vivo* tumor growth rates, compared with their non-aggressive counterparts (MCF7, OVCAR3, LNCaP, and MUM2C)[9,28]. We also profiled a human breast cancer progression model consisting of: 1) MCF10A nontransformed mammary epithelial cells; 2) MCF10A cells transformed with the activated HRAS (MCF10A-T1k cells or M2 cells); 3) M2 cells transduced with the constitutively activated transcription factor TAZ S89A (M2T cells) that have been previously shown to induce epithelial-to-mesenchymal transition (EMT), poor breast cancer prognosis, and stem-cell-like features in breast cancer; and 4) M4 (or MCF10A-CA1a) cells that are malignant derivatives of M2 cells through spontaneous malignant evolution *in vivo*. These cells are highly tumorigenic, metastatic, and display increased stem-like features and an upregulation of TAZ[187]. We then extracted the lipidome of these cells and quantitatively measured isotopic incorporation into cellular lipids using a

combination of targeted SRM-based and untargeted discovery-based metabolomic profiling[188,189] to globally track the isotopic incorporation and remodeling of exogenous fatty acids into cancer cells **(Figure 2-1)**. Our SRM methods included ~ 60 representative lipid species that could potentially incorporate isotopic palmitate, including phospholipids, neutral lipids, sphingolipids, and ether lipids. Our untargeted methods collected mass spectrometry data over a large mass range (m/z 50–1200) and subsequent datasets were analyzed by the XCMS Online software[190] to integrate all detectable ions (~5000–10,000 ions), and identify significant alterations in the metabolomes. We combined both targeted and untargeted data to gain a global understanding of exogenous FFA-derived lipid metabolism in cancer cells and mapped these data onto metabolic pathway maps.

Our metabolomic profiling of isotopic palmitic acid incorporation revealed that cancer cells robustly incorporate exogenous fatty acids into cancer cells, which are in turn remodeled into acyl carnitines (AC), phospholipids such as phosphatidyl cholines (PC), lysophosphatidyl cholines (LPC), phosphatidic acids (PA), lysophosphatidic acids (LPA), phosphatidyl ethanolamines (PE), lysophosphatidyl ethanolamines (LPE), phosphatidyl inositols (PI), phosphatidyl glycerols (PG) and phosphatidyl serines (PS), neutral lipids such as triacylglycerols (TAG) and diacylglycerols (DAGs), sphingolipids such as ceramide, sphingomyelin (SM), and ceramide-1-phosphate (C1P), and ether lipids such as alkyl PCs, alkyl PEs, alkyl PIs, alkyl PGs, alkyl PSs, alkyl PIs, platelet activating factor (PAF), and lysoPAF (Fig. 2-2A–E). These incorporated lipids not only include structural lipids (e.g. PC, LPC, SM, PE, LPE, PS, PG, PI, alkyl PCs, alkyl PEs, alkyl PIs, alkyl PGs, alkyl PSs, and alkyl PIs) and lipid stores (e.g. TAGs and DAGs), but also signaling lipids such as LPA, ceramide, DAG, and C1P. Several of these signaling lipids, such as LPA, DAG, and C1P or their associated signaling pathways have been shown to promote cancer pathogenicity[35,36,191,192]. We also find that C16:0 FFA also contributes to the generation of C18:0 FFA (stearic acid) and is incorporated into several C18:0 FFA-containing lipids. As such, with our targeted methods monitoring the m/z 184 phosphocholine ms2 fragment, we acknowledge the possibility that C16:0 PAF (1-O-hexadecyl-2-acetyl-sn-glycero-3-phosphocholine) may be a combination of C16:0 PAF and C18:0 LPC (1-stearoyl-2-hydroxysn-glycero-3-phosphocholine).

Isotopic Fatty Aids are Incorporated into Oncogenic Signaling Lipids in Tumors *in vivo*

We also wanted to investigate whether fatty acids can be incorporated *in vivo* into tumor xenografts in mice. Mice bearing M4 tumors were treated with d_4-C16:0 FFA (100 mg/kg oral gavage, 4 h), and isotopic incorporation into tumor lipids was measured by mass spectrometry. Consistent with our *in situ* studies, we found that exogenous d_4-C16:0 FFA was incorporated into certain lipid species including LPC, PAF, and C1P **(Figure 2-2F)**. Our studies suggest that exogenous fatty acid-derived lipids, which include oncogenic signaling lipids PAF and C1P, are found in tumors or tumor-associated cells *in vivo*.

Fatty Acid Incorporation into Structural and Oncogenic Signaling Lipids are Heightened in Aggressive Cancer Cells

We next wanted to understand alterations in lipid metabolism that may underlie cancer progression. We therefore compared isotopic fatty acid incorporation across aggressive versus non-aggressive cancer cells from multiple cancer types, and filtered for isotopic lipid levels that were commonly altered across three out of the five aggressive cancer cells (231MFP, M4, PC3, SKOV3, and C8161) compared to their non-aggressive counterparts (MCF7, MCF10A, LNCaP, OVCAR3, and MUM2C). We intriguingly found a common signature of altered lipid metabolism shared among aggressive cancer cells in which there are lower levels of isotopically labeled ACs, and increased levels of isotopically labeled phospholipids such as PA, PS, PC, and PI, sphingolipids such as ceramide and SM, ether lipids such as alkyl PE and alkyl PC, as well as oncogenic signaling lipids PAF, LPA, and C1P **(Figures 2-2A-E, 2-3)**. While we believe that these changes are reflective of reduced or heightened fatty acid incorporation into these lipids, we note that in this comparative analysis, we cannot formally distinguish between alterations in synthetic and degradation rates of each lipid. Using the KEGG pathway database[193] as a guide, fatty acid incorporation into cellular lipids was mapped onto a pathway diagram. We find that FFA incorporation and remodeling into phospholipid, sphingolipid, and ether lipids is heightened across aggressive cancer cells indicating that aggressive cancer cells rely more heavily on exogenous FFAs for cancer cell lipids **(Figure 2-4)**.

Conclusion

Taken together, our results reveal that cancer cells incorporate and utilize exogenous fatty acids not only for generation of cellular membranes for cell division, but also for synthesis of signaling lipids, such as C1P, PAF, DAG, and LPA, that have been previously shown to fuel cancer cell pathogenicity[35,36,191,192]. While recent studies have shown that carnitine palmitoyltransferase (CPT)1A or CPT1C activity promotes cell survival, tumor growth, or cellular motility in certain types of cancer cells and that blocking CPT may be a novel cancer therapeutic strategy[194–196], our data would suggest that CPT and fatty acid oxidation pathways are attenuated during cancer progression to shunt fatty acids from β-oxidation pathways (i.e. carnitine palmitoyltransferase (CPT)-mediated AC production) to generate more structural and oncogenic lipids. These results are reinforced by our previous genomic profiling efforts showing that the aggressive cancer cells used in this study possess lower levels of CPT expression compared to their non-aggressive counterparts **(Figure 2-5)**[9]. Nonetheless, blocking CPT may be an attractive therapeutic strategy for combatting less aggressive or low-grade tumors.

Of particular interest are the exogenous fatty acids that are incorporated significantly more into the signaling lipids C1P, PAF, and LPA across several types of aggressive human cancer cells compared with their less aggressive counterparts. C1P is formed by

ceramide kinase and has been shown to oppose the apoptotic effects of ceramide and promote cell proliferation and survival through activating intracellular signaling pathways such as MEK, ERK, PI3K/AKT, and JNK, activate inflammatory responses by activating cytosolic phospholipase A2 for generating pro-inflammatory prostaglandins, and stimulate cell migration through stimulating a yet unknown extracellular G_i-coupled receptor[191]. PAF, an inflammatory lipid that acts through PAF receptors and causes inflammation and platelet aggregation, has also been shown to be produced by melanoma cancer cells and promote invasiveness and metastasis through stimulating cancer cell PAF receptors in an autocrine mechanism[65,197]. LPA is a potent oncogenic signaling lipid that acts through stimulating LPA receptors leading to activation of multiple downstream effector pathways including phospholipase C, PI3K-AKT, RAS-ERK, and RHO and RAC GTPases leading to proliferation, survival, migration, invasion, and increased endothelial permeability[36]. Increased incorporation of exogenous fatty acids into C1P, PAF, and LPA in aggressive cancer cells can thus potentially fuel cancer initiation, progression, and metastasis.

Beyond the generation of these oncogenic signaling lipids, we also show that palmitic acid incorporation into complex lipids is globally increased in aggressive cancer cells into glycerophospholipid, sphingolipid, and ether lipid pathways. While there have been many studies into the bioactive roles of glycerophospholipids and sphingolipids[35], the role of ether lipids in cancer remains relatively poorly understood, despite its established correlation with aggressive cancers[198]. It will be of future interest to understand the role of heightened ether lipid synthesis in cancer progression.

Previous studies have indirectly suggested that cancer cells utilize exogenous fatty acids for energy or membrane formation. Nieman *et al*. showed that ovarian cancer cells use lipids derived from neighboring adipocyte stores *in vitro* by co-culture of ovarian cancer cells and adipocytes[33]. Studies have also shown that adipose stromal cells transplanted into mice promote tumor growth by serving as perivascular adipocyte progenitors. Intratumoral adipocytes can also fuel tumor vascularization and cancer cell proliferation[34].

While we show here that cancer cells take up exogenous free non-esterified palmitic acid, we do not yet understand the mechanism for palmitic acid uptake. Previous studies have shown that breast cancer and sarcoma cells expressing lipoprotein lipase and CD36, involved in lipoprotein-associated triglyceride lipolysis and fatty acid transport, respectively, treated with triglyceride-rich lipoproteins led to accelerated cell proliferation[199]. These authors also found that providing lipoprotein lipase to prostate cancer cells with triglyceride-rich lipoproteins prevented the cytotoxic effects of fatty acid synthesis inhibition. The expression of fatty acid binding proteins that are involved in fatty acid uptake and transport have also been associated with poor survival in triple-negative breast cancers[200]. Intriguingly, Kamphorst *et al*. recently demonstrated that under hypoxic conditions or Ras activation, cells switch from *de novo* lipogenic pathways to scavenging of serum fatty acids esterified to lysophospholipids to fuel membrane production[201]. Interestingly, this study also shows that this phenomenon is also linked to reduced glycolytic flux to acetyl-CoA and an increased flux of glutamine to

fatty acid synthesis. While these authors were also unable to ascertain the mechanism of lysophopholipid import, they show yet another mechanism through which cancer cells take up fatty acid sources. It will also be of future interest to determine the interplay between glycolytic and glutamine metabolism and fatty acid uptake and metabolism during cancer progression.

Our results provide a potential alternate and more direct mechanism linking obesity to increased incidence of cancer deaths by directly taking in exogenous fatty acids into structural and signaling lipids that can drive cancer pathogenicity. This mechanism adds to previous studies linking obesity-induced inflammation, hyperinsulinemia and increased insulin growth factor signaling, and heightened adipokine signaling to cancer cell proliferation and malignancy[202].

In summary, we have used advanced metabolomic platforms to globally map exogenous fatty acid incorporation and metabolism into cancer cells *in situ* and *in vivo*. We find a commonly dysregulated metabolic signature of lipid metabolism that underlies aggressive human cancer cells where there is an overall increase in exogenous fatty acid incorporation that is redirected from oxidative pathways to the generation of structural and signaling glycerophospholipids, sphingolipids, and ether lipids. Targeting fatty acid uptake into cancer cells, in combination with inhibitors of key nodal lipid metabolism pathways may provide a potential alternate strategy for treating cancer.

While we have described a potential strategy for treating cancers by disrupting lipid metabolism, the metabolic pathways that drive pathogenicity in certain types of cancer, specifically breast cancer subtypes that are highly malignant and have poor prognosis, remain poorly understood. In the following chapter, we utilized a reactivity-based chemoproteomic platform to identify novel metabolic enzymes that are heightened in TNBCs, a malignant subtype of breast cancers that have a high mortality rate and no targeted therapies.

Materials and Methods

Cell culture
C8161, MUM2C, 231MFP, MCF7, SKOV3, OVCAR3, PC3, and LNCaP cells were obtained from Benjamin Cravatt at The Scripps Research Institute or from ATCC. MCF10A, M2, M2T, and M4 cells were obtained from Stefano Piccolo at the University of Padua[187]. Cells were cultured as previously described[9,28,187].

Isotopic fatty acid labeling of cancer cells and mice
Cancer cells were seeded (1.5×10^6 cells) and upon adherence, cells were serum starved and treated with d_0-palmitic acid or (7,7,8,8-d_4)-palmitic acid (10 μM in 0.5% BSA) for 4 h. Cells were then washed twice in phosphate-buffered saline (PBS) and harvested by scraping. Cells were collected on ice and centrifuged at 1000 × *g* and cell pellets were frozen at −80 °C until lipid extraction. For isotopic fatty acid labeling of mouse tumor xenografts *in vivo*, M4 cancer cells (2×10^6 cells) were subcutaneously injected into the flank of immune-deficient SCID mice and tumors were grown out to 800 mm^3. Mice were treated with vehicle or d_4-palmitic acid (100 mg/kg oral gavage in polyethylene glycol 300 (PEG300)) for 4 h. Mice were then sacrificed and tumors were removed and flash frozen.

Metabolomic Analyses
Cell and tumor lipids were extracted as previously described[28]. Briefly, cells and tumors were extracted in 2:1:1 chloroform:methanol:phosphate-buffered saline with inclusion of internal standards (10 nmoles of dodecylglycerol and 10 nmoles of pentadecanoic acid). The organic layer was collected and the remaining aqueous layer was acidified with 0.1% formic acid and re-extracted in chloroform. Organic layers were combined and dried down under a stream of nitrogen. Dried extracts were resolubilized in 120 μl of chloroform and an aliquot (10 μl) was injected onto an Agilent 6430 triple quadrupole (QQQ)-liquid chromatography-mass spectrometry (LC-MS) instrument.

Targeted mass spectrometry analysis was performed as previously described[203,204]. Briefly, single-reaction monitoring (SRM) programs were derived from nonisotopic standards and databases. SRM programs for isotopic lipids were based on the ms2 fragments and optimized collision energies of nonisotopic standards. Metabolites were quantified by integrating the area under the curve and normalized against internal standards and external standard curves.

Untargeted mass spectrometry analysis was performed by LC-MS in scanning mode collecting mass spectral data from m/z 50 to 1200. Data files were extracted as m/z data files and analyzed by XCMS Online (xcmsserver.nutr.berkeley.edu) to identify isotopic fatty acid incorporation into cellular lipids[28,190]. Structures of metabolites from untargeted analysis were identified based on database searches (METLIN[205]) and incorporation of d_4-palmitate, as well as co-elution of metabolites with standards within the same class of metabolites. Lipids were separated by reverse phase chromatography with a Luna C5 column (Phenomenex) starting with 100% 95:5 water:methanol with a gradient to 100% 60:35:5 isopropanol:methanol:water as previously described. Formic

acid (0.1%) with 50 mM ammonium formate or ammonium hydroxide (0.1%) was added for positive and negative ionization mode, respectively. Metabolites were quantified by integrating the area under the curve, normalizing to internal standards, and then calculating levels based on external standard curves with representative lipid standards from each lipid species. For those metabolites for which there was a background peak for the isotopic d_4-lipid in the d_0-C16:0 FFA-treated group, we subtracted the average of the background from both d_0- and d_4-C16:0 FFA-treated groups. For all metabolites, the isotopic d_4-lipid peak for the d_0-C16:0 FFA-treated group was less than 20% of the d_4-C16:0 FFA-treated group.

Figures

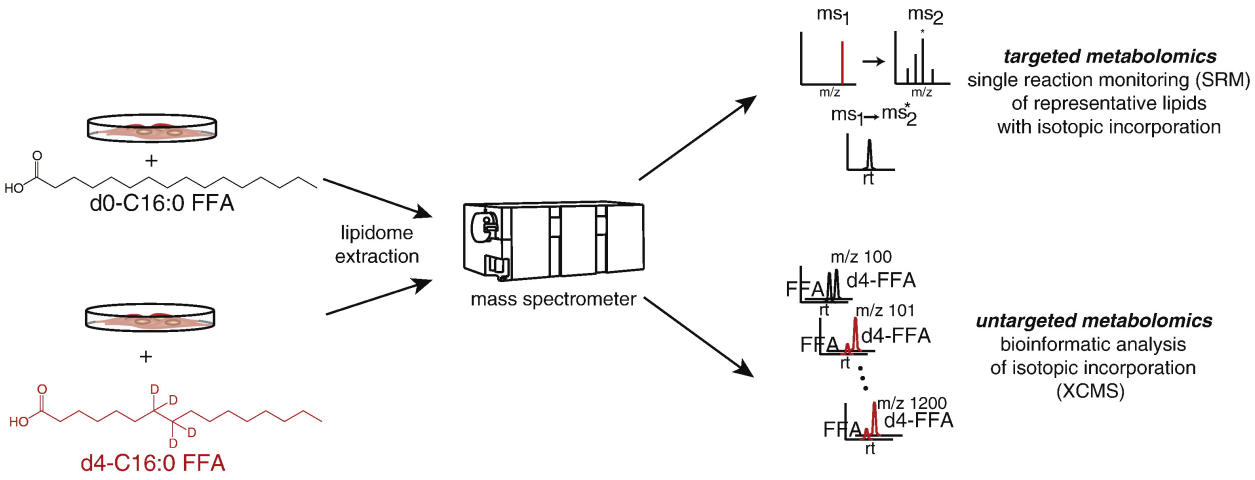

Figure 2-1. Metabolomic Mapping of Exogenously-Derived Isotopic FFA Metabolism in Cancer Cells

Cells were treated with either d_0-C16:0 FFA or d_4-C16:0 FFA for 4 h. Lipids were extracted and analyzed by LC-MS using targeted SRM-based approaches and untargeted approaches. The large datasets resulting from untargeted metabolomics were analyzed by XCMS Online to determine masses that were altered between d_0- and d_4-C16:0 FFA to identify isotopic-FFA-incorporated lipids.

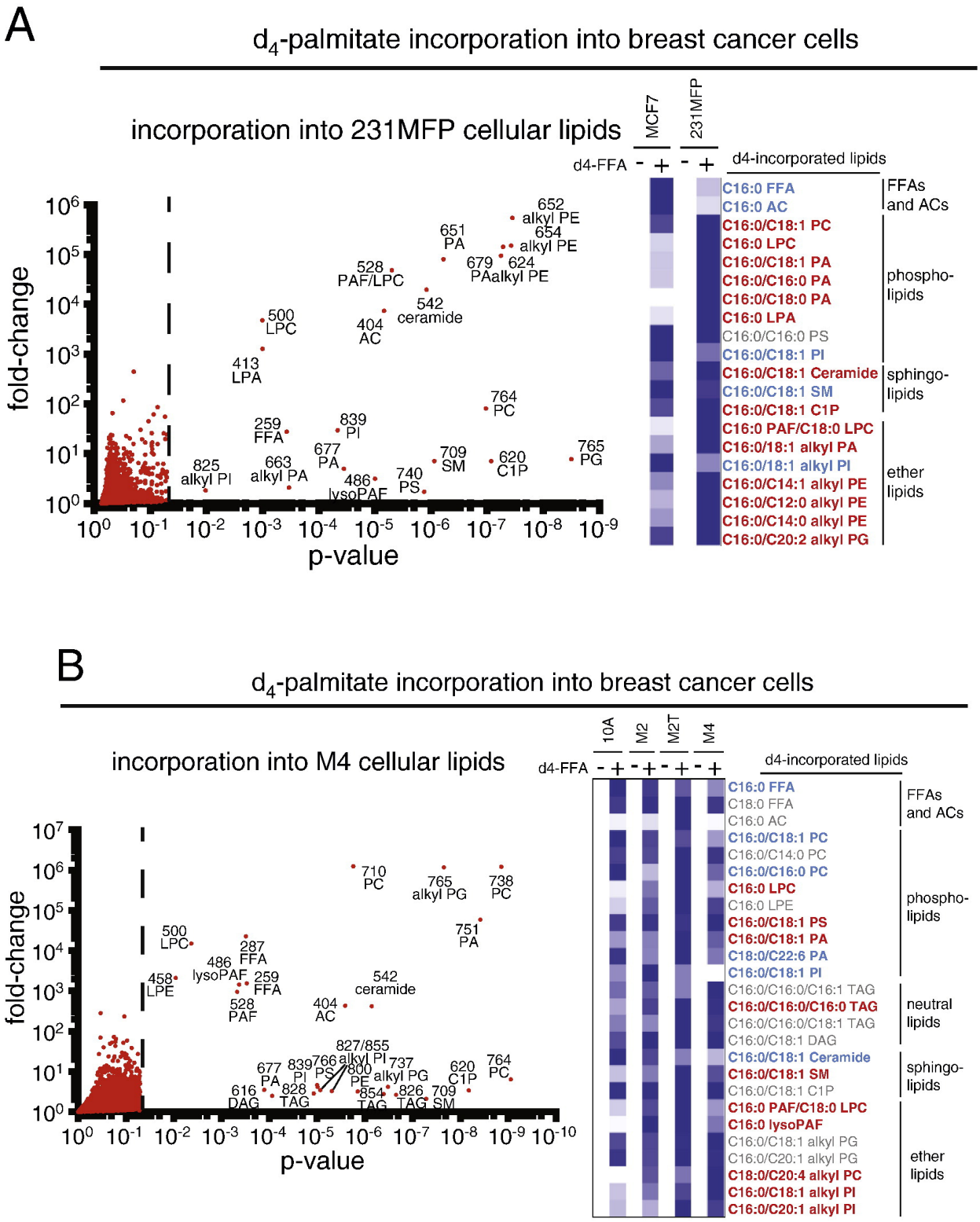
A
d4-palmitate incorporation into breast cancer cells
incorporation into 231MFP cellular lipids
fold-change
p-value
MCF7
231MFP
d4-FFA
d4-incorporated lipids
C16:0 FFA
C16:0 AC
C16:0/C18:1 PC
C16:0 LPC
C16:0/C18:1 PA
C16:0/C16:0 PA
C16:0/C18:0 PA
C16:0 LPA
C16:0/C16:0 PS
C16:0/C18:1 PI
C16:0/C18:1 Ceramide
C16:0/C18:1 SM
C16:0/C18:1 C1P
C16:0 PAF/C18:0 LPC
C16:0/18:1 alkyl PA
C16:0/18:1 alkyl PI
C16:0/C14:1 alkyl PE
C16:0/C12:0 alkyl PE
C16:0/C14:0 alkyl PE
C16:0/C20:2 alkyl PG
FFAs and ACs
phospho-lipids
sphingo-lipids
ether lipids
B
d4-palmitate incorporation into breast cancer cells
incorporation into M4 cellular lipids
fold-change
p-value
10A
M2
M2T
M4
d4-FFA
d4-incorporated lipids
C16:0 FFA
C18:0 FFA
C16:0 AC
C16:0/C18:1 PC
C16:0/C14:0 PC
C16:0/C16:0 PC
C16:0 LPC
C16:0 LPE
C16:0/C18:1 PS
C16:0/C18:1 PA
C18:0/C22:6 PA
C16:0/C18:1 PI
C16:0/C16:0/C16:1 TAG
C16:0/C16:0/C16:0 TAG
C16:0/C16:0/C18:1 TAG
C16:0/C18:1 DAG
C16:0/C18:1 Ceramide
C16:0/C18:1 SM
C16:0/C18:1 C1P
C16:0 PAF/C18:0 LPC
C16:0 lysoPAF
C16:0/C18:1 alkyl PG
C16:0/C20:1 alkyl PG
C18:0/C20:4 alkyl PC
C16:0/C18:1 alkyl PI
C16:0/C20:1 alkyl PI
FFAs and ACs
phospho-lipids
neutral lipids
sphingo-lipids
ether lipids

C

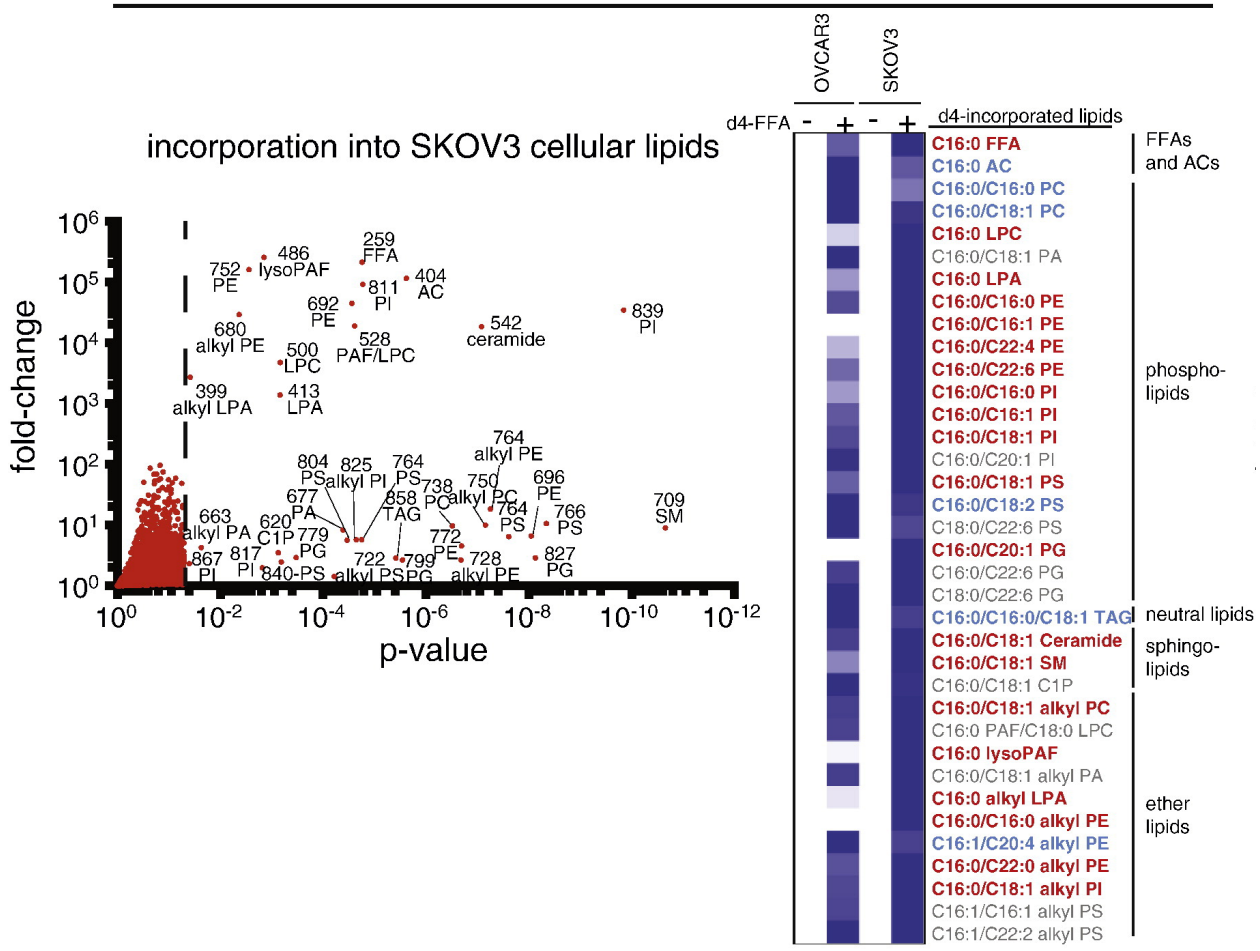
d4-palmitate incorporation into ovarian cancer cells
incorporation into SKOV3 cellular lipids
fold-change
p-value
OVCAR3
SKOV3
d4-FFA
d4-incorporated lipids
C16:0 FFA
C16:0 AC
C16:0/C16:0 PC
C16:0/C18:1 PC
C16:0 LPC
C16:0/C18:1 PA
C16:0 LPA
C16:0/C16:0 PE
C16:0/C16:1 PE
C16:0/C22:4 PE
C16:0/C22:6 PE
C16:0/C16:0 PI
C16:0/C16:1 PI
C16:0/C18:1 PI
C16:0/C20:1 PI
C16:0/C18:1 PS
C16:0/C18:2 PS
C18:0/C22:6 PS
C16:0/C20:1 PG
C16:0/C22:6 PG
C18:0/C22:6 PG
C16:0/C16:0/C18:1 TAG
C16:0/C18:1 Ceramide
C16:0/C18:1 SM
C16:0/C18:1 C1P
C16:0/C18:1 alkyl PC
C16:0 PAF/C18:0 LPC
C16:0 lysoPAF
C16:0/C18:1 alkyl PA
C16:0 alkyl LPA
C16:0/C16:0 alkyl PE
C16:1/C20:4 alkyl PE
C16:0/C22:0 alkyl PE
C16:0/C18:1 alkyl PI
C16:1/C16:1 alkyl PS
C16:1/C22:2 alkyl PS
FFAs and ACs
phospho-lipids
neutral lipids
sphingo-lipids
ether lipids

D

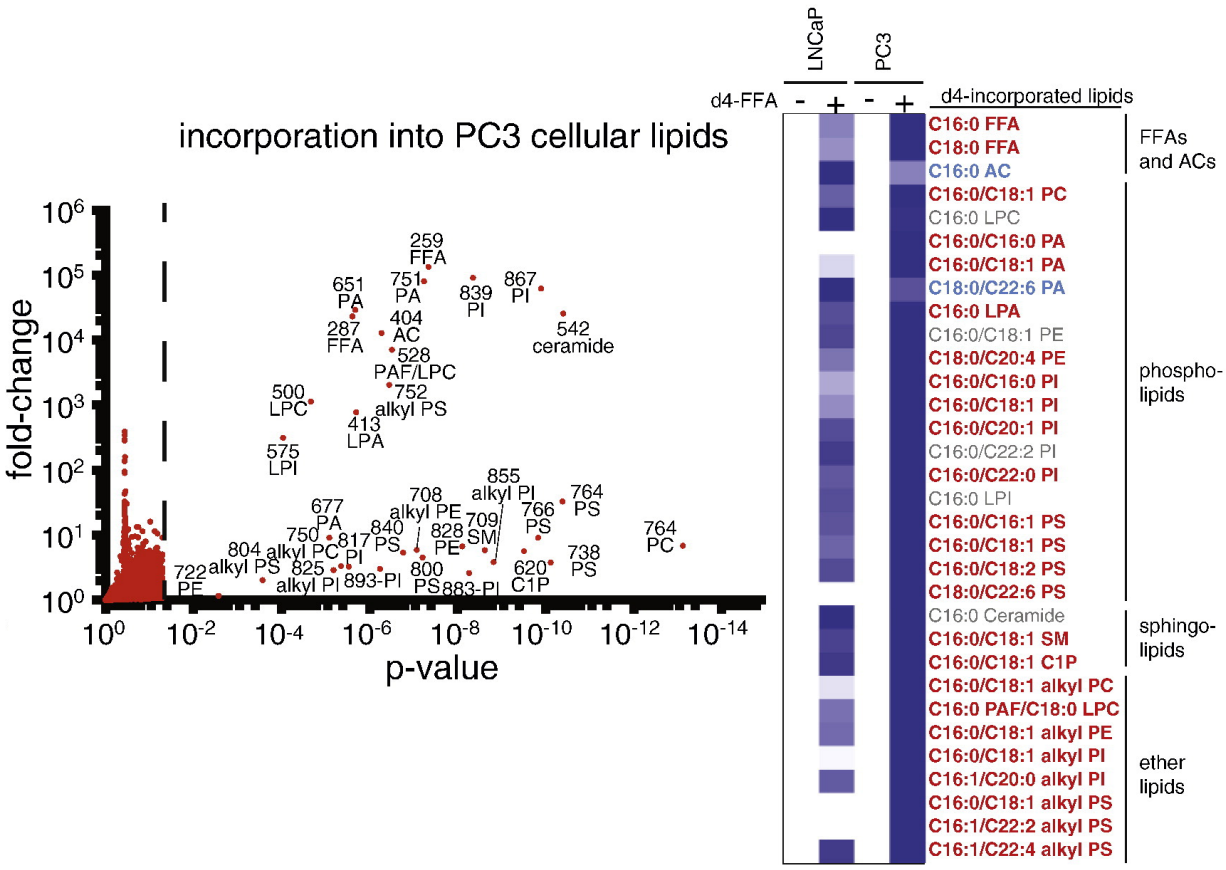
d4-palmitate incorporation into prostate cancer cells
incorporation into PC3 cellular lipids
fold-change
p-value
259 FFA
651 PA
751 PA
839 PI
867 PI
287 FFA
404 AC
542 ceramide
528 PAF/LPC
500 LPC
752 alkyl PS
413 LPA
575 LPI
855 alkyl PI
708 alkyl PE
764 PS
677 PA
766 PS
709 SM
840 PS
828 PE
764 PC
750
817 PI
804 alkyl PC
738 PS
722 PE
alkyl PS
825
620 C1P
alkyl PI
893-PI
800 PS
883-PI
LNCaP
PC3
d4-FFA
d4-incorporated lipids
C16:0 FFA
C18:0 FFA
C16:0 AC
C16:0/C18:1 PC
C16:0 LPC
C16:0/C16:0 PA
C16:0/C18:1 PA
C18:0/C22:6 PA
C16:0 LPA
C16:0/C18:1 PE
C18:0/C20:4 PE
C16:0/C16:0 PI
C16:0/C18:1 PI
C16:0/C20:1 PI
C16:0/C22:2 PI
C16:0/C22:0 PI
C16:0 LPI
C16:0/C16:1 PS
C16:0/C18:1 PS
C16:0/C18:2 PS
C18:0/C22:6 PS
C16:0 Ceramide
C16:0/C18:1 SM
C16:0/C18:1 C1P
C16:0/C18:1 alkyl PC
C16:0 PAF/C18:0 LPC
C16:0/C18:1 alkyl PE
C16:0/C18:1 alkyl PI
C16:1/C20:0 alkyl PI
C16:0/C18:1 alkyl PS
C16:1/C22:2 alkyl PS
C16:1/C22:4 alkyl PS
FFAs and ACs
phospho-lipids
sphingo-lipids
ether lipids

E

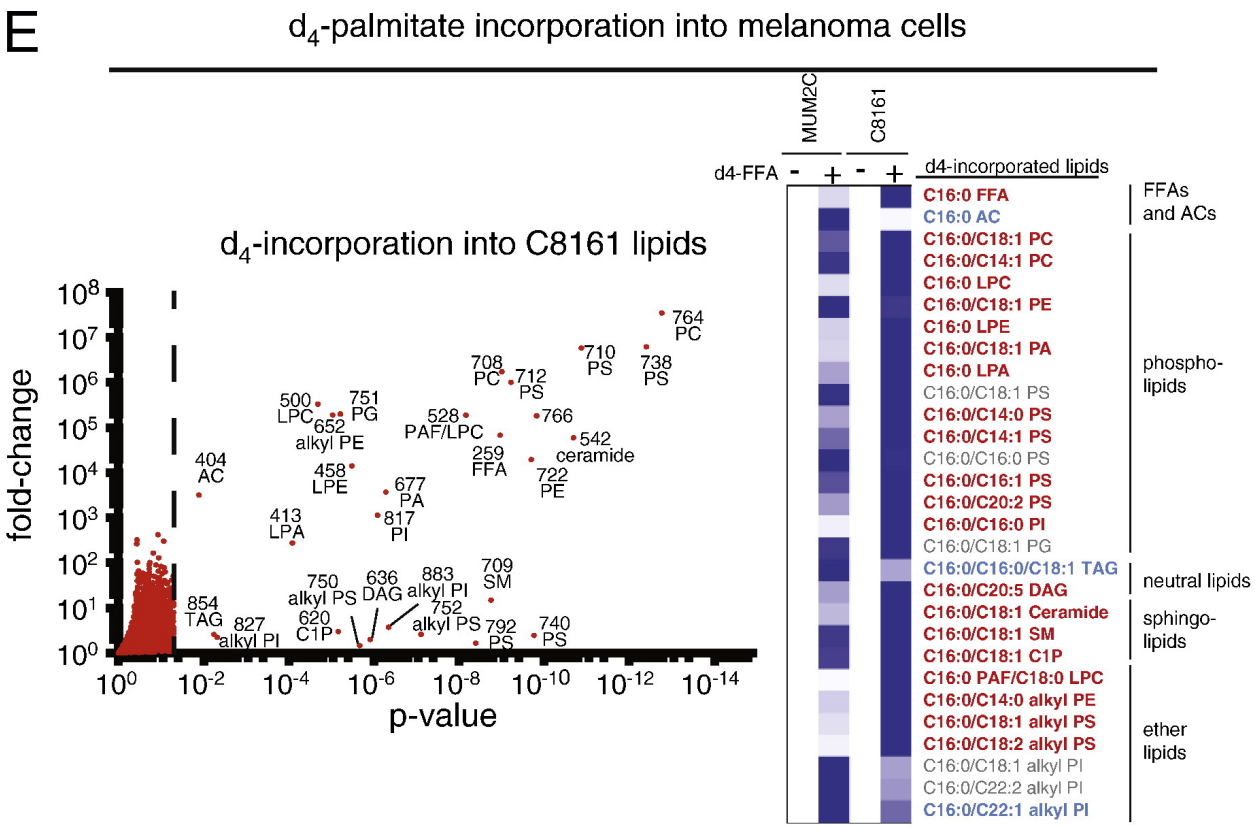
d4-palmitate incorporation into melanoma cells
d4-incorporation into C8161 lipids
fold-change
p-value
764 PC
710 PS
738 PS
708 PC
712 PS
500 LPC
751 PG
652 alkyl PE
528 PAF/LPC
766
542 ceramide
259 FFA
722 PE
404 AC
458 LPE
677 PA
413 LPA
817 PI
709 SM
750 alkyl PS
636 DAG
883 alkyl PI
752 alkyl PS
854 TAG
827 alkyl PI
620 C1P
792 PS
740 PS
MUM2C
C8161
d4-FFA - + - +
d4-incorporated lipids
C16:0 FFA
C16:0 AC
C16:0/C18:1 PC
C16:0/C14:1 PC
C16:0 LPC
C16:0/C18:1 PE
C16:0 LPE
C16:0/C18:1 PA
C16:0 LPA
C16:0/C18:1 PS
C16:0/C14:0 PS
C16:0/C14:1 PS
C16:0/C16:0 PS
C16:0/C16:1 PS
C16:0/C20:2 PS
C16:0/C16:0 PI
C16:0/C18:1 PG
C16:0/C16:0/C18:1 TAG
C16:0/C20:5 DAG
C16:0/C18:1 Ceramide
C16:0/C18:1 SM
C16:0/C18:1 C1P
C16:0 PAF/C18:0 LPC
C16:0/C14:0 alkyl PE
C16:0/C18:1 alkyl PS
C16:0/C18:2 alkyl PS
C16:0/C18:1 alkyl PI
C16:0/C22:2 alkyl PI
C16:0/C22:1 alkyl PI
FFAs and ACs
phospho-lipids
neutral lipids
sphingo-lipids
ether lipids

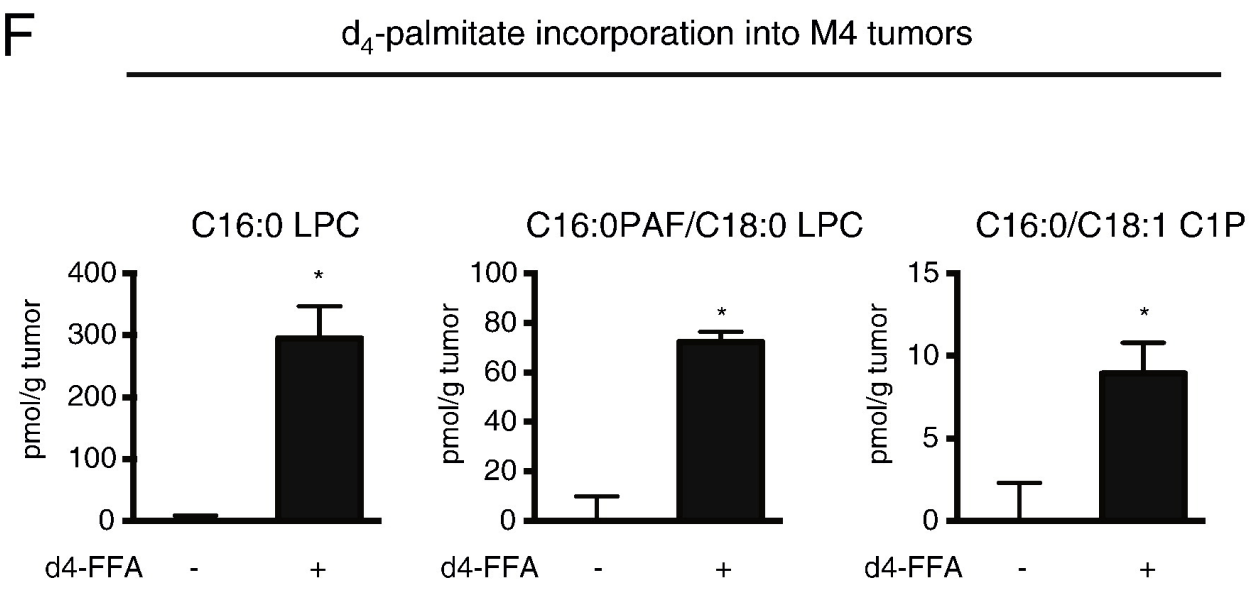

Figure 2-2. Mapping Exogenous Isotopic FFA-Derived Lipid Metabolism in Human Cancer Cells

(A–E) Shown are all ions detected in 231MFP, M4, SKOV3, PC3, or C8161 aggressive human cancer cells. For the volcano plot, points that are to the left of the dotted line ($P < 0.05$) represent ions that were not statistically altered in levels between d_0-C16:0 FFA versus d_4-C16:0 FFA-labeled cells. All points to the right of the dotted line ($P < 0.05$) represent ions that had significantly higher ion intensity in the d_4-C16:0 FFA labeled group compared to d_0-C16:0 FFA labeled group, i.e. d_4-incorporated lipids. In total, at least ~ 5000–10,000 ions were detected and analyzed between targeted and untargeted analysis comparing d_0-C16:0 FFA labeled to d_4-C16:0 FFA labeled M4, 231MFP, C8161, SKOV3, or PC3 cells. The y-axis denotes fold-change between raw integrated values of isotopically-incorporated ions by either targeted or untargeted analysis between d_0 versus d_4-C16:0 FFA-labeled samples. For the ions that exhibited no background peak corresponding to the m/z of the d_4-lipid in the d_0-C16:0 FFA-treated cells, we considered this value to be 1 to obtain a fold-change value compared to the raw integration values of d_4-C16:0 FFA-treated cells. For the ions for which there was a background peak, we obtained a fold-change value by dividing the ion intensity for the d_4-C16:0 FFA compared to d_0-C16:0 FFA groups. The heat map on the right shows relative levels of d_4-C16:0 FFA-incorporated lipids in non-aggressive (MCF7, OVCAR3, LNCaP, MUM2C) or non-transformed (MCF10A) cells compared to aggressive (231MFP, M2T, M4, SKOV3, PC3, C8161) or transformed (M2) cells. In the heat map, relative levels of each d_4-incorporated lipid metabolite are shown (darker blue shading corresponds to higher level of metabolite). The lipid designations next to the heat map are color-coded red for significantly higher, blue for significantly lower, and gray for unchanged d_4-metabolites in aggressive cancer cells (231MFP, M4, SKOV3, PC3, and C8161) compared to non-aggressive (MCF7, MCF10A, OVCAR3, LNCaP, and MUM2C, respectively) cells ($P < 0.05$).

(F) Shown are lipids species that exhibited significant d_4-C16:0 FFA incorporation *in vivo* in mice bearing a tumor xenograft from M4 cells. Mice were subcutaneously

injected with 2×10^6 M4 cells and tumors were grown out to ~ 800–1000 mm^3. Mice were treated with vehicle (polyethylene glycol 300 (PEG300)) or d_4-C16:0 FFA (100 mg/kg in PEG) by oral gavage (4 h). Tumors were harvested and lipids were extracted and analyzed by SRM-based metabolomics. For A–F, those metabolites where there was a background peak for the d_4-lipid m/z in the d_0-C16:0 FFA-treated cells, the average of the background ion intensity was subtracted from both d_0 and d_4-C16:0 FFA-treated groups. For all lipids shown here, any background peak for a d_4-lipid detected in d_0-C16:0 FFA-treated cells was assumed to either be a coeluting isobaric metabolite or natural isotopic abundance of the lipid. We have only presented here the d_4-incorporated lipids that showed > 5-fold significantly ($P < 0.05$) higher ion intensity in the d_4-C16:0 FFA-treated group compared to the d_0-C16:0 FFA-treated group. Data in (A–E) are average values of n = 4–6 biological replicates. Data in (F) are mean ± standard error of n = 4–6 biological replicates. Significance in (F) is represented as *$P < 0.05$ in d_4-C16:0 FFA-treated mice compared with vehicle-treatment.

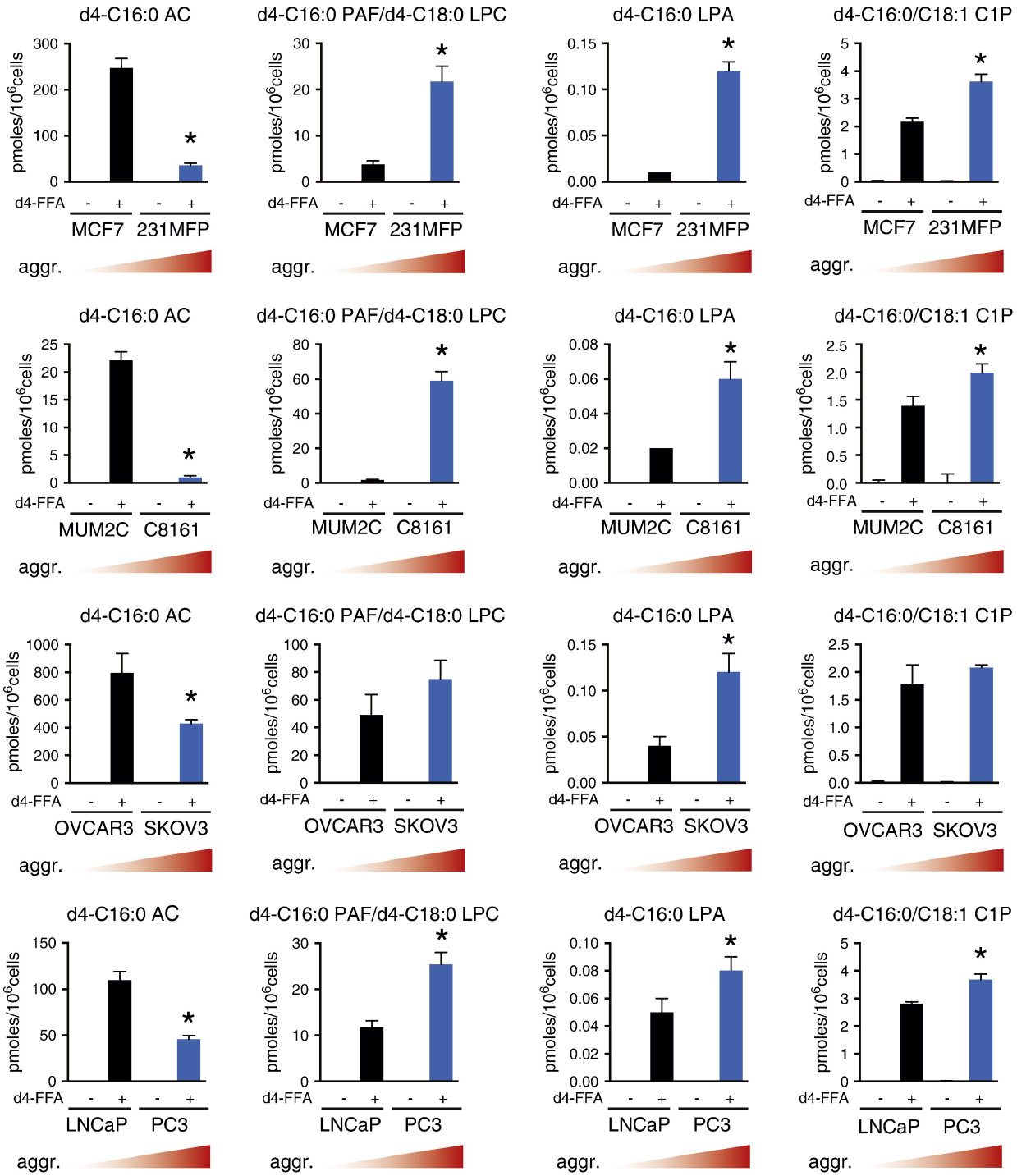

Figure 2-3. Aggressive Cancer Cells Increase Incorporation of Fatty Acids into Oncogenic Signaling Lipids and Reduce Incorporation into Oxidative Pathways
Representative lipids with significant fatty acid incorporation from Fig. 2-2 are quantitated and shown as bar graphs. In comparing d_4-C16:0 FFA incorporation into aggressive (C8161, PC3, SKOV3, and 231MFP cells) compared with non-aggressive cancer cells (MUM2C, LNCaP, OVCAR3, and MCF7 cells), we find that there is reduced

incorporation into C16:0 AC and increased incorporation into phospholipids, sphingolipids, and ether lipids, including the signaling lipids C1P, PAF/LPC, and LPA. Data are average values of n = 4–6 biological replicates and are presented as mean ± standard error. Significance is represented as *P < 0.05 comparing aggressive versus non-aggressive d_4-FFA groups.

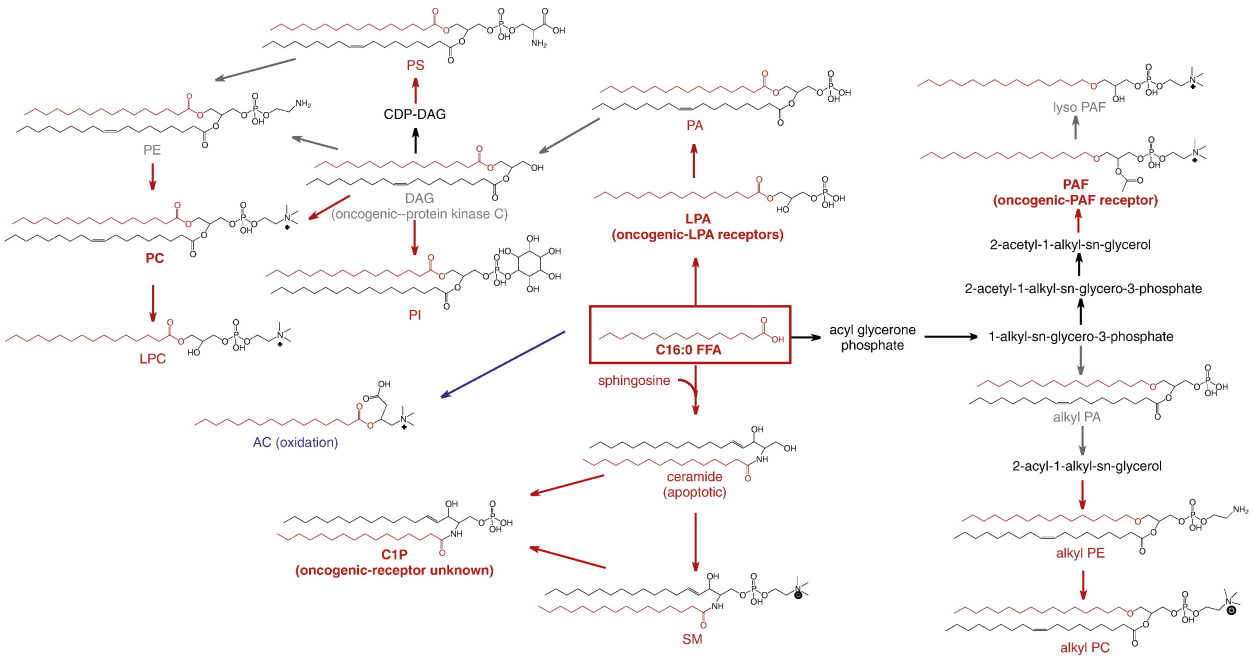

Figure 2-4. Map of Lipid Metabolism in Aggressive Cancer Cells
The data gathered from isotopic tracing of d_4-C16:0 FFA labeled cancer cells was compiled into a metabolic pathway map using the KEGG pathway database as a guide. d_4-C16:0 FFA incorporation into the lipid structures is noted in red. The color of arrows and metabolites notes increased (in red), decreased (in blue), or unchanged (in gray) levels of d_4-lipid in three out of five comparisons of aggressive (231MFP, M4, SKOV3, PC3, and C8161) versus non-aggressive (MCF7, MCF10A, OVCAR3, LNCaP, and MUM2C, respectively) cancer cells. Metabolites and arrows in black were not detected in either targeted or untargeted analysis. LPA, C1P, DAG, and PAF are oncogenic signaling lipids that act through LPA receptors, unknown receptor, protein kinase C, and PAF receptors, respectively.

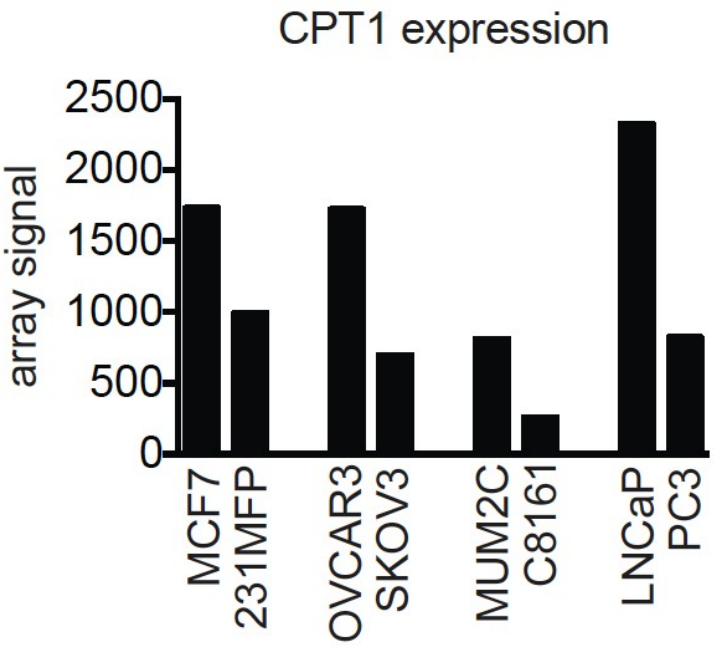

Figure 2-5. CPT1 Expression is Downregulated in Aggressive Cancer Cells
This data is derived from a microarray transcriptomic experiment derived from Nomura *et al*. 2011[9].

CHAPTER 3

GSTP1 is a Driver of Triple-Negative Breast Cancer Cell Metabolism and Pathogenicity

Introduction

Breast cancers possess fundamentally altered metabolism that drive their pathogenic features. A century ago, Otto Warburg proposed that cancer is a disease of aberrant metabolism, when he discovered that cancer cells have heightened glucose uptake and undergo aerobic glycolysis. Since then, others have identified many other biochemical alterations in cancer cells, including heightened glutamine-dependent anaplerosis and *de novo* lipid biosynthesis, which serve as metabolic platforms for breast cancer cells to generate biomass for cell division and metabolites that modulate cancer cell signaling, epigenetics, and pathogenicity[1–3]. While targeting dysregulated metabolism is a promising strategy for breast cancer treatment, the metabolic pathways that drive pathogenicity in breast cancer subtypes that are correlated with heightened malignancy and poor prognosis remain poorly understood.

Mortality from breast cancer is almost always attributed to metastatic spread of the disease to other organs, thus precluding resection as a treatment method. Unfortunately, conventional chemotherapy fails to eradicate most human cancers, including aggressive breast cancers. Studies over the past decade have uncovered certain breast cancer types and cell types that are associated with poor prognosis, such as estrogen/progesterone/HER2 receptor-negative (triple-negative) breast cancers (TNBCs) or cancer stem/precursor cells that possess self-renewing and tumor-initiating capabilities, epithelial-to-mesenchymal transition (EMT), poor prognosis, and chemotherapy resistance within breast tumors[206–208]. While eliminating these breast cancer types is critical in combatting breast cancer, there are currently few to no therapies that target this malignant population of breast cancer cells.

In this study, we used a reactivity-based chemoproteomic platform to identify metabolic enzymes that are heightened in TNBC cells or upon induction of an EMT-like programming of heightened malignancy in breast cancer cells. Through this profiling effort, we identified glutathione-*S*-transferase Pi 1 (GSTP1) as a critical metabolic driver that is heightened specifically in TNBCs to control multiple critical nodes in cancer metabolism and signaling pathways to drive breast cancer pathogenicity.

Profiling Dysregulated Metabolic Enzymes in TNBC Cells and CDH1 Knockdown Breast Cancer Cells

To identify metabolic drivers of breast cancer pathogenicity in aggressive breast cancer cell types associated with malignancy and poor prognosis, we used a reactivity-based chemical proteomic strategy to map cysteine and lysine reactivity in TNBC cells and breast cancer cells with EMT-like features **(Figure 3-1)**. Both TNBC cells and breast cancer cells that have undergone EMT have been linked to heightened aggressiveness and poor prognosis. Specifically, we wanted to (1) identify TNBC-specific metabolic enzyme targets by comparing a panel of four non-TNBC and five TNBC cell lines, and (2) identify upregulated enzyme targets in MCF7 breast cancer cells upon knockdown of CDH1, a critical mediator of EMT and cell-cell adhesion. We knocked down CDH1 in

MCF7 cells with short-hairpin (sh) oligonucleotides (shCDH1 cells) to induce an EMT-like state. These cells show upregulation of the mesenchymal marker vimentin and concordant increases in serum-free cell survival, proliferation, and migration **(Figure 3-6)**, consistent with EMT-like characteristics.

We labeled cell lysates from these two breast cancer models with previously validated lysine-reactive dichlorotriazine-alkyne or cysteine-reactive iodoacetamide-alkyne reactivity-based probes to tag proteins bearing functional lysines or cysteines, respectively, for subsequent attachment of a biotin handle by click chemistry, enrichment, and analysis by mass spectrometry (MS), using an adapted method established by Weerapana and co-workers **(Figures 3-1A and 3-1B)**[209,210]. We chose to profile cysteine and lysine reactivity in this study, since these amino acids are important mediators of enzyme activity or function through nucleophilic and redox catalysis, allosteric regulation, metal binding, and structural stabilization across a wide range of protein classes[211,212]. Upon proteomic analysis of probe-enriched protein targets, we filtered these proteins for metabolic enzyme targets that were significantly upregulated ($p < 0.01$, >5-fold) in TNBC cells or shCDH1 MCF7 cells compared with non-TNBC or shControl counterparts, respectively **(Figures 3-1C and 3-1D)**. GSTP1 was the most significantly upregulated target in TNBC cells that was also significantly heightened in shCDH1 cells, so we focused on investigating the pathogenic role of this target in breast cancer **(Figures 3-1C and 3-1D)**.

Many human cancers, including breast, lung, colon, and ovarian cancers, have been shown to express high levels of GSTP1, and its expression has been correlated with both disease progression and resistance to chemotherapeutic drugs[213]. GSTP1 inhibitors have been studied in the context of cancer for many years as adjuvant therapies with chemotherapy agents to prevent their detoxification by cancer cells, with the aim of improving chemotherapy efficacy[214,215]. Yet the majority of chemotherapeutic drugs have a relatively weak affinity for GSTP1 compared with other GST enzymes. This discrepancy between expression of GSTP1 and its correlation with the development of multidrug resistance suggests additional roles for GSTP1 on influencing metabolic and signaling pathways in cancer cells[213]. GSTP1 inhibitors have not yet been investigated for their potential as stand-alone therapies toward thwarting breast cancer. We thus focused our attention on further investigating the role of GSTP1 in driving breast cancer pathogenicity.

GSTP1 is a TNBC-Specific Target

We next investigated the expression pattern of GSTP1 in different types of breast cancer cell lines and primary human breast tumors. Interestingly, we show that GSTP1 is not expressed in any of the non-TNBC cells (MCF7, T47D, ZR751, and MDAMB-361), but is highly expressed across all of the TNBC cells (231MFP, HCC1143, HCC38, HCC70, and MDA-MB-468) (Figures 3-1E and 3-1F), shown both by dichlorotriazine-alkyne reactivity and western blotting. We also show that GSTP1 expression is significantly heightened in TNBC compared with receptor-positive primary human breast

tumors **(Figure 3-1G)**. Overall, our data indicate that GSTP1 may represent a TNBC-specific target.

Genetic or Pharmacological Inactivation of GSTP1 Impairs TNBC Pathogenicity

To investigate the role of GSTP1 in TNBC pathogenicity, we generated two knockdown lines of GSTP1 in TNBC 231MFP cells (shGSTP1-1 and shGSTP1-2) **(Figure 3-2A)**. We showed that GSTP1 knockdown impairs serum-free cell survival in 231MFP cells without affecting cell proliferation **(Figure 3-2B)**. GSTP1 knockdown also impaired *in vivo* 231MFP breast tumor xenograft growth in immune-deficient mice **(Figure 3-2C)**.

Intrigued by these results, we next tested whether pharmacological inhibition of GSTP1 with a highly selective GSTP1 inhibitor LAS17 also impaired breast cancer pathogenicity. LAS17 was recently developed as a highly potent, selective, and irreversible dichlorotriazine GSTP1 inhibitor that targets an active-site tyrosine **(Figure 3-2D)**[216]. In addition to its property as a GSTP1 inhibitor, LAS17 also bears a bioorthogonal alkyne handle, which can be coupled with copper catalyzed click chemistry[217] to append a fluorophore-azide or biotin-azide analytical handle for subsequent fluorescent or proteomics-based detection of GSTP1, respectively **(Figures 3-2D and 3-2E)**. LAS17 inhibits GSTP1 activity *in vitro* with a 50% inhibitory concentration (IC_{50}) value of 0.5 μM **(Figure 3-2F)**.

LAS17 treatment in 231MFP breast cancer cells recapitulated the serum-free cell survival impairments observed with genetic inactivation of GSTP1 **(Figure 3-2G)**. Daily administration of LAS17 (20 mg/kg intraperitoneally, once per day) significantly impaired 231MFP breast tumor xenograft growth in immune-deficient mice when treatment was initiated 2 days after subcutaneous injection of cells, and LAS17 even slowed tumor growth when initiated 16 days after tumor implantation (Figure 3-2H), with no observable toxicity and no weight change **(Figure 3-7A)**. LAS17 had no effect on serum-free survival of shControl MCF7 non-TNBC cells that do not express GSTP1, but significantly impaired the survival of shCDH1 MCF7 breast cancer cells **(Figure 3-2I)**. While GSTP1 inhibition selectively impaired survival in shCDH1 cells, LAS17 treatment in shCDH1 cells did not rescue vimentin expression or impair proliferation, indicating that GSTP1 is not a critical driver of the EMT process (data not shown). LAS17 treatment also impaired serum-free cell survival in additional TNBC lines HCC38, HCC70, and HCC1143 **(Figure 3-2J)**. We also show that GSTP1 knockdown in HCC38 cells impairs cell survival (**Figures 3-7B and 3-7C**). We thus show that pharmacological GSTP1 inactivation impairs breast cancer pathogenicity in culture and *in vivo* in a seemingly TNBC-specific manner, suggesting that GSTP1 inhibitors may be promising therapeutics for treating TNBCs.

Functional Metabolomic Profiling Reveals GSTP1 Control Over Glycolytic Metabolism, Energetics, and Macromolecular Building Blocks

We next wanted to understand the mechanisms through which GSTP1 was controlling breast cancer pathogenicity. Previous studies have shown that GSTP1 may directly affect cancer pathogenicity through protein-protein interactions with the MAPK family protein JNK, leading to JNK phosphorylation and activation[214,215]. However, GSTP1 genetic or pharmacological inactivation did not lead to JNK activation compared with treatment with the JNK activator anisomycin in 231MFP cells **(Figure 3-8A)**. We also postulated that GSTP1 could modulate glutathione levels and oxidative stress to cause cell-survival impairments. However, genetic or pharmacological inactivation of GSTP1 did not change oxidative stress levels or reduced oxidized glutathione (GSH/GSSG) ratios under both basal and menadione-induced oxidative stress conditions compared with controls **(Figures 3-8B–3-8D)**.

To identify alternative mechanisms, we next performed functional metabolomic profiling to comprehensively map metabolic alterations conferred by genetic or pharmacological inactivation of GSTP1 in 231MFP breast cancer cells **(Figures 3-3A–3-3C and 3-9A–3-9F)**. We used a targeted single-reaction monitoring (SRM)-based liquid chromatography-tandem MS (LC-MS/MS) approach to comparatively measure the levels of 200 metabolites encompassing glycolytic, tricarboxylic acid (TCA) cycle, amino acid, nucleotide, and lipid metabolism. We also used an untargeted LC-MS approach in which we collected mass spectra from mass-to-charge ratios (m/z) of 100–1,200 and analyzed the resulting features by XCMSOnline[218] to identify metabolites that were altered upon GSTP1 inactivation. We subsequently analyzed any changing m/z by METLIN to identify candidate metabolites, used targeted SRM-based LC-MS/MS to quantify the levels of these metabolites, and added these data to our total targeted analyses. Through these approaches we identified several metabolites that were commonly changing between both shGSTP1 231MFP lines, including lowered levels of lactic acid, ATP, nucleotides, diacylated phospholipids, and alkylacyl ether lipids, and increased levels of acyl carnitines (ACs), ceramides, and lysophospholipids **(Figures 3-3A–3-3C)**. LAS17 treatment in 231MFP cells also showed reduced levels of ATP, lactic acid, purine nucleotides, diacylated phospholipids, and alkylacyl ether lipids, and increased levels of ACs, ceramides, and lysophospholipids **(Figures 3-9B–3-9F)**. While there were many metabolomic changes that were unique to either shGSTP1 or LAS17 treatment, we attributed these differences to metabolic alterations that may manifest under chronic and stable knockdown versus acute inhibition of GSTP1. Nonetheless, between the common changes and even the uncommon changes in metabolite levels, we were able to identify overlapping metabolic pathways that were altered upon GSTP1 inhibition.

Upon mapping the observed metabolomic changes to metabolic pathway maps, our data suggested that GSTP1 inactivation led to impairments in glycolytic metabolism, leading to reduced lactic acid and ATP levels as well as reductions in the levels of macromolecular building blocks, including purine nucleotides, fatty acids, diacylphospholipids, and alkylacyl ether lipids **(Figure 3-3C)**. Consistent with this

premise, we observed significant and time-dependent reductions in lactic acid secretion or glucose consumption upon GSTP1 knockdown in shGSTP1 cells or upon LAS17 treatment in 231MFP cells, compared with shControl or vehicle-treated controls, respectively **(Figures 3-3D and 3-9E)**, indicating reduced glycolytic metabolism.

GSTP1 Inhibition Impairs Oncogenic Signaling Pathways

The reduced levels of ATP and increased levels of ACs (C18:0 AC), a product of carnitine palmitoyltransferase 1 (CPT1), suggested heightened phosphorylation and activity of AMP kinase (AMPK) and also phosphorylation and inhibition of the downstream substrate acetyl coenzyme A (CoA) carboxylase (ACC). Inhibited ACC would presumably lead to decreased malonyl CoA levels and derepression of CPT1, and thus the observed increase in AC levels. We show that GSTP1 knockdown in both shGSTP1 cells and LAS17 treatment in 231MFP cells result in increased levels of phosphorylated AMPK and ACC **(Figures 3-4A and 3-4B)**.

Activation of AMPK has been previously shown to impair breast cancer pathogenicity, partly by inhibiting mammalian target of rapamycin (mTOR) activity and downstream protein synthesis[219]. Consistent with the role of AMPK in driving the GSTP1 inhibition-mediated breast cancer pathogenicity impairments, we show that the cell survival impairments conferred by GSTP1 knockdown are partially rescued upon treatment with the AMPK inhibitor dorsomorphin **(Figure 3-4C)**. We also show that the levels of phosphorylated S6, downstream of mTOR and S6 kinase, are lower in shGSTP1- and LAS17-treated 231MFP breast cancer cells compared with shControl or vehicle-treated control cells, respectively **(Figure 3-4D)**. Consistent with the role of impaired mTOR signaling in GSTP1 inhibition-mediated survival defects, treatment of 231MFP cells with the mTOR inhibitor Torin 1 alone causes survival impairments, but co-treatment of 231MFP cells with Torin 1 and LAS17 does not cause additional survival impairments beyond those observed with LAS17 treatment alone **(Figure 3-4E)**.

GSTP1 Interacts with and Activates GAPDH Activity to Influence Glycolytic Metabolism

We next wanted to investigate the mechanism through which GSTP1 controlled glycolytic metabolism. GSTP1 has been previously shown to control signaling pathways through protein-protein interactions. We thus generated a 231MFP cell line stably overexpressing a FLAG-tagged GSTP1 and performed a pulldown study to identify GSTP1 interacting proteins through proteomic profiling **(Figures 3-10A–3-10C)**. We found that anti-FLAG pulldown in GSTP1-FLAG-overexpressing cell lysates significantly enriched seven proteins compared with mock-infected control cell lysates **(Figure 3-10C)**. Among these seven proteins was glyceraldehyde-3-phosphate dehydrogenase (GAPDH), which was significantly enriched in GSTP1-FLAG-expressing cells compared with mock-infected control 231MFP cells **(Figure 3-5A)**. While we could not confirm this GSTP1 interaction with endogenous GAPDH, we showed that addition of exogenous

pure and active GAPDH enzyme could lead to enrichment of GAPDH upon anti-FLAG pulldown in GSTP1-FLAG-overexpressing cell lysates compared with mock-infected control lysates **(Figure 3-5B)**.

We thus postulated that GSTP1 may interact with GAPDH to influence its activity. Consistent with this hypothesis, we show that GSTP1 greatly activates GAPDH activity *in vitro* **(Figure 3-5C)**. This activation in GAPDH activity was independent of glutathione (GSH) or oxidized glutathione (GSSG), indicating that this activity was not due to glutathione conjugation of a small-molecule metabolite or glutathionylation of GAPDH **(Figure 3-10D)**. LAS17 itself does not inhibit GAPDH activity **(Figure 3-10E)**. This GSTP1- induced GAPDH activity was, however, partially suppressed by LAS17 pre-treatment, indicating that LAS17 binding to GSTP1 at least partially disrupts the GSTP1-GAPDH protein-protein interaction **(Figure 3-5C)**.

To complement our steady-state metabolomic profiling data and further confirm our proposed mechanism that GSTP1 inhibition indirectly inhibits glycolysis through impairing GAPDH activity, we performed [^{13}C]glucose isotopic tracing analysis in 231MFP cells to follow ^{13}C into relevant metabolic pathways using SRM-based LC-MS/MS methods **(Figures 3-5D and 3-5E)**. GSTP1 inhibition with LAS17 led to an accumulation of the GAPDH substrate [^{13}C]glyceraldehyde-3-phosphate/dihydroxyacetone phosphate (G3P/DHAP) and lowered [^{13}C]glycolytic intermediates downstream of GAPDH, which represent the ATP-generating steps of glycolysis **(Figures 3-5D and 3-5E)**. We also show an accumulation in the levels of [^{13}C]glycolytic and [^{13}C]pentose phosphate pathway (PPP) metabolites upstream of GAPDH **(Figures 3-5D and 3-5E)**. Overall, these data are consistent with an inhibition of GAPDH activity from GSTP1 inhibition. [^{13}C]Fructose-1,6-bisphosphate levels were reduced, indicating that GSTP1 may potentially also affect additional nodes in glycolysis. We also show that the impaired glycolytic metabolism downstream of GAPDH also affects other related downstream pathways, including lowered levels of [^{13}C]TCA cycle and [^{13}C]glycine metabolites. This reduction of carbon into the TCA cycle and particularly into [^{13}C]citrate is also consistent with reduced *de novo* lipogenic pools of [^{13}C]palmitate levels **(Figures 3-5D and 3-5E)**, and the reductions in the levels of phospholipid and ether lipid levels **(Figures 3-3B, 3-3C, and 3-5E)**. Our steady-state metabolomic data also showed reduced levels of purine nucleotides such as adenine and guanine, which is counter-indicative to heightened PPP observed from our tracing studies. However, detailed tracing analysis shows that the levels of [^{13}C]adenine AMP (m+7), derived from isotopic incorporation of glucose into PPP metabolites (m+5) and glycine (m+2), are lowered, whereas levels of [^{13}C]AMP (m+5), derived only from glucose incorporation into PPP metabolites, are elevated **(Figure 3-5D)**. These data indicate that the observed reductions in nucleotide levels are likely due to the reduction in glycine necessary for *de novo* synthesis of purines **(Figures 3-3B, 3-3C, 3-5D, and 3-5E)**.

While GSTP1 expression is heightened in TNBC compared with non-TNBC cells, we also showed that GSTP1 is expressed in non-transformed MCF10A mammary epithelial cells. We find that GSTP1 inhibition in MCF10A cells does not impair cell survival

compared with significantly impaired survival in 231MFP cells **(Figure 3-10F)**. Interestingly, LAS17 treatment in MCF10A cells also impairs lactic acid secretion, indicating that glycolytic metabolism may also be impaired in these cells **(Figure 3-10G)**. We postulated that TNBC cells may be more addicted to glycolytic metabolism compared with MCF10A cells. Consistent with this premise, 231MFP cell survival is significantly impaired by the glycolytic hexokinase inhibitor 2-deoxyglucose (2DG) to a degree comparable to that of LAS17, but MCF10A cells show no survival impairment upon 2DG treatment **(Figure 3-10H)**.

Conclusion

Taken together, our data point to GSTP1 as a novel TNBC target that, when inactivated, impairs glycolytic metabolism through a unique mechanism of disrupting GSTP1-induced activation of GAPDH, leading to lower levels of macromolecular building blocks (e.g., lipids and nucleotides) and ATP levels. This reduction in energy levels in turn also leads to impaired oncogenic signaling through activation of AMPK and inhibition of mTOR signaling **(Figure 3-5E)**.

While our interpretations presented here are consistent with the metabolomic and signaling changes that we observe with GSTP1 inactivation in breast cancer cells, we expect that there are also additional mechanisms involved that may arise from the metabolomic changes we observed. For example, we showed increased levels of ACs with GSTP1 inhibition, which we presume to be downstream of ACC inhibition and derepression of CPT1. These results could indicate that fatty acid β-oxidation pathways may be activated upon GSTP1 inactivation. While we did not observe rescue of cell-survival impairments with the CPT1 inhibitor etomoxir (data not shown), the observed increase in AC levels may play a role in other aspects of GSTP1-mediated effects[220].

GSTP1 has also been linked to many other functions in cancer and other human pathologies and even in drug addiction. Beyond glutathionylation and detoxification functions, GSTP1 has been shown to possess chaperone functions, regulation of nitric oxide pathways, and control over various kinase signaling pathways[221]. For example, GSTP1 inhibits JNK signaling and prevents downstream transcriptional activation of cell-stress pathways. Under cellular stress conditions whereby reactive oxygen stress is heightened, GSTP1 has been shown to dimerize into larger aggregates and preclude binding to JNK, enabling JNK activation. In the context of hematopoiesis, GSTP1 inhibition has been shown to play a cytoprotective role in both erythroid and lymphoid cells, and the GSTP1 inhibitor ezatiostat has been shown to be clinically effective for myelodysplastic syndrome[221,222]. While we report here that GSTP1 inhibition does not activate JNK signaling in our TNBC cells, GSTP1 may still directly regulate other signaling pathways through protein interactions or glutathionylation-mediated pathways[221].

We also acknowledge that the apparent activation of GAPDH activity by GSTP1 is only modestly reduced upon LAS17 treatment, indicating that there may be additional

complexities involved in the mechanism underlying the GSTP1 induction of GAPDH activity. While our isotopic tracing data clearly indicate that GSTP1 inhibition leads to an impairment in the ATP-generating steps of glycolysis downstream of GAPDH, we do not yet understand the mechanism through which this occurs. GAPDH activity is dependent on a highly reactive catalytic cysteine that coordinates the interconversion between glyceraldehyde-3-phosphate into 1,3-bisphosphoglycerate and is particularly sensitive to oxidation by agents such as hydrogen peroxide or other oxidants that can inhibit GAPDH activity[223]. Reports have also shown that GAPDH can even be inhibited by its reactive 1,3-bisphosphoglycerate product on a hyperreactive and functional lysine to inhibit its activity[224]. It would be of future interest to investigate whether GSTP1 interacts with GAPDH to protect hyperreactive sites from being adducted and inhibited. GSTP1 has also been shown to glutathionylate cysteines on proteins to post-translationally regulate protein structure and function and protect proteins from degradation from sulfhydryl overoxidation or proteolysis[225]. While we were not able to detect GAPDH glutathionylation by GSTP1 and the activation of GAPDH by GSTP1 was independent of GSSG and GSH, it may still be possible that GAPDH activity and glycolytic metabolism may be regulated by GSTP1-mediated glutathionylation. Furthermore, while GAPDH is not generally considered to be a rate-limiting step of glycolysis, a recent study has shown that GAPDH is rate limiting in cancer cells that possess aerobic glycolysis[223,224,226]. Our studies with GSTP1 provide additional support for how GAPDH may act as a major regulatory hub for TNBC glycolytic activity.

We show that pharmacological inactivation of GSTP1 over a sustained period does not show any observable toxicity, and not only prevents breast tumor growth but even slows established breast tumor growth in mice. A highly potent GSTP1 inhibitor, ezatiostat (developed by Telik Inc.) has passed phase II clinical trials in patients for the treatment of myelodysplastic syndrome, indicating that GSTP1 inhibitors are likely to be well tolerated in humans[222]. Beyond the many previously reported biochemical and therapeutic roles of GSTP1[214,215,225], our study suggests that GSTP1 inhibitors may also be promising stand-alone therapeutics for TNBCs. Our study also underscores the utility of using reactivity-based chemoproteomic platforms coupled with functional metabolomic approaches to identify novel metabolic drivers and pathways underlying breast cancer malignancy.

Materials and Methods

Chemicals
The AMPK inhibitor dorsomorphin dihydrochloride and the mTOR inhibitor Torin 1 were obtained from Tocris. LAS17 was synthesized as described previously[216]. Menadione was obtained from Spectrum Chemical.

Cell culture
The 231MFP cells were obtained from Prof. Benjamin Cravatt and were generated from explanted tumor xenografts of MDA-MB-231 cells. MCF7, MCF10A, T47D, ZR751, MDA-MB-361, HCC1143, HCC38, HCC70, MDA-MB-468, and HEK293T cells were obtained from the American Type Culture Collection. HEK293T cells were cultured in DMEM containing 10% (v/v) fetal bovine serum (FBS) and maintained at 37 °C with 5% CO_2. 231MFP, MDA-MB-361, and MDA-MB 468 cells were cultured in L15 medium containing 10% FBS and maintained at 37 °C with 0% CO_2. MCF10A cells were cultured in DMEM/F12K medium containing 5% horse serum, 20 ng/ml epidermal growth factor, 100 ng/ml cholera toxin, 10 ng/ml insulin, and 500 ng/ml hydrocortisone, and maintained at 37 °C with 5% CO_2. MCF7, T47D, ZR751, HCC1143, HCC38, and HCC70 cells were cultured in RPMI medium containing 10% FBS and maintained at 37 °C with 5% CO_2.

Gene expression by qPCR
qPCR was performed using the manufacturer's protocol for Fisher Maxima SYBR Green with 10 μM primer concentrations or for Bio-Rad SsoAdvanced Universal Probes Supermix. Primer sequences for Fisher Maxima SYBR Green were derived from Primer Bank. Primer sequences for Bio-Rad SsoAdvanced Universal Probes Supermix were designed with Primer 3 Plus.

Constructing knockdown cell lines
Constructing Knockdown Cell Lines We used two independent short-hairpin oligonucleotides to knock down the expression of GSTP1 and one short-hairpin oligonucleotide to knock down the expression of CDH1 using previously described methods[227]. For generation of stable shRNA lines, lentiviral plasmids in the pLKO.1 backbone containing shRNA (Sigma) against human GSTP1 were transfected into HEK293T cells using Fugene (Roche). Lentivirus was collected from filtered cultured medium and used to infect the target cancer cell line with Polybrene. Target cells were selected over 3 days with 1 mg/ml puromycin. The short-hairpin sequences used for generation of the GSTP1 knockdown lines were: shGSTP1-1, CCGGCGCTGACTACAACCTGCTGGACTCGAGTCCAGC AGGTTGTAGTCAGCGTTTTTG; shGSTP1-2, CCGGCCTCACCCTGTACCAG TCCAACTCGAGTTGGACTGGTACAGGGTGAGGTTTTTG.
The short-hairpin sequence used for generation of the CDH1 knockdown line was CCGGAGAAGGGTCTGTTCACGTATTCTCGAGAATACGTGAACAGA CCCTTCTTTTTTG.

The control shRNA was targeted against GFP with the target sequence GCAAGCTGACCCTGAAGTTCAT. Knockdown was confirmed by qPCR or western blotting.

Cellular phenotype studies
GSTP1 cDNA (Dharmacon) was subcloned into the pENTR4-FLAG vector (Addgene). This entry vector was recombined via an attL-attR (LR) reaction into a pLenti CMV puro DEST vector (Addgene). For generation of the FLAG-tagged GSTP1 line, the lentiviral plasmid containing FLAG-GSTP1 was transfected into HEK293T cells using Fugene (Roche). Lentivirus was collected from filtered cultured medium and used to infect the target cancer cell line with Polybrene. Target cells were selected over 3 days with 1 μg/ml puromycin.

Tumor xenograft studies
Human tumor xenografts were established by transplanting cancer cells ectopically into the flank of C.B17 severe combined immunodeficiency (SCID) mice (Taconic Farms) as previously described[28]. In brief, cells were washed twice with PBS, trypsinized, and harvested in serum-containing medium. Harvested cells were washed twice with serum-free medium and resuspended at a concentration of 2.0×10^4 cells/μl, and 100 μl was injected. Tumors were measured every 2 days with calipers. Animal experiments were conducted in accordance with the guidelines of the Institutional Animal Care and Use Committees of the University of California, Berkeley.

Metabolomic profiling of cancer cells
Metabolomic analyses were conducted using previously described methods[227–231].

Lactic acid secretion
Lactic acid secretion from L-15 medium was measured by collecting medium and performing a colorimetric lactic acid assay using a kit purchased from Abcam in accordance with the manufacturer's protocol.

Glucose consumption
Glucose consumption from RPMI medium was measured by collecting medium and performing a colorimetric glucose assay using a kit purchased from Abcam following the manufacturer's protocol.

Western blotting
E-cadherin antibody was obtained from BD Biosciences. Vimentin antibody was obtained from Sigma. Antibodies to cyclophilin, GSTP1, β-actin, phospho-AMPK-α (Thr172), AMPK-α, phospho-ACC (Ser79), ACC, phospho-S6, total S6, phospho-JNK (Thr183/Tyr185), JNK, and GAPDH were obtained from Cell Signaling Technology. FLAG antibody was obtained from Cayman Chemicals.

Cells were lysed in lysis buffer (CST) containing both protease and phosphatase inhibitors. Proteins were resolved by electrophoresis on 4%–15% Tris-glycine precast Mini-PROTEAN TGX gel (Bio-Rad) and transferred to nitrocellulose membranes using

the iBlot system (Invitrogen). Blots were blocked with 5% nonfat milk in Tris-buffered saline containing Tween 20 (TBST) solution for 1 h at room temperature, washed in TBST, and probed with primary antibody diluted in recommended diluent per manufacturer overnight at 4 °C. Following washes with TBST, the blots were incubated in the dark with an IR-linked secondary antibody at room temperature for 1 h. Blots were visualized using an Odyssey Li-Cor scanner after additional washes.

Anti-FLAG pulldown studies
Pulldown studies were performed used Anti-FLAG M2 magnetic beads (Sigma) according to the manufacturer's protocol. FLAG-tagged GSTP1-overexpressing and GFP-overexpressing control cells were lysed in lysis buffer (CST), and 500 mg of lysate was incubated with 32 µl of anti-FLAG magnetic beads for 2 h at 4 °C. Beads were collected and washed three times with Tris-buffered saline before elution with 4% SDS (w/v) in 120 mM Tris-HCl. Samples were heated to 95 °C for 3 min. Eluent was subsequently prepared for proteomic profiling with a shotgun proteomic analysis protocol as described below.

Shotgun proteomic profiling of anti-FLAG pulldown
Pulldown products were precipitated in 20% trichloroacetic acid at 80 °C overnight and centrifuged at 10,000 × *g* at 4 °C for 10 min to pellet protein. Pelleted proteins were washed three times with 8 M urea in PBS. After solubilization, 30 µl of 0.2% ProteaseMAX Surfactant (Promega) was added and the resulting mixture was vortexed followed by the addition of 40 µl of 100 mM ammonium bicarbonate and 10 mM tris(2-carboxyethyl)phosphine (TCEP). After 30 min, 12.5 mM iodoacetamide was added and allowed to react for 30 min in the dark before adding 120 µl of PBS and 1.2 µl of 1% ProteaseMAX Surfactant. The protein solution was vortexed, and 0.5 µg/µl sequencing-grade trypsin (Promega) was added and allowed to react overnight at 37 °C. The peptide solution was then centrifuged at 10,000 × *g* before the supernatant was subsequently analyzed by LC-MS/MS.

GAPDH activity assay
GAPDH activity was measured using a colorimetric kit purchased from BioVision and performed according to the manufacturer's protocol. Active human GSTP1 and active human GAPDH full-length proteins were purchased from Abcam. Proteins were co-incubated at 37 °C for 1 h before GAPDH activity was measured using the kit.

Oxidative stress
Oxidative stress was measured using CellROX Green Reagent (Invitrogen) according to the manufacturer's protocol.

Cysteine and lysine reactivity profiling
Cysteine and lysine reactivity profiling was performed based on an adapted method that has been previously described[210,232]. Tryptic digests for proteomic profiling were analyzed using a Thermo LTQ-XL and quantified by spectral counting using previously described methods[28].

GSTP1 activity assay

The IC_{50} of LAS17 was determined using a GSTP1 activity assay. 1-Chloro-2,4-dinitrobenzene (CDNB) was incubated with 200 mM reduced glutathione and 1 µg of active GSTP1 protein with 100, 10, 1, 0.1, 0.01, 0.001, and 0 µM LAS17. GSTP1 catalyzes the conjugation of glutathione to CDNB, generating the reaction product glutathione-DNB conjugate, which absorbs at 340 nm. The rate of increase in the absorption of the product is proportional to GSTP1 activity and was used to measure GSTP1 activity.

In vitro labeling of GSTP1 with LAS17

50 µg of protein was incubated with 5 µM LAS17 for 30 min at room temperature. Following probe labeling, 25 µM rhodamine-azide, 1 mM TCEP, 100 µM tris(benzyltriazoylmethyl)amine, and 1 mM Cu(II)SO4 were added and incubated for 1 h at room temperature. Laemmli sample buffer was added, heated to 95 °C for 5 min, and cooled to room temperature. Samples were loaded onto an SDS-PAGE gel and imaged by in-gel fluorescence using a Typhoon flatbed scanner.

Figures

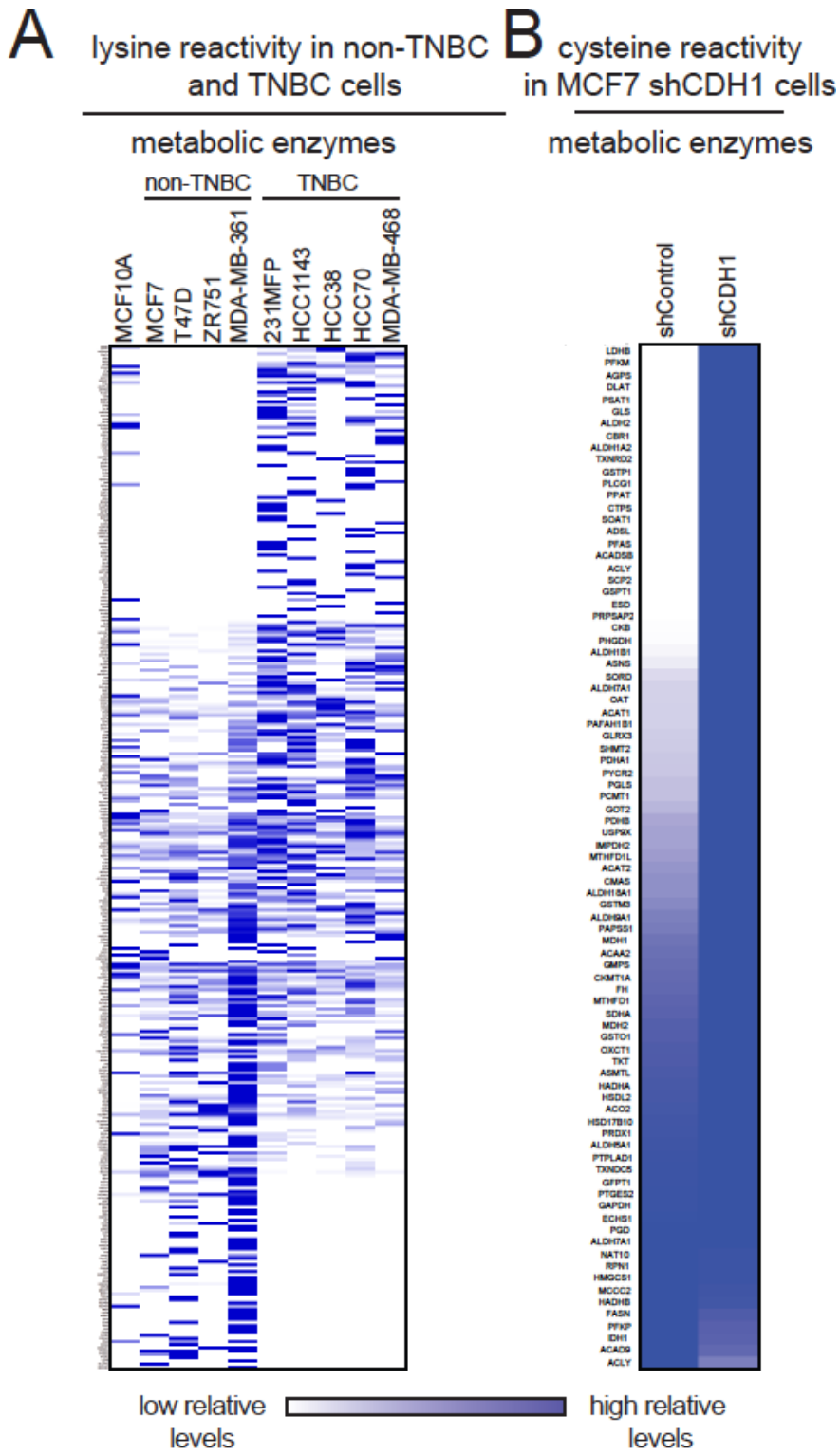
A
lysine reactivity in non-TNBC and TNBC cells
metabolic enzymes
non-TNBC
TNBC
MCF10A
MCF7
T47D
ZR751
MDA-MB-361
231MFP
HCC1143
HCC38
HCC70
MDA-MB-468
B
cysteine reactivity in MCF7 shCDH1 cells
metabolic enzymes
shControl
shCDH1
low relative levels
high relative levels

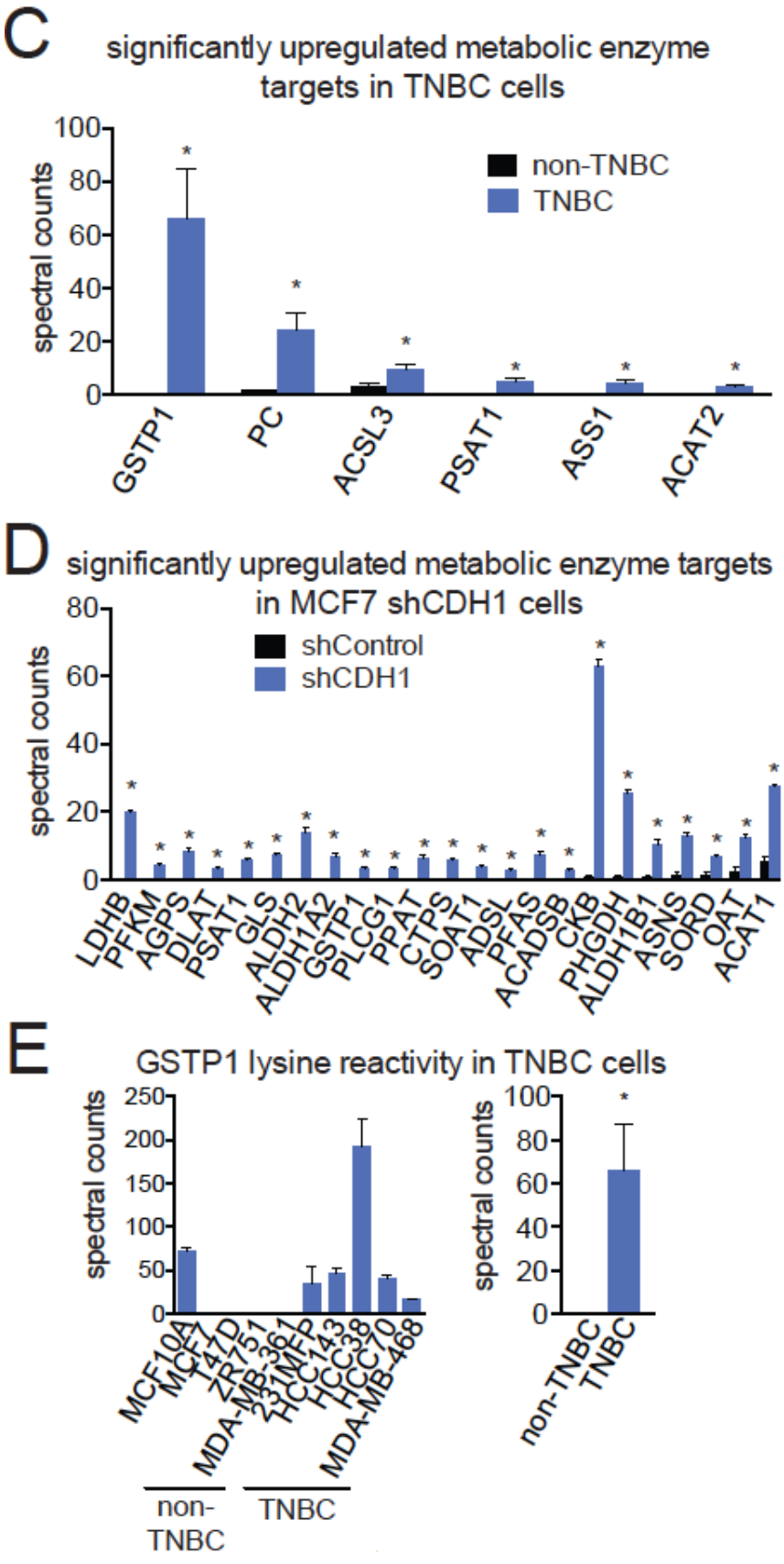
C
significantly upregulated metabolic enzyme targets in TNBC cells
spectral counts
non-TNBC
TNBC
GSTP1
PC
ACSL3
PSAT1
ASS1
ACAT2
D
significantly upregulated metabolic enzyme targets in MCF7 shCDH1 cells
shControl
shCDH1
LDHB
PFKM
AGPS
DLAT
PSAT1
GLS
ALDH2
ALDH1A2
GSTP1
PLCG1
PPAT
CTPS
SOAT1
ADSL
PFAS
ACADSB
CKB
PHGDH
ALDH1B1
ASNS
SORD
OAT
ACAT1
E
GSTP1 lysine reactivity in TNBC cells
MCF10A
MCF7
T47D
ZR751
MDA-MB-361
231MFP
HCC143
HCC38
HCC70
MDA-MB-468
non-TNBC
TNBC

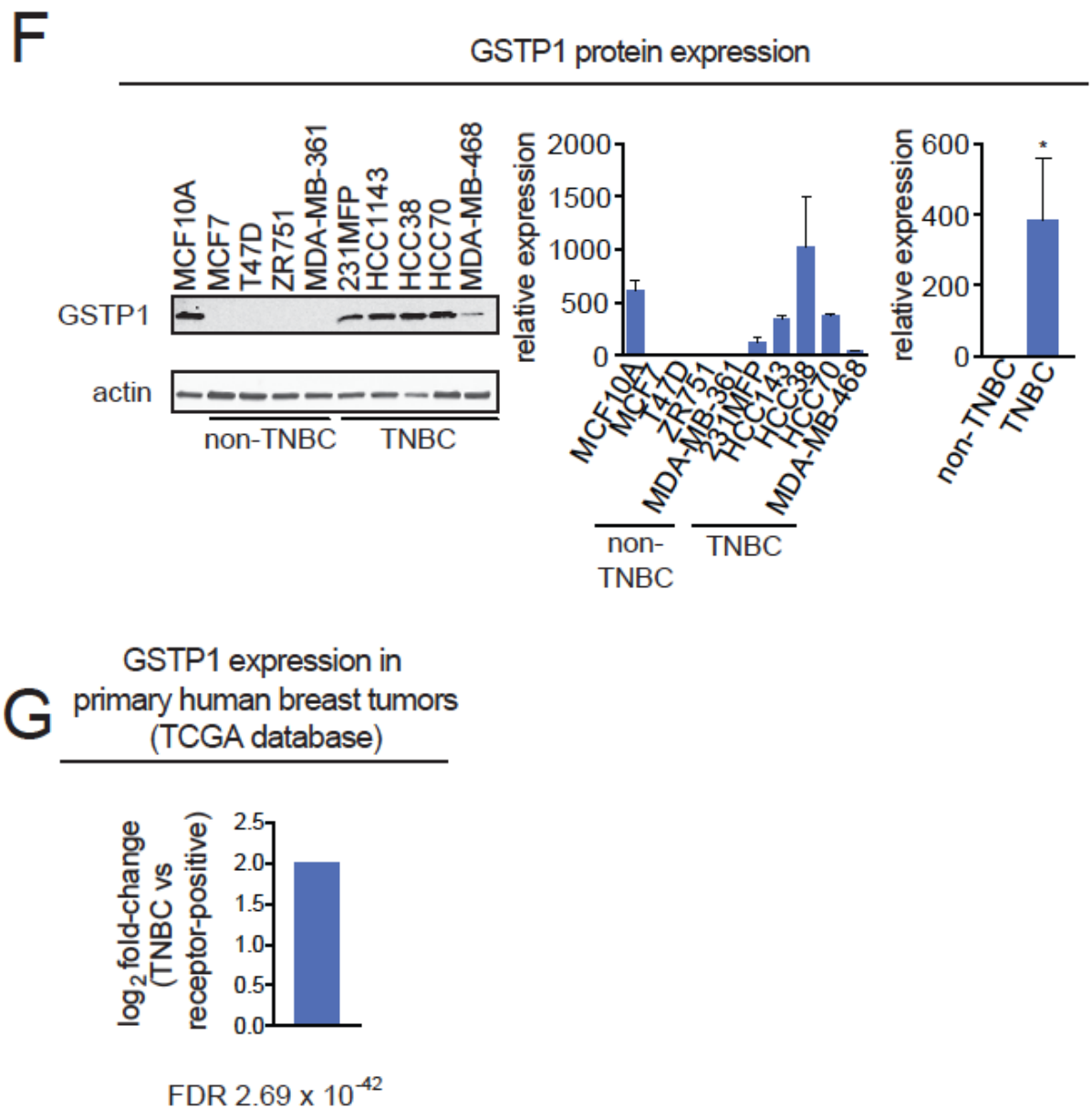

Figure 3-1. Profiling Dysregulated Metabolic Enzyme Targets in TNBC Cells and CDH1 Knockdown Breast Cancer Cells

(A and B) Chemoproteomic profiling of a panel of MCF10A non-transformed mammary epithelial cells, non-TNBC, and TNBC cell lines **(A)** and shControl and shCDH1 MCF7 breast cancer cells **(B)** with the lysine-reactive dichlorotriazine-alkyne and cysteine-reactive iodoacetamide-alkyne probes, respectively. Probe-labeled proteins were avidin enriched, and enriched proteins were trypsinized and analyzed by LC-MS/MS and quantified by spectral counting. Heat maps represent relative levels for each protein, where dark and light blue indicate higher and lower enrichment of the protein, respectively.

(C and D) Significantly upregulated metabolic enzyme targets in TNBC cells **(C)** and shCDH1 MCF7 cells **(D)**.
(E) GSTP1 lysine reactivity in TNBC cells from each individual cell line and combined averaged spectral counts from non-TNBC and TNBC cells.
(F) GSTP1 expression was measured across a panel of MCF10A non-transformed mammary epithelial cells, non-TNBC, and TNBC cell lines by western blotting. Western blotting image shown is representative of n = 3/group. GSTP1 expression was normalized to actin loading control and quantified by densitometry.
(G) GSTP1 expression in receptor-positive and TNBC primary human breast tumors from The Cancer Genome Atlas (TCGA) database. FDR, false-discovery rate.
Data in (C–G) are presented as mean ± SEM, n = 3–5/group. Significance is presented as *$p < 0.05$ compared with non-TNBC or shControl cells.

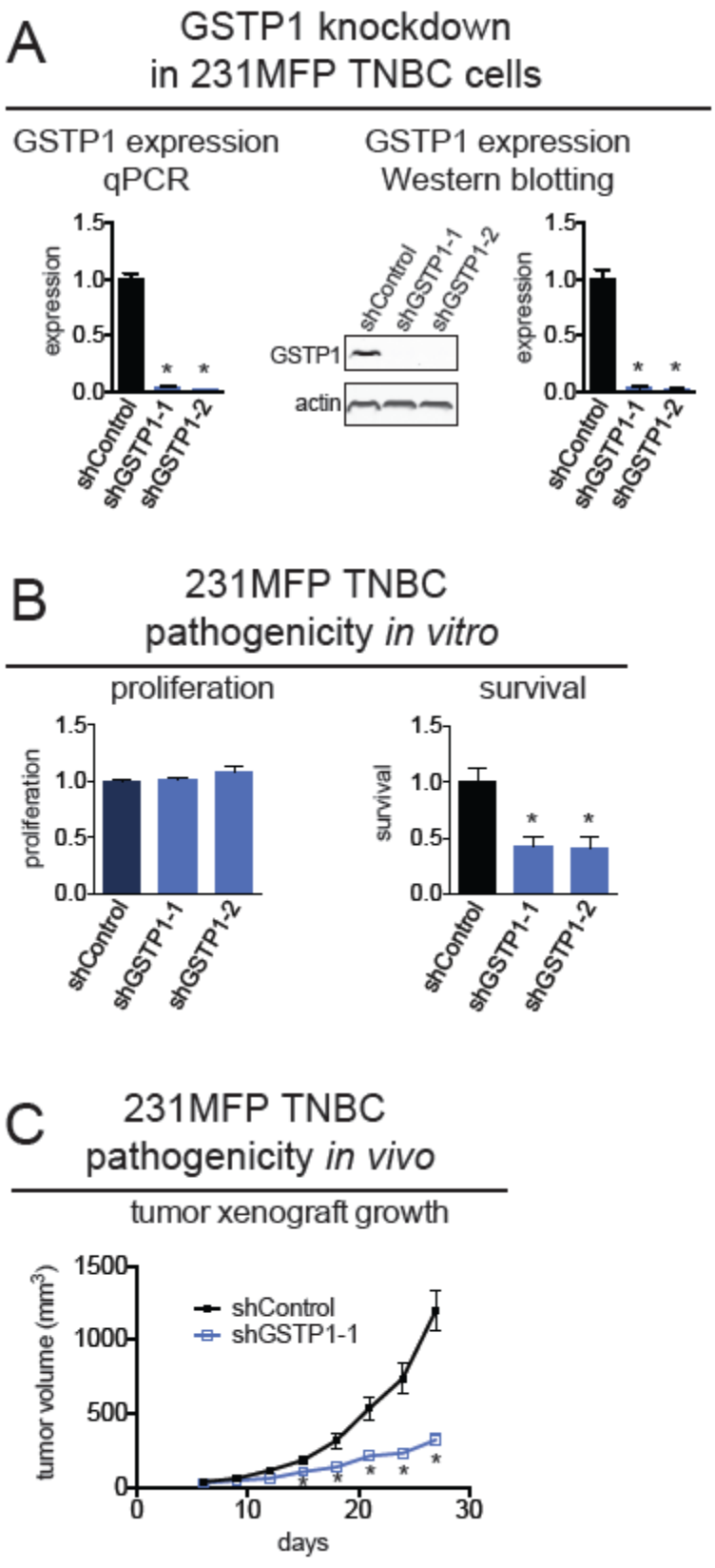
A
GSTP1 knockdown
in 231MFP TNBC cells
GSTP1 expression
qPCR
GSTP1 expression
Western blotting
expression
1.5
1.0
0.5
0.0
shControl
shGSTP1-1
shGSTP1-2
GSTP1
actin
B
231MFP TNBC
pathogenicity in vitro
proliferation
survival
C
231MFP TNBC
pathogenicity in vivo
tumor xenograft growth
tumor volume (mm3)
1500
1000
500
0
shControl
shGSTP1-1
0
10
20
30
days

D GSTP1 inhibitor

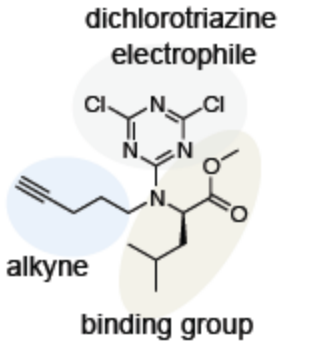

LAS-17

E LAS17 labeling of shCDH1 cells

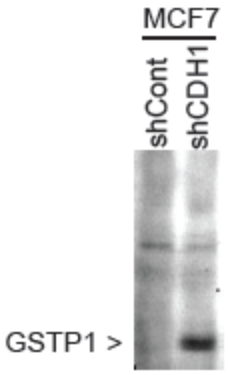

F LAS17 inhibition of GSTP1 activity

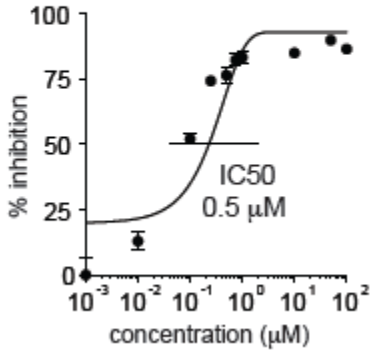

G 231MFP TNBC pathogenicity *in vitro*

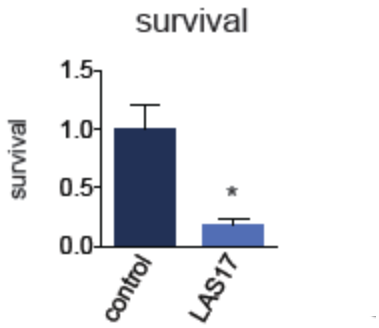

H tumor xenograft

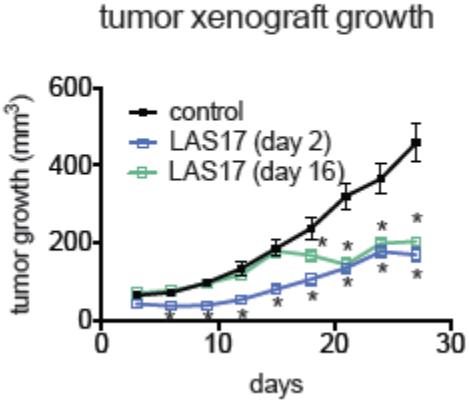

I GSTP1 inhibitor sensitivity in shCDH1 cells

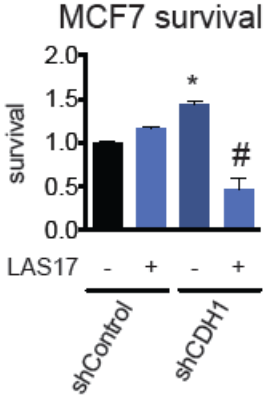

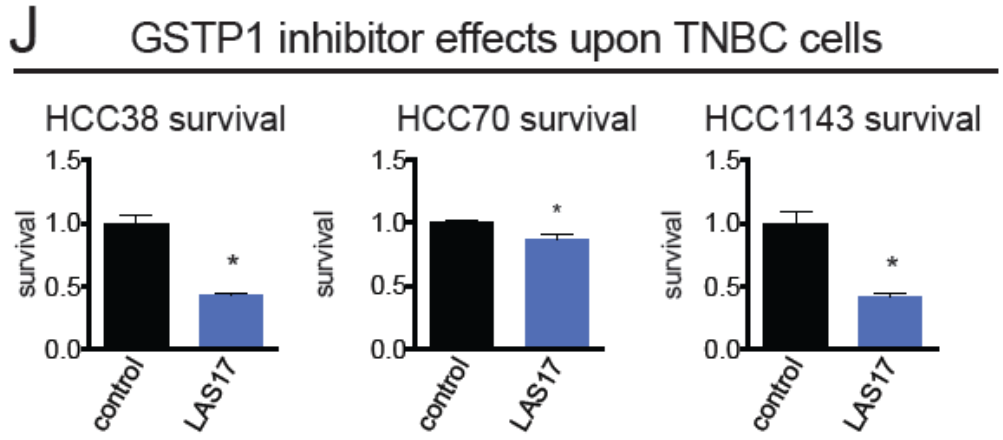

Figure 3-2. The Effect of Genetic and Pharmacological Inactivation of GSTP1 on Breast Cancer Pathogenicity

(A) GSTP1 was knocked down in 231MFP TNBC cells using two independent shRNA, and expression was confirmed by both qPCR and western blotting. Western blotting image is representative of n = 3/group and protein expression was quantified by densitometry.

(B) GSTP1 knockdown in 231MFP cells shows impaired serum-free cell survival, with no change in cell proliferation 48 h after seeding. Survival and proliferation were assessed using Hoechst stain.

(C) shGSTP1 231MFP cells show impaired tumor growth in SCID mice compared with shControl cells.

(D) Selective and irreversible dichlorotriazine GSTP1 inhibitor LAS17 bearing a dichlorotriazine electrophile, GSTP1 binding group, and an alkyne handle for subsequent click chemistry.

(E) LAS17 labeling of shControl and shCDH1 MCF7 cells showing heightened GSTP1 in shCDH1 cells. Cell lysates were labeled with LAS17 for 30 min prior to click chemistry with rhodamine-azide. Proteomes were separated on SDS-PAGE and visualized by in-gel fluorescence.

(F) LAS17 inhibits GSTP1 activity with a 50% inhibitory concentration (IC_{50}) of 0.5 μM. GSTP1 activity was assessed by pre-incubating vehicle DMSO or LAS17 with pure GSTP1 protein for 30 min prior to measuring the rate of conjugation of glutathione to CDNB and quantifying the rate of increase in the absorption of the reaction product, glutathione-DNB conjugate.

(G) Serum-free survival 48 h after seeding in 231MFP cells treated with DMSO vehicle or LAS17 (10 μM), determined by Hoechst staining.

(H) 231MFP tumor xenograft growth in SCID mice upon once-per-day daily treatment with vehicle (18:1:1 PBS/ethanol/PEG 40) or LAS17 (20 mg/kg, intraperitoneally) initiated either 2 or 16 days after subcutaneous injection of 2×10^6 231MFP cells.

(I) Serum-free cell survival in shControl and shCDH1 MCF7 cells treated with DMSO vehicle or LAS17 treatment (10 μM) in shControl and shCDH1 MCF7 cells, determined by WST-1 assay.
(J) Serum-free cell survival 48 h after seeding in HCC38, HCC70, and HCC1143 cells treated with DMSO vehicle or LAS17 (10 μM), determined by Hoechst staining.
Data in (A–C), (F), and (G–J) are presented as mean ± SEM, n = 3/group in (A), n = 5/group in (B), n = 8/group in (C), n = 3/group in (F), n = 5/group in (G), n = 8/group in (H), and n = 5/group in (I) and (J). Significance is presented as *$p < 0.05$ compared with shControl and #$p < 0.05$ compared to shCDH1 vehicle-treated control.

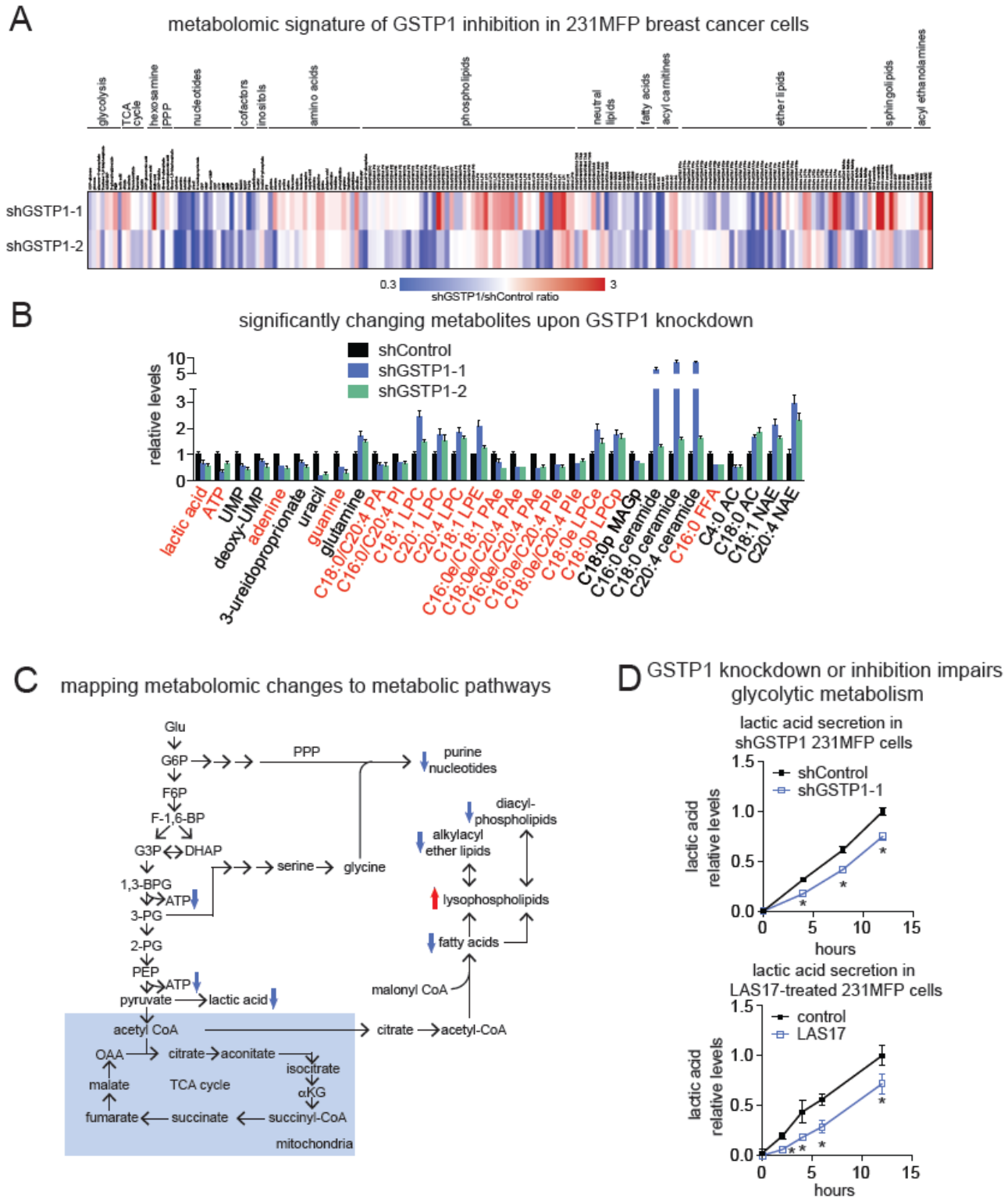

Figure 3-3. Functional Metabolomic Profiling and Pathway Mapping of GSTP1 Inactivation in TNBC Cells

(A) We performed untargeted and targeted SRM-based metabolomic profiling of shControl and shGSTP1 231MFP cancer cells. Shown is a heat map of shGSTP1/shControl ratios of all the metabolites that were measured by SRM analysis.
(B) Shown are metabolites that were significantly ($p < 0.05$) changing in the same direction in both shGSTP1-1 and shGSTP1-2 cells compared with shControl cells. Highlighted in red are the metabolite changes that were mapped to metabolic pathways in **(C)**. UMP, uridine monophosphate; PA, phosphatidic acid; PI, phosphatidylinositol; LPC, lysophosphatidylcholine; PAe, phosphatidic acid-ether; PIe, phosphatidylinositol-ether; LPCe, lysophosphatidylcholine-ether; LPCp, lysophosphatidylcholine-plasmalogen; MAGp, monoalkylglycerol-plasmalogen; FFA, free fatty acid; AC, acyl carnitine; NAE, N-acyl ethanolamine.
(C) Pathway mapping of many of the metabolic changes observed in shGSTP1 231MFP cells indicates a primary impairment in glycolysis with resulting secondary impairments in nucleotide and lipid metabolism.
(D) Lactic acid secretion into the media in shControl and shGSTP1-1 231MFP cells or DMSO vehicle-treated or LAS17-treated (10 μM) 231MFP cells. Lactic acid was measured using a lactic acid measurement kit.
Data in (B) and (D) are presented as mean ± SEM, n = 5/group. Significance in (D) is presented as $*p < 0.05$ compared with shControl or DMSO vehicle-treated controls.

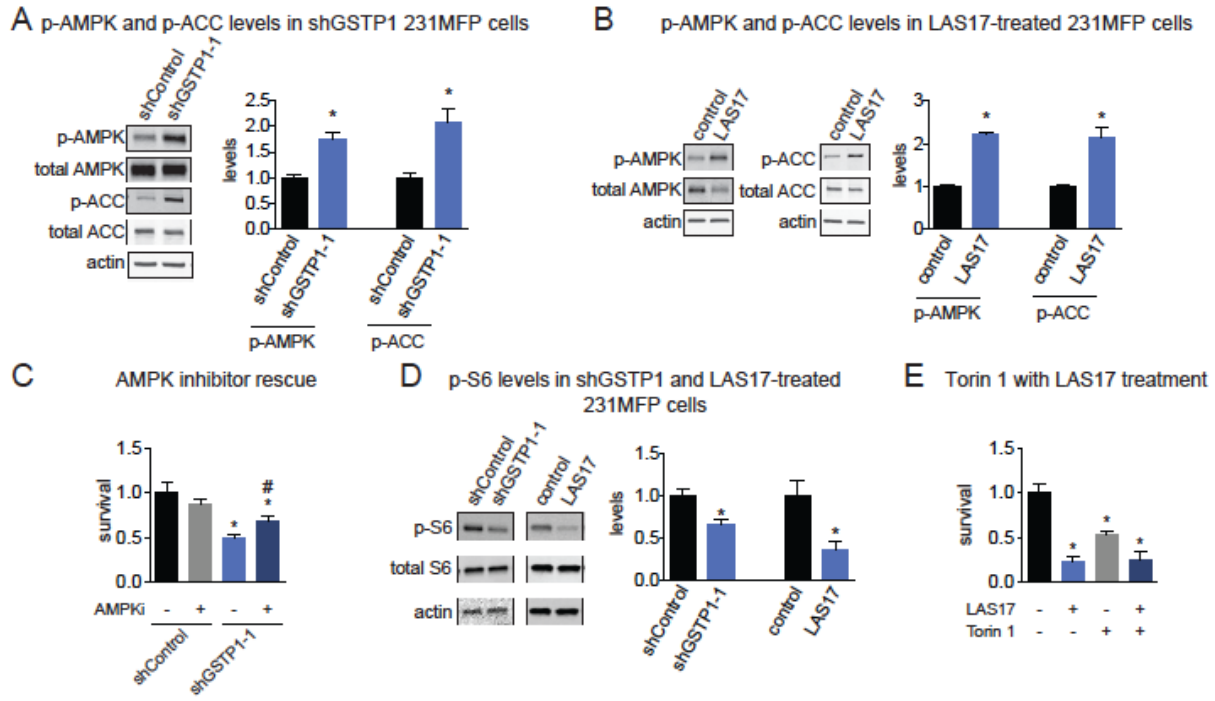

Figure 3-4. GSTP1 Inhibition Impairs Oncogenic Signaling Pathways
(A and B) shGSTP1 **(A)** and LAS17-treated **(B)** 231MFP cells show increased levels of phosphorylated AMPK and ACC compared with shControl and DMSO vehicle-treated controls, respectively, as assessed by western blotting.
(C) Serum-free cell survival impairments 48 h post seeding in shControl and shGSTP1 231MFP cells treated with DMSO vehicle or AMPK inhibitor dorsomorphin (10 μM).
(D) Phosphorylated S6 levels, a readout of mTOR activity, in shControl and shGSTP1 or DMSO vehicle or LAS17-treated (10 μM) 231MFP cells.
(E) Serum-free cell survival 48 h post seeding in 231MFP cells treated with DMSO vehicle or LAS17 (10 μM) and DMSO vehicle or mTOR inhibitor Torin 1 (250 nM).
Western blotting images in (A), (B), and (D) are representative images from n = 3/group. Quantification was performed by normalizing to actin or total S6 loading controls by densitometry. Data in (A–E) are presented as mean ± SEM, n = 3–5/group. Significance is presented as *$p < 0.05$ compared with shControl or DMSO vehicle-treated controls, respectively in (A–E) and $^{\#}p < 0.05$ compared with DMSO vehicle-treated shGSTP1 in (C).

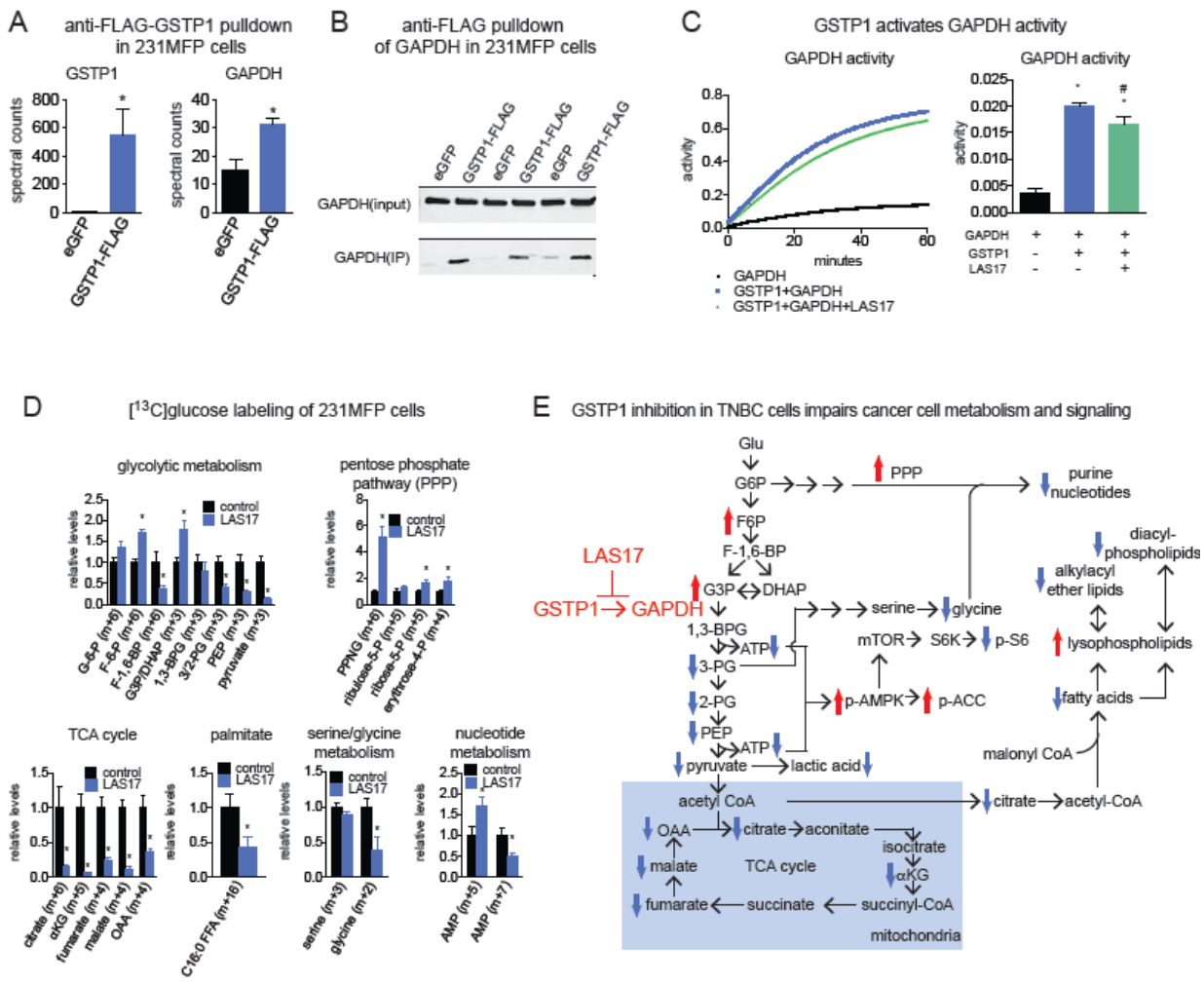

Figure 3-5. GSTP1 Interacts with and Activates GAPDH Activity to Influence Glycolytic Metabolism

(A) We generated stable GFP-expressing control and GSTP1-FLAG-overexpressing 231MFP cells to identify GSTP1 interaction partners. Upon anti-FLAG pulldown of GFP-expressing control (EGFP) or GSTP1-FLAG-overexpressing 231MFP lysates and subsequent proteomic analysis of pulled-down proteins, we found enrichment of GSTP1 and GAPDH.

(B) This GSTP1-GAPDH interaction was confirmed by incubation of pure and active GAPDH enzyme with GFP-expressing or GSTP1-FLAG-overexpressing 231MFP cell lysates, subsequent anti-FLAG pulldown, and western blotting of GAPDH. Shown are GAPDH blots for input and immunoprecipitation fractions.

(C) Effect of co-incubating pure and active GSTP1 and GAPDH proteins individually or together on GAPDH activity, assessed by a GAPDH activity assay measuring NADH, a by-product of the conversion of glyceraldehyde-3-phosphate to 1,3-bisphosphoglycerate. GAPDH was treated with DMSO vehicle and GAPDH + GSTP1

was treated with DMSO vehicle or LAS17 (10 μM) 30 min prior to assessment of GAPDH activity.
(D) Isotopic tracing of [^{13}C]glucose into metabolic pathways in 231MFP cells. Cells were pre-treated with DMSO vehicle or LAS17 (10 μM) 1 h prior to labeling of 231MFP cells with [^{13}C]glucose (10 mM, 8 h). Cell metabolomes were analyzed by SRM-based LC-MS/MS.
(E) Model of mechanisms underlying GSTP1 control over breast cancer pathogenicity, based on steady-state metabolomics, isotopic tracing, and western blotting data.
Data in (A) and (D) are presented as mean ± SEM, n = 3–5/group. Significance is presented as *$p < 0.05$ compared with EGFP or DMSO vehicle-treated controls, respectively. Data in (C) are presented as mean ± SEM, n = 3/group. Significance in (C) is presented as *$p < 0.05$ compared with GAPDH only and $^{\#}p < 0.05$ compared with the GAPDH and GSTP1 group.

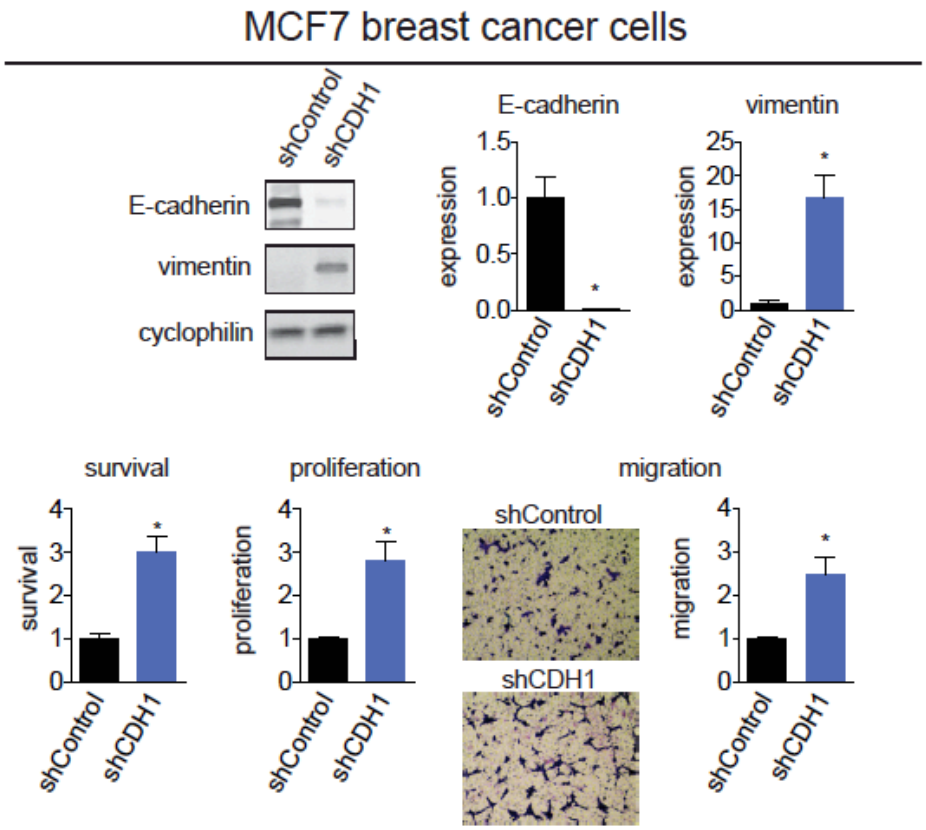

Figure 3-6. CDH1 Knockdown in MCF7 Breast Cancer Cells
CDH1 was stably knocked down in MCF7 breast cancer cells using a short-hairpin oligonucleotide targeting CDH1. Knockdown was confirmed by Western blotting of E-cadherin. The EMT marker vimentin is heightened in shCDH1 cells as determined by Western blotting. Western blotting images shown are represented images from n=3/group and CDH1 and vimentin expression were normalized to the cyclophilin loading control and quantified by densitometry. Serum-free survival, proliferation, and migration were significantly enhanced upon CDH1 knockdown in both MCF7 and LNCaP cells. Survival and proliferation were assessed 3 days post-seeding of cells by the WST-1 cell viability assay. Cell migration assays were performed by transferring cancer cells to serum-free media prior to seeding cells into inserts with 8 mm pore size containing membranes coated with collagen (10 µg/ml). Migrated cells were subsequently fixed, stained, and counted. Data is presented as mean ± SEM, n=3-5/group. Significance is presented as *p<0.05 compared to shControl cells.

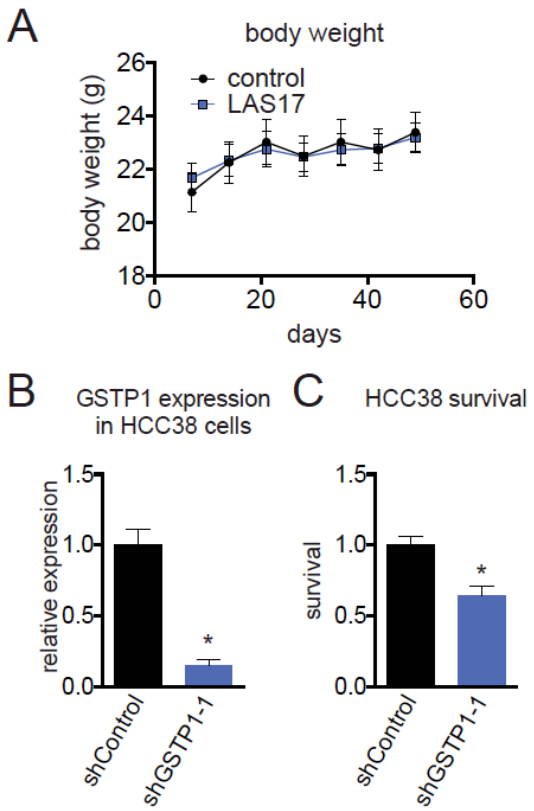

Figure 3-7. Effect of GSTP1 Inhibition on Mouse Body Weight and in Breast Cancer Cells

(A) Body weight in SCID mice treated once per day with LAS17 (20 mg/kg ip). **(B)** GSTP1 expression in HCC38 shControl and shGSTP1-1 cells, determined by qPCR. **(C)** Serum-free cell survival 48 h after seeding in shControl and shGSTP1-1 HCC38 cells determined by WST-1 assay. Data are presented as mean ± SEM, n=5-6/group. Significance is presented as *$p<0.05$ compared to vehicle-treated or shControl cells.

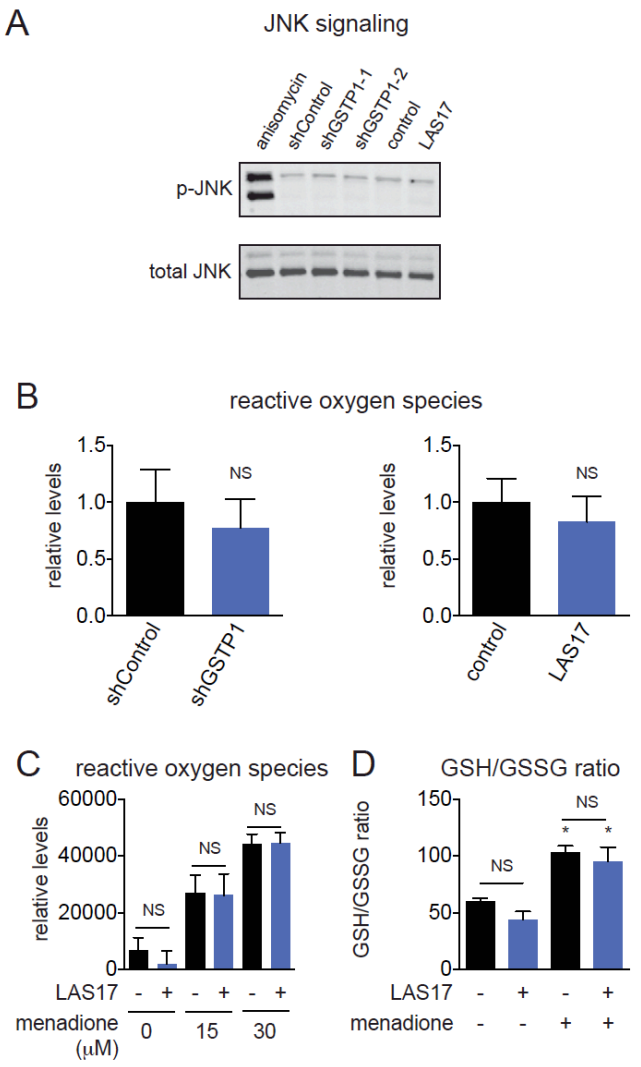

Figure 3-8. Effect of GSTP1 Inactivation on JNK Signaling, Reactive Oxygen Species, or GSH/GSSG Ratios

(A) shGSTP1 and LAS17-treated 231MFP cells do not show any changes in phosphorylated JNK levels compared to shControl or DMSO vehicle-treated control cells. Treatment of 231MFP cells with anisomycin (1 mM, 1 h), a JNK activator, dramatically elevated p-JNK levels. **(B)** Reactive oxygen species in shGSTP1 and LAS17-treated 231MFP cells, compared to shControl or DMSO vehicle-treated control cells, as measured by CellROX green reagent. **(C)** Reactive oxygen species in DMSO vehicle-treated or LAS17-treated 231MFP cells treated with DMSO vehicle or the oxidant menadione. **(D)** Ratio of reduced (GSH) or oxidized glutathione (GSSG) levels in 231MFP cells treated with DMSO or LAS17 also treated with DMSO or menadione. Data are presented as mean ± SEM, n=3/group. NS refers to not significantly changing compared to control groups ($p>0.05$).

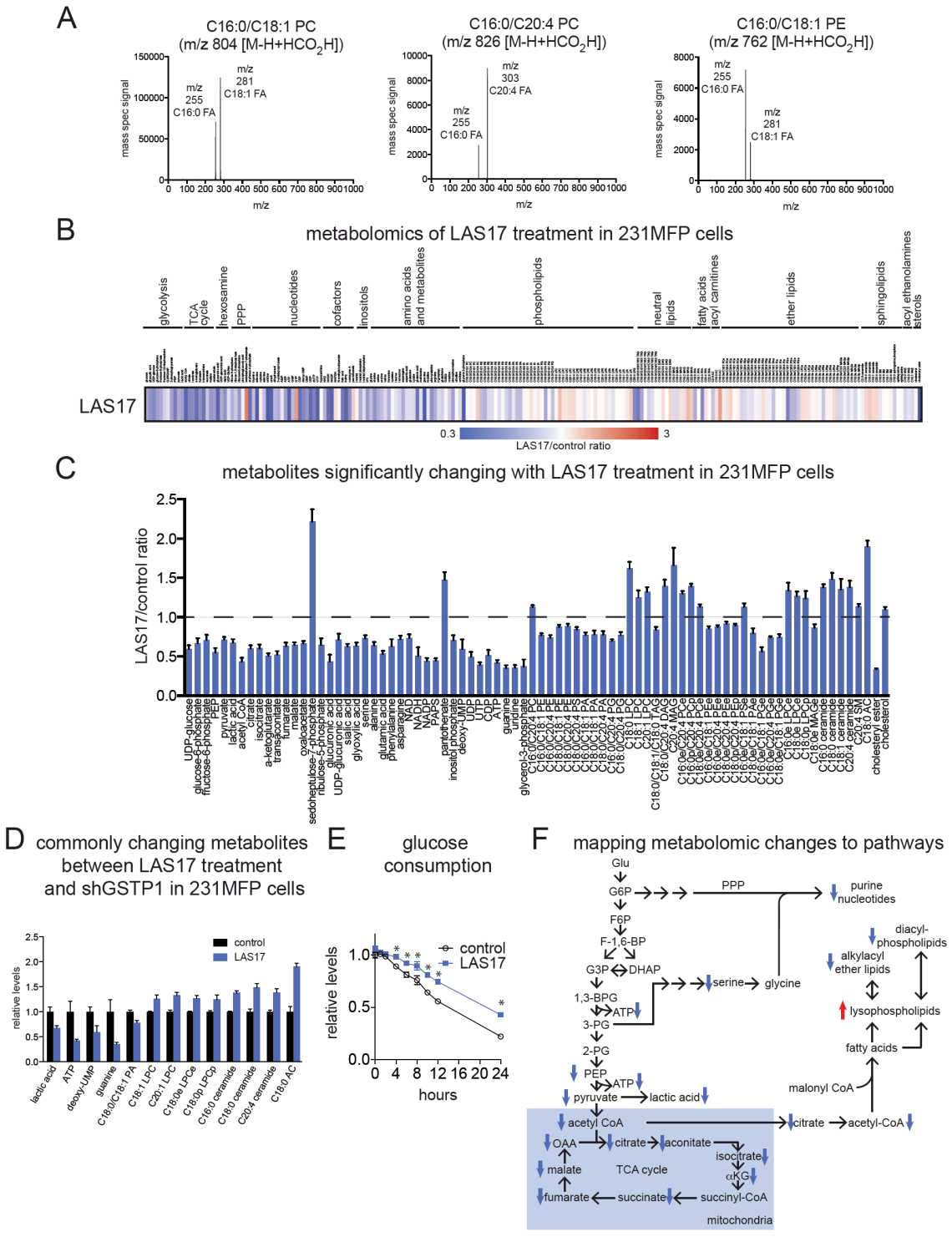

Figure 3-9. Functional Metabolomic Profiling and Pathway Mapping of GSTP1 Inhibition in 231MFP TNBC Cells

(A) Representative ms2 spectra of phospholipid formate adducts in 231MFP cell metabolomes fragmented with 40 V collision energy under LC/MS solvent conditions containing both ammonium hydroxide and formic acid to ascertain acyl chain lengths of

phospholipids targeted by SRM analyses. **(B)** Targeted and untargeted SRM-based metabolomic profiling of DMSO vehicle and LAS17 (10 μM, 8h)-treated 231MFP cells. Shown is a heat map of the LAS17/control ratios of all the metabolites that were measured by SRM analysis. **(C)** Shown are metabolites that were significantly ($p<0.05$) changed in levels upon LAS17 treatment (10 μM, 20 h) compared to DMSO-vehicle-treated controls. **(D)** Metabolites that were commonly changed between LAS17 treatment and shGSTP1 in 231MFP breast cancer cells ($p<0.05$). **(E)** Glucose consumption of 231MFP cells treated with DMSO vehicle or LAS17 (10 μM). **(F)** Pathway mapping of many of the metabolic changes observed in LAS17-treated 231MFP cells indicates a primary impairment in glycolysis with resulting secondary impairments in nucleotide and lipid metabolism. Data in (C and D) are presented as mean ± SEM, n=4-5/group. Significance in (E) is presented as *$p<0.05$ compared to vehicle-treated controls.

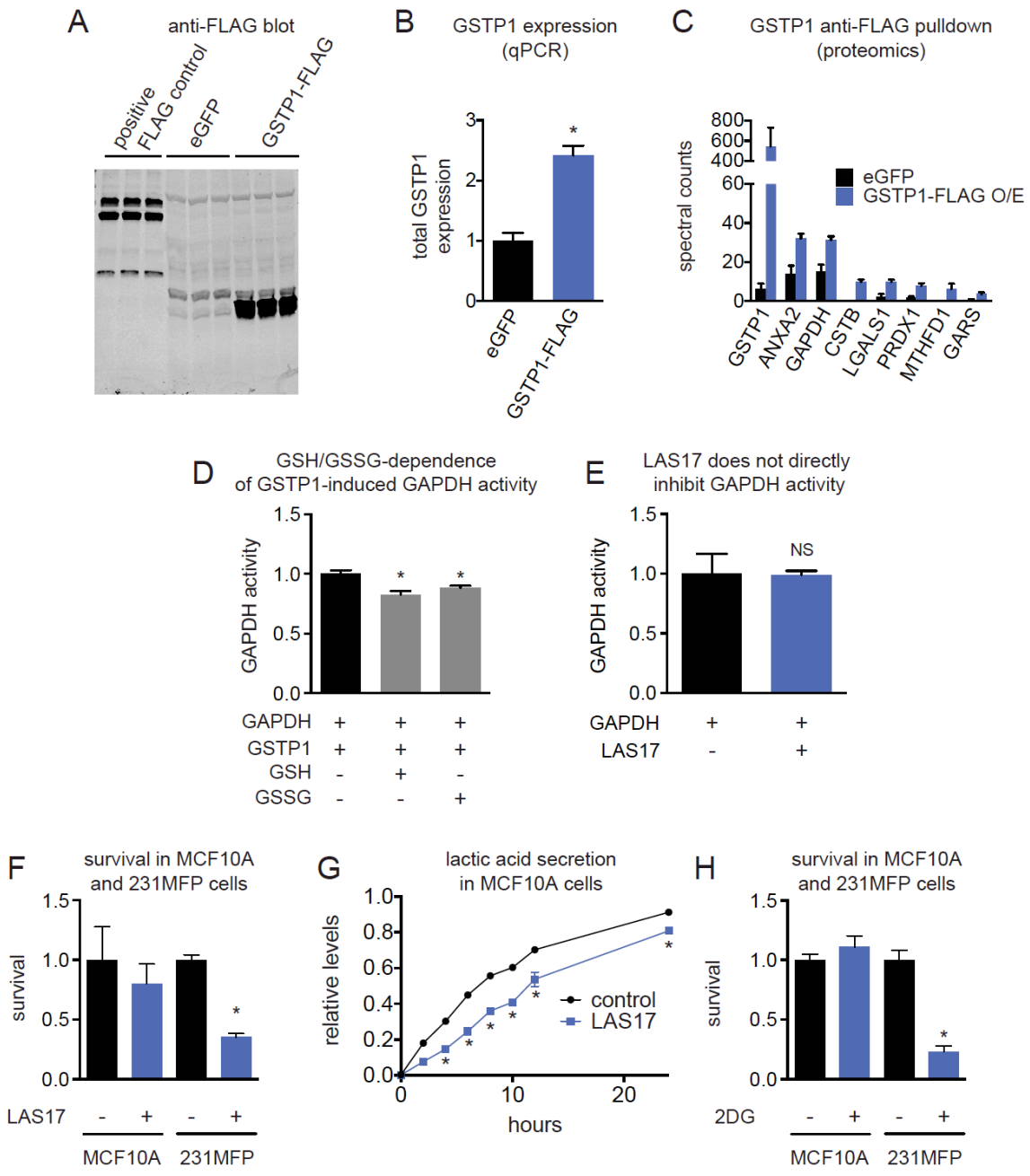

Figure 3-10. Characterizing the Role of GSTP1 in Regulating GAPDH Activity and Glycolysis

(A) We generated stable control GFP-infected (eGFP) and GSTP1-FLAG overexpressing 231MFP cells to identify GSTP1 interaction partners. GSTP1-FLAG expression was confirmed by an anti-FLAG Western blot that includes a positive FLAG-labeled protein control. **(B)** qPCR analysis of total GSTP1 expression in eGFP infected versus GSTP1-FLAG overexpressing 231MFP cells. **(C)** Proteins significantly enriched ($p<0.05$ compared to eGFP controls) by anti-FLAG pulldown of mock-infected or GSTP1-FLAG 231MFP cell lysates and subsequent proteomic analysis of pulled-down

proteins. **(D)** The effect of GSH or GSSG treatment on GSTP1-induced GAPDH activity. Indeed, it significantly inhibits the activity, indicating that GSTP1-induced GAPDH activity is not due to glutathionylation properties of GSTP1. GSH or GSSG (1 mM) were co-incubated with pure and active GAPDH and GSTP1 for 1 h. **(E)** LAS17 does not inhibit GAPDH activity. LAS17 (10 μM) was incubated with pure GAPDH for 30 min before initiation of the GAPDH assay. GAPDH assay was performed using the GAPDH activity assay kit, which measures the rate of production of NADH, a byproduct of the conversion of glyceraldehyde-3-phosphate to 1,3-bisphosphoglycerate.
(F) Serum-free cell survival of MCF10A and 231MFP cells treated with vehicle DMSO or LAS17 (10 μM) 48 h after seeding. **(G)** Lactic acid secretion in MCF10A cells treated with vehicle DMSO or LAS17 (10 μM) over a 24 h period. **(H)** Serum-free cell survival of MCF10A and 231MFP cells treated with vehicle DMSO or 2-deoxyglucose (20 mM) 48 h after seeding. Data are presented as mean ± SEM, n=3-5/group. Significance is expressed as *$p<0.05$ compared to mock (B), GAPDH+GSTP1 (D), vehicle-treated DMSO control in each respective cell line (F, G, H). NS denotes no significant change ($p>0.05$).

CONCLUSION

Cancer is currently the leading cause of death in developed countries and second in developing countries[14]. A fundamental hallmark of cancer is aberrant metabolism. Since Otto Warburg's discovery in the 1920s that cancer cells increase uptake of glucose and undergo aerobic glycolysis, scientists have sought to understand the metabolic pathways that are conferred upon tumorigenesis. Identifying these critical metabolic nodes can uncover novel therapeutic strategies to treat cancer.

In chapter one, we focus on a well-established relationship between obesity and the prevalence of cancers and highlight the molecular mechanisms that have been proposed to explain this relationship, focusing on elevated lipids and lipid signaling, inflammation, insulin signaling, and adipokines. These findings have led to potential therapeutic interventions for patients with obesity, such as the recommendation to take insulin-sensitizing drugs rather than insulin, which has been shown to have a worse cancer outcome compared to those taking the former[181,182].

In chapter two, we describe a potential alternate and more direct mechanism linking obesity to increased incidence of cancers. Previously, cancer cells were thought to rely solely on *de novo* lipogenesis for cellular lipids[186]. Using an isotopic tracing metabolomic platform, we show that cancer cells can uptake exogenous fatty acids and remodel them into structural and signaling lipids that can drive cancer pathogenicity. We find a dysregulated metabolic signature of lipid metabolism that is common amongst aggressive cancer cells where there is an overall increase in exogenous fatty acid incorporation to generate structural and oncogenic signaling lipids. This mechanism adds to previous studies linking obesity-induced inflammation, hyperinsulinemia, increased insulin growth factor signaling, and heightened adipokine signaling to cancer cell proliferation and malignancy[202].

Although targeting key nodal lipid metabolism pathways provides a potential strategy for treating cancers, the metabolic pathways that drive tumorigenesis in some cancer subtypes are not well defined. In chapter three, we focus on TNBCs, a subtype of breast cancers with heightened malignancy, poor prognosis, and few therapeutic options. We used a reactivity-based chemoproteomic platform to identify GSTP1 as a novel potential therapeutic target for TNBCs. We show that GSTP1 interacts with GAPDH to activate its activity and that GSTP1 inactivation impairs glycolytic metabolism after the GAPDH step in glycolysis to impair ATP generation, nucleotide and fatty acid metabolism, and oncogenic signaling pathways. We show that GSTP1 inhibitors show selective killing of TNBC cells over non-TNBC or non-transformed mammary epithelial cells and that long-term GSTP1 inhibition in mice does not cause overt toxicity or weight loss. Altogether, we show that GSTP1 inhibitors may potentially be novel therapeutic agents to specifically target TNBCs.

In summary, we have described several aspects of cancer metabolism, including mechanisms linking adiposity to cancer, the role of exogenous fatty acids in lipid metabolism, and the role of GSTP1 in glycolytic metabolism. Besides providing critical insights into several dysregulated metabolic pathways in cancer, these findings can lead to the development of novel therapeutic options for the treatment of cancer.

REFERENCES

1. Benjamin, D. I., Cravatt, B. F. & Nomura, D. K. Global profiling strategies for mapping dysregulated metabolic pathways in cancer. *Cell Metab.* **16,** 565–577 (2012).
2. Cantor, J. R. & Sabatini, D. M. Cancer cell metabolism: one hallmark, many faces. *Cancer Discov.* **2,** 881–898 (2012).
3. Pavlova, N. N. & Thompson, C. B. The Emerging Hallmarks of Cancer Metabolism. *Cell Metab.* **23,** 27–47 (2016).
4. Vander Heiden, M. G., Cantley, L. C. & Thompson, C. B. Understanding the Warburg effect: the metabolic requirements of cell proliferation. *Science* **324,** 1029–1033 (2009).
5. Fantuzzi, G. Adipose tissue, adipokines, and inflammation. *J. Allergy Clin. Immunol.* **115,** 911–919; quiz 920 (2005).
6. Calle, E. E. & Kaaks, R. Overweight, obesity and cancer: epidemiological evidence and proposed mechanisms. *Nat. Rev. Cancer* **4,** 579–591 (2004).
7. Renehan, A. G., Tyson, M., Egger, M., Heller, R. F. & Zwahlen, M. Body-mass index and incidence of cancer: a systematic review and meta-analysis of prospective observational studies. *Lancet Lond. Engl.* **371,** 569–578 (2008).
8. Merino Salvador, M. *et al.* Lipid metabolism and lung cancer. *Crit. Rev. Oncol. Hematol.* **112,** 31–40 (2017).
9. Nomura, D. K. *et al.* Monoacylglycerol lipase exerts dual control over endocannabinoid and fatty acid pathways to support prostate cancer. *Chem. Biol.* **18,** 846–856 (2011).

10. Alli, P. M., Pinn, M. L., Jaffee, E. M., McFadden, J. M. & Kuhajda, F. P. Fatty acid synthase inhibitors are chemopreventive for mammary cancer in neu-N transgenic mice. *Oncogene* **24,** 39–46 (2005).

11. Vander Heiden, M. G. Targeting cancer metabolism: a therapeutic window opens. *Nat. Rev. Drug Discov.* **10,** 671–684 (2011).

12. Flegal, K. M., Carroll, M. D., Kit, B. K. & Ogden, C. L. Prevalence of obesity and trends in the distribution of body mass index among US adults, 1999-2010. *JAMA* **307,** 491–497 (2012).

13. Finucane, M. M. *et al.* National, regional, and global trends in body-mass index since 1980: systematic analysis of health examination surveys and epidemiological studies with 960 country-years and 9·1 million participants. *Lancet Lond. Engl.* **377,** 557–567 (2011).

14. Jemal, A. *et al.* Global cancer statistics. *CA. Cancer J. Clin.* **61,** 69–90 (2011).

15. Lichtman, M. A. Obesity and the risk for a hematological malignancy: leukemia, lymphoma, or myeloma. *The Oncologist* **15,** 1083–1101 (2010).

16. Li, D. *et al.* Body mass index and risk, age of onset, and survival in patients with pancreatic cancer. *JAMA* **301,** 2553–2562 (2009).

17. MacInnis, R. J. & English, D. R. Body size and composition and prostate cancer risk: systematic review and meta-regression analysis. *Cancer Causes Control CCC* **17,** 989–1003 (2006).

18. Key, T. J. *et al.* Body mass index, serum sex hormones, and breast cancer risk in postmenopausal women. *J. Natl. Cancer Inst.* **95,** 1218–1226 (2003).

19. Vucenik, I. & Stains, J. P. Obesity and cancer risk: evidence, mechanisms, and recommendations. *Ann. N. Y. Acad. Sci.* **1271,** 37–43 (2012).

20. Rocchini, A. P. Childhood obesity and a diabetes epidemic. *N. Engl. J. Med.* **346,** 854–855 (2002).

21. Biro, F. M. & Wien, M. Childhood obesity and adult morbidities. *Am. J. Clin. Nutr.* **91,** 1499S–1505S (2010).

22. Hunt, D. A., Lane, H. M., Zygmont, M. E., Dervan, P. A. & Hennigar, R. A. MRNA stability and overexpression of fatty acid synthase in human breast cancer cell lines. *Anticancer Res.* **27,** 27–34 (2007).

23. Gansler, T. S., Hardman, W., Hunt, D. A., Schaffel, S. & Hennigar, R. A. Increased expression of fatty acid synthase (OA-519) in ovarian neoplasms predicts shorter survival. *Hum. Pathol.* **28,** 686–692 (1997).

24. Nguyen, P. L. *et al.* Fatty acid synthase polymorphisms, tumor expression, body mass index, prostate cancer risk, and survival. *J. Clin. Oncol. Off. J. Am. Soc. Clin. Oncol.* **28,** 3958–3964 (2010).

25. Menendez, J. A. & Lupu, R. Fatty acid synthase and the lipogenic phenotype in cancer pathogenesis. *Nat. Rev. Cancer* **7,** 763–777 (2007).

26. Kridel, S. J., Axelrod, F., Rozenkrantz, N. & Smith, J. W. Orlistat is a novel inhibitor of fatty acid synthase with antitumor activity. *Cancer Res.* **64,** 2070–2075 (2004).

27. Boizard, M. *et al.* Obesity-related overexpression of fatty-acid synthase gene in adipose tissue involves sterol regulatory element-binding protein transcription factors. *J. Biol. Chem.* **273,** 29164–29171 (1998).

28. Nomura, D. K. *et al.* Monoacylglycerol lipase regulates a fatty acid network that promotes cancer pathogenesis. *Cell* **140,** 49–61 (2010).

29. Das, S. K. *et al.* Adipose triglyceride lipase contributes to cancer-associated cachexia. *Science* **333,** 233–238 (2011).

30. Gercel-Taylor, C., Doering, D. L., Kraemer, F. B. & Taylor, D. D. Aberrations in normal systemic lipid metabolism in ovarian cancer patients. *Gynecol. Oncol.* **60,** 35–41 (1996).

31. Argilés, J. M., Alvarez, B. & López-Soriano, F. J. The metabolic basis of cancer cachexia. *Med. Res. Rev.* **17,** 477–498 (1997).

32. Mulligan, H. D., Beck, S. A. & Tisdale, M. J. Lipid metabolism in cancer cachexia. *Br. J. Cancer* **66,** 57–61 (1992).

33. Nieman, K. M. *et al.* Adipocytes promote ovarian cancer metastasis and provide energy for rapid tumor growth. *Nat. Med.* **17,** 1498–1503 (2011).

34. Zhang, Y. *et al.* Stromal progenitor cells from endogenous adipose tissue contribute to pericytes and adipocytes that populate the tumor microenvironment. *Cancer Res.* **72,** 5198–5208 (2012).

35. Wymann, M. P. & Schneiter, R. Lipid signalling in disease. *Nat. Rev. Mol. Cell Biol.* **9,** 162–176 (2008).

36. Mills, G. B. & Moolenaar, W. H. The emerging role of lysophosphatidic acid in cancer. *Nat. Rev. Cancer* **3,** 582–591 (2003).

37. Erickson, J. R. *et al.* Lysophosphatidic acid and ovarian cancer: a paradigm for tumorogenesis and patient management. *Prostaglandins Other Lipid Mediat.* **64,** 63–81 (2001).

38. Liu, S. *et al.* Expression of autotaxin and lysophosphatidic acid receptors increases mammary tumorigenesis, invasion, and metastases. *Cancer Cell* **15,** 539–550 (2009).

39. Yang, M. *et al.* G protein-coupled lysophosphatidic acid receptors stimulate proliferation of colon cancer cells through the {beta}-catenin pathway. *Proc. Natl. Acad. Sci. U. S. A.* **102,** 6027–6032 (2005).

40. van Corven, E. J., Groenink, A., Jalink, K., Eichholtz, T. & Moolenaar, W. H. Lysophosphatidate-induced cell proliferation: identification and dissection of signaling pathways mediated by G proteins. *Cell* **59,** 45–54 (1989).

41. Fang, X. *et al.* Lysophosphatidic acid prevents apoptosis in fibroblasts via G(i)-protein-mediated activation of mitogen-activated protein kinase. *Biochem. J.* **352 Pt 1,** 135–143 (2000).

42. Takeda, H. *et al.* PI 3-kinase gamma and protein kinase C-zeta mediate RAS-independent activation of MAP kinase by a Gi protein-coupled receptor. *EMBO J.* **18,** 386–395 (1999).

43. van Corven, E. J., Hordijk, P. L., Medema, R. H., Bos, J. L. & Moolenaar, W. H. Pertussis toxin-sensitive activation of p21ras by G protein-coupled receptor agonists in fibroblasts. *Proc. Natl. Acad. Sci. U. S. A.* **90,** 1257–1261 (1993).

44. Boucharaba, A. *et al.* Bioactive lipids lysophosphatidic acid and sphingosine 1-phosphate mediate breast cancer cell biological functions through distinct mechanisms. *Oncol. Res.* **18,** 173–184 (2009).

45. Marshall, J.-C. A. *et al.* Effect of inhibition of the lysophosphatidic acid receptor 1 on metastasis and metastatic dormancy in breast cancer. *J. Natl. Cancer Inst.* **104,** 1306–1319 (2012).

46. Costa, C. *et al.* Cyclo-oxygenase 2 expression is associated with angiogenesis and lymph node metastasis in human breast cancer. *J. Clin. Pathol.* **55,** 429–434 (2002).

47. Howe, L. R. *et al.* HER2/neu-induced mammary tumorigenesis and angiogenesis are reduced in cyclooxygenase-2 knockout mice. *Cancer Res.* **65,** 10113–10119 (2005).

48. Tsujii, M. & DuBois, R. N. Alterations in cellular adhesion and apoptosis in epithelial cells overexpressing prostaglandin endoperoxide synthase 2. *Cell* **83,** 493–501 (1995).

49. Gupta, G. P. *et al.* Mediators of vascular remodelling co-opted for sequential steps in lung metastasis. *Nature* **446,** 765–770 (2007).

50. Chang, S.-H. *et al.* Role of prostaglandin E2-dependent angiogenic switch in cyclooxygenase 2-induced breast cancer progression. *Proc. Natl. Acad. Sci. U. S. A.* **101,** 591–596 (2004).

51. Castellone, M. D., Teramoto, H., Williams, B. O., Druey, K. M. & Gutkind, J. S. Prostaglandin E2 promotes colon cancer cell growth through a Gs-axin-beta-catenin signaling axis. *Science* **310,** 1504–1510 (2005).

52. Heasley, L. E. *et al.* Induction of cytosolic phospholipase A2 by oncogenic Ras in human non-small cell lung cancer. *J. Biol. Chem.* **272,** 14501–14504 (1997).

53. Weiser-Evans, M. C. M. *et al.* Depletion of cytosolic phospholipase A2 in bone marrow-derived macrophages protects against lung cancer progression and metastasis. *Cancer Res.* **69,** 1733–1738 (2009).

54. Gómez-Muñoz, A. *et al.* Ceramide-1-phosphate promotes cell survival through activation of the phosphatidylinositol 3-kinase/protein kinase B pathway. *FEBS Lett.* **579,** 3744–3750 (2005).

55. Park, K. S. *et al.* S1P stimulates chemotactic migration and invasion in OVCAR3 ovarian cancer cells. *Biochem. Biophys. Res. Commun.* **356,** 239–244 (2007).

56. Li, W. *et al.* Sphingosine kinase 1 is associated with gastric cancer progression and poor survival of patients. *Clin. Cancer Res. Off. J. Am. Assoc. Cancer Res.* **15,** 1393–1399 (2009).

57. Kawamori, T. *et al.* Role for sphingosine kinase 1 in colon carcinogenesis. *FASEB J. Off. Publ. Fed. Am. Soc. Exp. Biol.* **23,** 405–414 (2009).

58. Bektas, M. *et al.* Sphingosine kinase activity counteracts ceramide-mediated cell death in human melanoma cells: role of Bcl-2 expression. *Oncogene* **24,** 178–187 (2005).

59. Limaye, V. *et al.* Sphingosine kinase-1 enhances endothelial cell survival through a PECAM-1-dependent activation of PI-3K/Akt and regulation of Bcl-2 family members. *Blood* **105,** 3169–3177 (2005).

60. Liu, S.-Q. *et al.* Sphingosine kinase 1 promotes tumor progression and confers malignancy phenotypes of colon cancer by regulating the focal adhesion kinase pathway and adhesion molecules. *Int. J. Oncol.* **42,** 617–626 (2013).

61. Oskouian, B. *et al.* Sphingosine-1-phosphate lyase potentiates apoptosis via p53- and p38-dependent pathways and is down-regulated in colon cancer. *Proc. Natl. Acad. Sci. U. S. A.* **103,** 17384–17389 (2006).

62. Shindou, H. *et al.* A single enzyme catalyzes both platelet-activating factor production and membrane biogenesis of inflammatory cells. Cloning and characterization of acetyl-CoA:LYSO-PAF acetyltransferase. *J. Biol. Chem.* **282,** 6532–6539 (2007).

63. Denizot, Y. *et al.* Platelet-activating factor and human thyroid cancer. *Eur. J. Endocrinol.* **153,** 31–40 (2005).

64. Bussolati, B. *et al.* PAF produced by human breast cancer cells promotes migration and proliferation of tumor cells and neo-angiogenesis. *Am. J. Pathol.* **157,** 1713–1725 (2000).

65. Melnikova, V. O., Mourad-Zeidan, A. A., Lev, D. C. & Bar-Eli, M. Platelet-activating factor mediates MMP-2 expression and activation via phosphorylation of cAMP-response element-binding protein and contributes to melanoma metastasis. *J. Biol. Chem.* **281,** 2911–2922 (2006).

66. Denley, A., Gymnopoulos, M., Kang, S., Mitchell, C. & Vogt, P. K. Requirement of phosphatidylinositol(3,4,5)trisphosphate in phosphatidylinositol 3-kinase-induced oncogenic transformation. *Mol. Cancer Res. MCR* **7,** 1132–1138 (2009).

67. Hernandez-Aya, L. F. & Gonzalez-Angulo, A. M. Targeting the phosphatidylinositol 3-kinase signaling pathway in breast cancer. *The Oncologist* **16,** 404–414 (2011).

68. Wang, Y. *et al.* Mitogenic and anti-apoptotic effects of insulin in endometrial cancer are phosphatidylinositol 3-kinase/Akt dependent. *Gynecol. Oncol.* **125,** 734–741 (2012).

69. Krystal, G. W., Sulanke, G. & Litz, J. Inhibition of phosphatidylinositol 3-kinase-Akt signaling blocks growth, promotes apoptosis, and enhances sensitivity of small cell lung cancer cells to chemotherapy. *Mol. Cancer Ther.* **1,** 913–922 (2002).

70. Gregor, M. F. & Hotamisligil, G. S. Inflammatory mechanisms in obesity. *Annu. Rev. Immunol.* **29,** 415–445 (2011).

71. Neels, J. G. & Olefsky, J. M. Inflamed fat: what starts the fire? *J. Clin. Invest.* **116,** 33–35 (2006).

72. van Kruijsdijk, R. C. M., van der Wall, E. & Visseren, F. L. J. Obesity and cancer: the role of dysfunctional adipose tissue. *Cancer Epidemiol. Biomark. Prev. Publ. Am. Assoc. Cancer Res. Cosponsored Am. Soc. Prev. Oncol.* **18,** 2569–2578 (2009).

73. Cottam, D. R. *et al.* The chronic inflammatory hypothesis for the morbidity associated with morbid obesity: implications and effects of weight loss. *Obes. Surg.* **14,** 589–600 (2004).

74. Weisberg, S. P. *et al.* Obesity is associated with macrophage accumulation in adipose tissue. *J. Clin. Invest.* **112,** 1796–1808 (2003).

75. Carswell, E. A. *et al.* An endotoxin-induced serum factor that causes necrosis of tumors. *Proc. Natl. Acad. Sci. U. S. A.* **72,** 3666–3670 (1975).

76. Leibovich, S. J. *et al.* Macrophage-induced angiogenesis is mediated by tumour necrosis factor-alpha. *Nature* **329,** 630–632 (1987).

77. Orosz, P. *et al.* Enhancement of experimental metastasis by tumor necrosis factor. *J. Exp. Med.* **177,** 1391–1398 (1993).

78. Liu, Z. G., Hsu, H., Goeddel, D. V. & Karin, M. Dissection of TNF receptor 1 effector functions: JNK activation is not linked to apoptosis while NF-kappaB activation prevents cell death. *Cell* **87,** 565–576 (1996).

79. Duyao, M. P., Buckler, A. J. & Sonenshein, G. E. Interaction of an NF-kappa B-like factor with a site upstream of the c-myc promoter. *Proc. Natl. Acad. Sci. U. S. A.* **87,** 4727–4731 (1990).

80. Guttridge, D. C., Albanese, C., Reuther, J. Y., Pestell, R. G. & Baldwin, A. S. NF-kappaB controls cell growth and differentiation through transcriptional regulation of cyclin D1. *Mol. Cell. Biol.* **19,** 5785–5799 (1999).

81. Calado, D. P. *et al.* Constitutive canonical NF-κB activation cooperates with disruption of BLIMP1 in the pathogenesis of activated B cell-like diffuse large cell lymphoma. *Cancer Cell* **18,** 580–589 (2010).

82. Wang, W. *et al.* The nuclear factor-kappa B RelA transcription factor is constitutively activated in human pancreatic adenocarcinoma cells. *Clin. Cancer Res. Off. J. Am. Assoc. Cancer Res.* **5,** 119–127 (1999).

83. Pikarsky, E. *et al.* NF-kappaB functions as a tumour promoter in inflammation-associated cancer. *Nature* **431,** 461–466 (2004).

84. Bours, V. *et al.* Nuclear factor-kappa B, cancer, and apoptosis. *Biochem. Pharmacol.* **60,** 1085–1089 (2000).

85. Kern, P. A., Ranganathan, S., Li, C., Wood, L. & Ranganathan, G. Adipose tissue tumor necrosis factor and interleukin-6 expression in human obesity and insulin resistance. *Am. J. Physiol. Endocrinol. Metab.* **280,** E745-751 (2001).

86. Yan, S. F. *et al.* Induction of interleukin 6 (IL-6) by hypoxia in vascular cells. Central role of the binding site for nuclear factor-IL-6. *J. Biol. Chem.* **270,** 11463–11471 (1995).

87. Bromberg, J. F. *et al.* Stat3 as an oncogene. *Cell* **98,** 295–303 (1999).

88. Darnell, J. E., Kerr, I. M. & Stark, G. R. Jak-STAT pathways and transcriptional activation in response to IFNs and other extracellular signaling proteins. *Science* **264,** 1415–1421 (1994).

89. Yadav, A., Kumar, B., Datta, J., Teknos, T. N. & Kumar, P. IL-6 promotes head and neck tumor metastasis by inducing epithelial-mesenchymal transition via the JAK-STAT3-SNAIL signaling pathway. *Mol. Cancer Res. MCR* **9,** 1658–1667 (2011).

90. Park, E. J. *et al.* Dietary and genetic obesity promote liver inflammation and tumorigenesis by enhancing IL-6 and TNF expression. *Cell* **140,** 197–208 (2010).

91. Park, J., Tadlock, L., Gores, G. J. & Patel, T. Inhibition of interleukin 6-mediated mitogen-activated protein kinase activation attenuates growth of a cholangiocarcinoma cell line. *Hepatol. Baltim. Md* **30,** 1128–1133 (1999).

92. Danø, K. *et al.* Plasminogen activation and cancer. *Thromb. Haemost.* **93,** 676–681 (2005).

93. Foekens, J. A. *et al.* Plasminogen activator inhibitor-1 and prognosis in primary breast cancer. *J. Clin. Oncol. Off. J. Am. Soc. Clin. Oncol.* **12,** 1648–1658 (1994).

94. Isogai, C. *et al.* Plasminogen activator inhibitor-1 promotes angiogenesis by stimulating endothelial cell migration toward fibronectin. *Cancer Res.* **61,** 5587–5594 (2001).

95. Bajou, K. *et al.* Absence of host plasminogen activator inhibitor 1 prevents cancer invasion and vascularization. *Nat. Med.* **4,** 923–928 (1998).

96. Hotamisligil, G. S., Arner, P., Caro, J. F., Atkinson, R. L. & Spiegelman, B. M. Increased adipose tissue expression of tumor necrosis factor-alpha in human obesity and insulin resistance. *J. Clin. Invest.* **95,** 2409–2415 (1995).

97. Uysal, K. T., Wiesbrock, S. M., Marino, M. W. & Hotamisligil, G. S. Protection from obesity-induced insulin resistance in mice lacking TNF-alpha function. *Nature* **389,** 610–614 (1997).

98. Samuel, V. T., Petersen, K. F. & Shulman, G. I. Lipid-induced insulin resistance: unravelling the mechanism. *Lancet Lond. Engl.* **375,** 2267–2277 (2010).

99. Carey, D. G., Jenkins, A. B., Campbell, L. V., Freund, J. & Chisholm, D. J. Abdominal fat and insulin resistance in normal and overweight women: Direct measurements reveal a strong relationship in subjects at both low and high risk of NIDDM. *Diabetes* **45,** 633–638 (1996).

100. Cnop, M. *et al.* The concurrent accumulation of intra-abdominal and subcutaneous fat explains the association between insulin resistance and plasma leptin concentrations : distinct metabolic effects of two fat compartments. *Diabetes* **51,** 1005–1015 (2002).

101. Gan, S. K. *et al.* Insulin action, regional fat, and myocyte lipid: altered relationships with increased adiposity. *Obes. Res.* **11,** 1295–1305 (2003).

102. Mu, N., Zhu, Y., Wang, Y., Zhang, H. & Xue, F. Insulin resistance: a significant risk factor of endometrial cancer. *Gynecol. Oncol.* **125,** 751–757 (2012).

103. Barone, B. B. *et al.* Long-term all-cause mortality in cancer patients with preexisting diabetes mellitus: a systematic review and meta-analysis. *JAMA* **300,** 2754–2764 (2008).

104. Ma, J. *et al.* Prediagnostic body-mass index, plasma C-peptide concentration, and prostate cancer-specific mortality in men with prostate cancer: a long-term survival analysis. *Lancet Oncol.* **9,** 1039–1047 (2008).

105. Harris, L. N. *et al.* Predictors of resistance to preoperative trastuzumab and vinorelbine for HER2-positive early breast cancer. *Clin. Cancer Res. Off. J. Am. Assoc. Cancer Res.* **13,** 1198–1207 (2007).

106. Stansbie, D., Brownsey, R. W., Crettaz, M. & Denton, R. M. Acute effects in vivo of anti-insulin serum on rates of fatty acid synthesis and activities of acetyl-coenzyme A carboxylase and pyruvate dehydrogenase in liver and epididymal adipose tissue of fed rats. *Biochem. J.* **160,** 413–416 (1976).

107. Monaco, M. E., Osborne, C. K. & Lippman, M. E. Insulin stimulation of fatty acid synthesis in human breast cancer cells. *J. Natl. Cancer Inst.* **58,** 1591–1593 (1977).

108. Gross, G. E., Boldt, D. H. & Osborne, C. K. Perturbation by insulin of human breast cancer cell cycle kinetics. *Cancer Res.* **44,** 3570–3575 (1984).

109. Liu, Z. *et al.* Epidermal growth factor induces tumour marker AKR1B10 expression through activator protein-1 signalling in hepatocellular carcinoma cells. *Biochem. J.* **442,** 273–282 (2012).

110. Pollak, M. Insulin and insulin-like growth factor signalling in neoplasia. *Nat. Rev. Cancer* **8,** 915–928 (2008).

111. Böni-Schnetzler, M., Schmid, C., Meier, P. J. & Froesch, E. R. Insulin regulates insulin-like growth factor I mRNA in rat hepatocytes. *Am. J. Physiol.* **260,** E846-851 (1991).

112. Engelman, J. A. Targeting PI3K signalling in cancer: opportunities, challenges and limitations. *Nat. Rev. Cancer* **9,** 550–562 (2009).

113. Schubbert, S., Shannon, K. & Bollag, G. Hyperactive Ras in developmental disorders and cancer. *Nat. Rev. Cancer* **7,** 295–308 (2007).

114. Cully, M., You, H., Levine, A. J. & Mak, T. W. Beyond PTEN mutations: the PI3K pathway as an integrator of multiple inputs during tumorigenesis. *Nat. Rev. Cancer* **6,** 184–192 (2006).

115. Zoncu, R., Efeyan, A. & Sabatini, D. M. mTOR: from growth signal integration to cancer, diabetes and ageing. *Nat. Rev. Mol. Cell Biol.* **12,** 21–35 (2011).

116. Kalaany, N. Y. & Sabatini, D. M. Tumours with PI3K activation are resistant to dietary restriction. *Nature* **458,** 725–731 (2009).

117. Ma, J. *et al.* IGF-1 mediates PTEN suppression and enhances cell invasion and proliferation via activation of the IGF-1/PI3K/Akt signaling pathway in pancreatic cancer cells. *J. Surg. Res.* **160,** 90–101 (2010).

118. Wrobel, G. *et al.* Microarray-based gene expression profiling of benign, atypical and anaplastic meningiomas identifies novel genes associated with meningioma progression. *Int. J. Cancer* **114,** 249–256 (2005).

119. Hartmann, W. *et al.* Insulin-like growth factor II is involved in the proliferation control of medulloblastoma and its cerebellar precursor cells. *Am. J. Pathol.* **166,** 1153–1162 (2005).

120. Perks, C. M. & Holly, J. M. P. The insulin-like growth factor (IGF) family and breast cancer. *Breast Dis.* **18,** 45–60 (2003).

121. Chan, J. M. *et al.* Plasma insulin-like growth factor-I and prostate cancer risk: a prospective study. *Science* **279,** 563–566 (1998).

122. Barozzi, C. *et al.* Relevance of biologic markers in colorectal carcinoma: a comparative study of a broad panel. *Cancer* **94,** 647–657 (2002).

123. Hakam, A. *et al.* Expression of insulin-like growth factor-1 receptor in human colorectal cancer. *Hum. Pathol.* **30,** 1128–1133 (1999).

124. Sesti, G. *et al.* Plasma concentration of IGF-I is independently associated with insulin sensitivity in subjects with different degrees of glucose tolerance. *Diabetes Care* **28,** 120–125 (2005).

125. Nam, S. Y. *et al.* Effect of obesity on total and free insulin-like growth factor (IGF)-1, and their relationship to IGF-binding protein (BP)-1, IGFBP-2, IGFBP-3, insulin, and growth hormone. *Int. J. Obes. Relat. Metab. Disord. J. Int. Assoc. Study Obes.* **21,** 355–359 (1997).

126. de Ostrovich, K. K. *et al.* Paracrine overexpression of insulin-like growth factor-1 enhances mammary tumorigenesis in vivo. *Am. J. Pathol.* **173,** 824–834 (2008).

127. DiGiovanni, J. *et al.* Deregulated expression of insulin-like growth factor 1 in prostate epithelium leads to neoplasia in transgenic mice. *Proc. Natl. Acad. Sci. U. S. A.* **97,** 3455–3460 (2000).

128. Bol, D. K., Kiguchi, K., Gimenez-Conti, I., Rupp, T. & DiGiovanni, J. Overexpression of insulin-like growth factor-1 induces hyperplasia, dermal abnormalities, and spontaneous tumor formation in transgenic mice. *Oncogene* **14,** 1725–1734 (1997).

129. Moorehead, R. A., Sanchez, O. H., Baldwin, R. M. & Khokha, R. Transgenic overexpression of IGF-II induces spontaneous lung tumors: a model for human lung adenocarcinoma. *Oncogene* **22,** 853–857 (2003).

130. Pravtcheva, D. D. & Wise, T. L. Metastasizing mammary carcinomas in H19 enhancers-Igf2 transgenic mice. *J. Exp. Zool.* **281,** 43–57 (1998).

131. Carboni, J. M. *et al.* Tumor development by transgenic expression of a constitutively active insulin-like growth factor I receptor. *Cancer Res.* **65,** 3781–3787 (2005).

132. Lopez, T. & Hanahan, D. Elevated levels of IGF-1 receptor convey invasive and metastatic capability in a mouse model of pancreatic islet tumorigenesis. *Cancer Cell* **1,** 339–353 (2002).

133. Wu, Y. *et al.* Insulin-like growth factor-I regulates the liver microenvironment in obese mice and promotes liver metastasis. *Cancer Res.* **70,** 57–67 (2010).

134. Baskin, D. G. *et al.* Insulin and leptin: dual adiposity signals to the brain for the regulation of food intake and body weight. *Brain Res.* **848,** 114–123 (1999).

135. Snoussi, K. *et al.* Leptin and leptin receptor polymorphisms are associated with increased risk and poor prognosis of breast carcinoma. *BMC Cancer* **6,** 38 (2006).

136. Howard, J. M., Pidgeon, G. P. & Reynolds, J. V. Leptin and gastro-intestinal malignancies. *Obes. Rev. Off. J. Int. Assoc. Study Obes.* **11,** 863–874 (2010).

137. Friedman, J. M. & Halaas, J. L. Leptin and the regulation of body weight in mammals. *Nature* **395,** 763–770 (1998).

138. Maffei, M. *et al.* Leptin levels in human and rodent: measurement of plasma leptin and ob RNA in obese and weight-reduced subjects. *Nat. Med.* **1,** 1155–1161 (1995).

139. Hoda, M. R. & Popken, G. Mitogenic and anti-apoptotic actions of adipocyte-derived hormone leptin in prostate cancer cells. *BJU Int.* **102,** 383–388 (2008).

140. Wu, M.-H. *et al.* Circulating levels of leptin, adiposity and breast cancer risk. *Br. J. Cancer* **100,** 578–582 (2009).

141. Drew, J. E. Molecular mechanisms linking adipokines to obesity-related colon cancer: focus on leptin. *Proc. Nutr. Soc.* **71,** 175–180 (2012).

142. Cheng, S.-P. *et al.* Differential roles of leptin in regulating cell migration in thyroid cancer cells. *Oncol. Rep.* **23,** 1721–1727 (2010).

143. Ptak, A., Kolaczkowska, E. & Gregoraszczuk, E. L. Leptin stimulation of cell cycle and inhibition of apoptosis gene and protein expression in OVCAR-3 ovarian cancer cells. *Endocrine* **43,** 394–403 (2013).

144. Saxena, N. K., Vertino, P. M., Anania, F. A. & Sharma, D. leptin-induced growth stimulation of breast cancer cells involves recruitment of histone acetyltransferases and mediator complex to CYCLIN D1 promoter via activation of Stat3. *J. Biol. Chem.* **282,** 13316–13325 (2007).

145. Sharma, D., Saxena, N. K., Vertino, P. M. & Anania, F. A. Leptin promotes the proliferative response and invasiveness in human endometrial cancer cells by

activating multiple signal-transduction pathways. *Endocr. Relat. Cancer* **13,** 629–640 (2006).

146. Banks, A. S., Davis, S. M., Bates, S. H. & Myers, M. G. Activation of downstream signals by the long form of the leptin receptor. *J. Biol. Chem.* **275,** 14563–14572 (2000).

147. Bates, S. H. *et al.* STAT3 signalling is required for leptin regulation of energy balance but not reproduction. *Nature* **421,** 856–859 (2003).

148. Giordano, C. *et al.* Leptin increases HER2 protein levels through a STAT3-mediated up-regulation of Hsp90 in breast cancer cells. *Mol. Oncol.* **7,** 379–391 (2013).

149. Inagaki-Ohara, K. *et al.* Enhancement of leptin receptor signaling by SOCS3 deficiency induces development of gastric tumors in mice. *Oncogene* **33,** 74–84 (2014).

150. Dieudonne, M.-N. *et al.* Leptin mediates a proliferative response in human MCF7 breast cancer cells. *Biochem. Biophys. Res. Commun.* **293,** 622–628 (2002).

151. Hardwick, J. C., Van Den Brink, G. R., Offerhaus, G. J., Van Deventer, S. J. & Peppelenbosch, M. P. Leptin is a growth factor for colonic epithelial cells. *Gastroenterology* **121,** 79–90 (2001).

152. Catalano, S. *et al.* Leptin induces, via ERK1/ERK2 signal, functional activation of estrogen receptor alpha in MCF-7 cells. *J. Biol. Chem.* **279,** 19908–19915 (2004).

153. Zheng, Q. *et al.* Leptin deficiency suppresses MMTV-Wnt-1 mammary tumor growth in obese mice and abrogates tumor initiating cell survival. *Endocr. Relat. Cancer* **18,** 491–503 (2011).

154. Park, J., Kusminski, C. M., Chua, S. C. & Scherer, P. E. Leptin receptor signaling supports cancer cell metabolism through suppression of mitochondrial respiration in vivo. *Am. J. Pathol.* **177,** 3133–3144 (2010).

155. Paz-Filho, G., Lim, E. L., Wong, M.-L. & Licinio, J. Associations between adipokines and obesity-related cancer. *Front. Biosci. Landmark Ed.* **16,** 1634–1650 (2011).

156. Kelesidis, I., Kelesidis, T. & Mantzoros, C. S. Adiponectin and cancer: a systematic review. *Br. J. Cancer* **94,** 1221–1225 (2006).

157. Yamauchi, T. *et al.* The fat-derived hormone adiponectin reverses insulin resistance associated with both lipoatrophy and obesity. *Nat. Med.* **7,** 941–946 (2001).

158. Ouchi, N. *et al.* Adiponectin, an adipocyte-derived plasma protein, inhibits endothelial NF-kappaB signaling through a cAMP-dependent pathway. *Circulation* **102,** 1296–1301 (2000).

159. An, W. *et al.* Adiponectin levels in patients with colorectal cancer and adenoma: a meta-analysis. *Eur. J. Cancer Prev. Off. J. Eur. Cancer Prev. Organ. ECP* **21,** 126–133 (2012).

160. Petridou, E. *et al.* Plasma adiponectin concentrations in relation to endometrial cancer: a case-control study in Greece. *J. Clin. Endocrinol. Metab.* **88,** 993–997 (2003).

161. Konturek, P. C., Burnat, G., Rau, T., Hahn, E. G. & Konturek, S. Effect of adiponectin and ghrelin on apoptosis of Barrett adenocarcinoma cell line. *Dig. Dis. Sci.* **53,** 597–605 (2008).

162. Goktas, S. *et al.* Prostate cancer and adiponectin. *Urology* **65,** 1168–1172 (2005).

163. Tworoger, S. S. *et al.* Plasma adiponectin concentrations and risk of incident breast cancer. *J. Clin. Endocrinol. Metab.* **92,** 1510–1516 (2007).

164. Bub, J. D., Miyazaki, T. & Iwamoto, Y. Adiponectin as a growth inhibitor in prostate cancer cells. *Biochem. Biophys. Res. Commun.* **340,** 1158–1166 (2006).

165. Kim, A. Y. *et al.* Adiponectin represses colon cancer cell proliferation via AdipoR1- and -R2-mediated AMPK activation. *Mol. Endocrinol. Baltim. Md* **24,** 1441–1452 (2010).

166. Taliaferro-Smith, L. *et al.* LKB1 is required for adiponectin-mediated modulation of AMPK-S6K axis and inhibition of migration and invasion of breast cancer cells. *Oncogene* **28,** 2621–2633 (2009).

167. Lam, J. B. B. *et al.* Adiponectin haploinsufficiency promotes mammary tumor development in MMTV-PyVT mice by modulation of phosphatase and tensin homolog activities. *PloS One* **4,** e4968 (2009).

168. Fogarty, S. & Hardie, D. G. Development of protein kinase activators: AMPK as a target in metabolic disorders and cancer. *Biochim. Biophys. Acta* **1804,** 581–591 (2010).

169. Igata, M. *et al.* Adenosine monophosphate-activated protein kinase suppresses vascular smooth muscle cell proliferation through the inhibition of cell cycle progression. *Circ. Res.* **97,** 837–844 (2005).

170. Inoki, K., Zhu, T. & Guan, K.-L. TSC2 mediates cellular energy response to control cell growth and survival. *Cell* **115,** 577–590 (2003).

171. Villa, N. Y. *et al.* Sphingolipids function as downstream effectors of a fungal PAQR. *Mol. Pharmacol.* **75,** 866–875 (2009).

172. Holland, W. L. & Scherer, P. E. PAQRs: a counteracting force to ceramides? *Mol. Pharmacol.* **75,** 740–743 (2009).

173. Takabe, K., Paugh, S. W., Milstien, S. & Spiegel, S. 'Inside-out' signaling of sphingosine-1-phosphate: therapeutic targets. *Pharmacol. Rev.* **60,** 181–195 (2008).

174. Levine, Y. C., Li, G. K. & Michel, T. Agonist-modulated regulation of AMP-activated protein kinase (AMPK) in endothelial cells. Evidence for an AMPK -> Rac1 -> Akt -> endothelial nitric-oxide synthase pathway. *J. Biol. Chem.* **282,** 20351–20364 (2007).

175. Holland, W. L. *et al.* Receptor-mediated activation of ceramidase activity initiates the pleiotropic actions of adiponectin. *Nat. Med.* **17,** 55–63 (2011).

176. Landskroner-Eiger, S. *et al.* Proangiogenic contribution of adiponectin toward mammary tumor growth in vivo. *Clin. Cancer Res. Off. J. Am. Assoc. Cancer Res.* **15,** 3265–3276 (2009).

177. Trujillo, M. E. & Scherer, P. E. Adiponectin--journey from an adipocyte secretory protein to biomarker of the metabolic syndrome. *J. Intern. Med.* **257,** 167–175 (2005).

178. Grossmann, M. E. *et al.* Role of the adiponectin leptin ratio in prostate cancer. *Oncol. Res.* **18,** 269–277 (2009).

179. Currie, C. J., Poole, C. D. & Gale, E. a. M. The influence of glucose-lowering therapies on cancer risk in type 2 diabetes. *Diabetologia* **52,** 1766–1777 (2009).

180. Jonasson, J. M. *et al.* Insulin glargine use and short-term incidence of malignancies-a population-based follow-up study in Sweden. *Diabetologia* **52,** 1745–1754 (2009).

181. Bowker, S. L., Majumdar, S. R., Veugelers, P. & Johnson, J. A. Increased cancer-related mortality for patients with type 2 diabetes who use sulfonylureas or insulin. *Diabetes Care* **29,** 254–258 (2006).

182. Erickson, K. *et al.* Clinically defined type 2 diabetes mellitus and prognosis in early-stage breast cancer. *J. Clin. Oncol. Off. J. Am. Soc. Clin. Oncol.* **29,** 54–60 (2011).

183. Govindarajan, R. *et al.* Thiazolidinediones and the risk of lung, prostate, and colon cancer in patients with diabetes. *J. Clin. Oncol. Off. J. Am. Soc. Clin. Oncol.* **25,** 1476–1481 (2007).

184. Kim, S. *et al.* Aspirin may be more effective in preventing colorectal adenomas in patients with higher BMI (United States). *Cancer Causes Control CCC* **17,** 1299–1304 (2006).

185. Ookhtens, M., Kannan, R., Lyon, I. & Baker, N. Liver and adipose tissue contributions to newly formed fatty acids in an ascites tumor. *Am. J. Physiol.* **247,** R146-153 (1984).

186. DeBerardinis, R. J., Lum, J. J., Hatzivassiliou, G. & Thompson, C. B. The biology of cancer: metabolic reprogramming fuels cell growth and proliferation. *Cell Metab.* **7,** 11–20 (2008).

187. Cordenonsi, M. *et al.* The Hippo transducer TAZ confers cancer stem cell-related traits on breast cancer cells. *Cell* **147,** 759–772 (2011).

188. Nomura, D. K., Dix, M. M. & Cravatt, B. F. Activity-based protein profiling for biochemical pathway discovery in cancer. *Nat. Rev. Cancer* **10,** 630–638 (2010).

189. Medina-Cleghorn, D. & Nomura, D. K. Chemical approaches to study metabolic networks. *Pflugers Arch.* **465,** 427–440 (2013).

190. Tautenhahn, R., Patti, G. J., Rinehart, D. & Siuzdak, G. XCMS Online: a web-based platform to process untargeted metabolomic data. *Anal. Chem.* **84,** 5035–5039 (2012).

191. Arana, L., Gangoiti, P., Ouro, A., Trueba, M. & Gómez-Muñoz, A. Ceramide and ceramide 1-phosphate in health and disease. *Lipids Health Dis.* **9,** 15 (2010).

192. Tsoupras, A. B., Iatrou, C., Frangia, C. & Demopoulos, C. A. The implication of platelet activating factor in cancer growth and metastasis: potent beneficial role of PAF-inhibitors and antioxidants. *Infect. Disord. Drug Targets* **9,** 390–399 (2009).

193. Ogata, H., Goto, S., Fujibuchi, W. & Kanehisa, M. Computation with the KEGG pathway database. *Biosystems* **47,** 119–128 (1998).

194. Pacilli, A. *et al.* Carnitine-acyltransferase system inhibition, cancer cell death, and prevention of myc-induced lymphomagenesis. *J. Natl. Cancer Inst.* **105,** 489–498 (2013).

195. Zaugg, K. *et al.* Carnitine palmitoyltransferase 1C promotes cell survival and tumor growth under conditions of metabolic stress. *Genes Dev.* **25,** 1041–1051 (2011).

196. Liu, L., Wang, Y.-D., Wu, J., Cui, J. & Chen, T. Carnitine palmitoyltransferase 1A (CPT1A): a transcriptional target of PAX3-FKHR and mediates PAX3-FKHR-dependent motility in alveolar rhabdomyosarcoma cells. *BMC Cancer* **12,** 154 (2012).

197. Fallani, A. *et al.* Platelet-activating factor (PAF) is the effector of IFN gamma-stimulated invasiveness and motility in a B16 melanoma line. *Prostaglandins Other Lipid Mediat.* **81,** 171–177 (2006).

198. Snyder, F. & Wood, R. Alkyl and alk-1-enyl ethers of glycerol in lipids from normal and neoplastic human tissues. *Cancer Res.* **29,** 251–257 (1969).

199. Kuemmerle, N. B. *et al.* Lipoprotein lipase links dietary fat to solid tumor cell proliferation. *Mol. Cancer Ther.* **10,** 427–436 (2011).

200. Liu, R.-Z. *et al.* Association of FABP5 expression with poor survival in triple-negative breast cancer: implication for retinoic acid therapy. *Am. J. Pathol.* **178,** 997–1008 (2011).

201. Kamphorst, J. J. *et al.* Hypoxic and Ras-transformed cells support growth by scavenging unsaturated fatty acids from lysophospholipids. *Proc. Natl. Acad. Sci. U. S. A.* **110,** 8882–8887 (2013).

202. Louie, S. M., Roberts, L. S. & Nomura, D. K. Mechanisms linking obesity and cancer. *Biochim. Biophys. Acta* **1831,** 1499–1508 (2013).

203. Nomura, D. K. *et al.* Endocannabinoid hydrolysis generates brain prostaglandins that promote neuroinflammation. *Science* **334,** 809–813 (2011).

204. Piro, J. R. *et al.* A dysregulated endocannabinoid-eicosanoid network supports pathogenesis in a mouse model of Alzheimer's disease. *Cell Rep.* **1,** 617–623 (2012).

205. Smith, C. A. *et al.* METLIN: a metabolite mass spectral database. *Ther. Drug Monit.* **27,** 747–751 (2005).

206. Dawson, S. J., Provenzano, E. & Caldas, C. Triple negative breast cancers: clinical and prognostic implications. *Eur. J. Cancer Oxf. Engl. 1990* **45 Suppl 1,** 27–40 (2009).

207. Dietze, E. C., Sistrunk, C., Miranda-Carboni, G., O'Regan, R. & Seewaldt, V. L. Triple-negative breast cancer in African-American women: disparities versus biology. *Nat. Rev. Cancer* **15,** 248–254 (2015).

208. Polyak, K. & Weinberg, R. A. Transitions between epithelial and mesenchymal states: acquisition of malignant and stem cell traits. *Nat. Rev. Cancer* **9,** 265–273 (2009).

209. Shannon, D. A. *et al.* Investigating the proteome reactivity and selectivity of aryl halides. *J. Am. Chem. Soc.* **136,** 3330–3333 (2014).

210. Weerapana, E. *et al.* Quantitative reactivity profiling predicts functional cysteines in proteomes. *Nature* **468,** 790–795 (2010).

211. Pace, N. J. & Weerapana, E. Diverse functional roles of reactive cysteines. *ACS Chem. Biol.* **8,** 283–296 (2013).

212. Shannon, D. A. & Weerapana, E. Covalent protein modification: the current landscape of residue-specific electrophiles. *Curr. Opin. Chem. Biol.* **24,** 18–26 (2015).

213. Laborde, E. Glutathione transferases as mediators of signaling pathways involved in cell proliferation and cell death. *Cell Death Differ.* **17,** 1373–1380 (2010).

214. Tew, K. D. & Townsend, D. M. Regulatory functions of glutathione S-transferase P1-1 unrelated to detoxification. *Drug Metab. Rev.* **43,** 179–193 (2011).

215. Townsend, D. M. & Tew, K. D. The role of glutathione-S-transferase in anti-cancer drug resistance. *Oncogene* **22,** 7369–7375 (2003).

216. Crawford, L. A. & Weerapana, E. A tyrosine-reactive irreversible inhibitor for glutathione S-transferase Pi (GSTP1). *Mol. Biosyst.* **12,** 1768–1771 (2016).

217. Martell, J. & Weerapana, E. Applications of copper-catalyzed click chemistry in activity-based protein profiling. *Mol. Basel Switz.* **19,** 1378–1393 (2014).

218. Gowda, H. *et al.* Interactive XCMS Online: simplifying advanced metabolomic data processing and subsequent statistical analyses. *Anal. Chem.* **86,** 6931–6939 (2014).

219. Dowling, R. J. O., Zakikhani, M., Fantus, I. G., Pollak, M. & Sonenberg, N. Metformin inhibits mammalian target of rapamycin-dependent translation initiation in breast cancer cells. *Cancer Res.* **67,** 10804–10812 (2007).

220. Carracedo, A., Cantley, L. C. & Pandolfi, P. P. Cancer metabolism: fatty acid oxidation in the limelight. *Nat. Rev. Cancer* **13,** 227–232 (2013).

221. Zhang, J. *et al.* Pleiotropic functions of glutathione S-transferase P. *Adv. Cancer Res.* **122,** 143–175 (2014).

222. Mahadevan, D. & Sutton, G. R. Ezatiostat hydrochloride for the treatment of myelodysplastic syndromes. *Expert Opin. Investig. Drugs* **24,** 725–733 (2015).

223. Hildebrandt, T., Knuesting, J., Berndt, C., Morgan, B. & Scheibe, R. Cytosolic thiol switches regulating basic cellular functions: GAPDH as an information hub? *Biol. Chem.* **396,** 523–537 (2015).

224. Moellering, R. E. & Cravatt, B. F. Functional lysine modification by an intrinsically reactive primary glycolytic metabolite. *Science* **341,** 549–553 (2013).

225. Grek, C. L., Zhang, J., Manevich, Y., Townsend, D. M. & Tew, K. D. Causes and consequences of cysteine S-glutathionylation. *J. Biol. Chem.* **288,** 26497–26504 (2013).

226. Shestov, A. A. *et al.* Quantitative determinants of aerobic glycolysis identify flux through the enzyme GAPDH as a limiting step. *eLife* **3,** (2014).

227. Benjamin, D. I. *et al.* Ether lipid generating enzyme AGPS alters the balance of structural and signaling lipids to fuel cancer pathogenicity. *Proc. Natl. Acad. Sci. U. S. A.* **110,** 14912–14917 (2013).

228. Benjamin, D. I. *et al.* Inositol phosphate recycling regulates glycolytic and lipid metabolism that drives cancer aggressiveness. *ACS Chem. Biol.* **9,** 1340–1350 (2014).

229. Benjamin, D. I. *et al.* Diacylglycerol Metabolism and Signaling Is a Driving Force Underlying FASN Inhibitor Sensitivity in Cancer Cells. *ACS Chem. Biol.* **10,** 1616–1623 (2015).

230. Long, J. Z. *et al.* Metabolomics annotates ABHD3 as a physiologic regulator of medium-chain phospholipids. *Nat. Chem. Biol.* **7,** 763–765 (2011).

231. Mulvihill, M. M. *et al.* Metabolic profiling reveals PAFAH1B3 as a critical driver of breast cancer pathogenicity. *Chem. Biol.* **21,** 831–840 (2014).

232. Medina-Cleghorn, D. *et al.* Mapping Proteome-Wide Targets of Environmental Chemicals Using Reactivity-Based Chemoproteomic Platforms. *Chem. Biol.* **22,** 1394–1405 (2015).